Organic & Biomolecular Chemistry

REVIEW

View Article Online
View Journal | View Issue

Cite this: *Org. Biomol. Chem.*, 2016, **14**, 7392

Studies in organic and physical photochemistry – an interdisciplinary approach

Michael Oelgemöller*[a] and Norbert Hoffmann*[b]

Received 19th April 2016,
Accepted 22nd June 2016

DOI: 10.1039/c6ob00842a

www.rsc.org/obc

Traditionally, organic photochemistry when applied to synthesis strongly interacts with physical chemistry. The aim of this review is to illustrate this very fruitful interdisciplinary approach and cooperation. A profound understanding of the photochemical reactivity and reaction mechanisms is particularly helpful for optimization and application of these reactions. Some typical reactions and particular aspects are reported such as the Norrish-Type II reaction and the Yang cyclization and related transformations, the [2 + 2] photocycloadditions, particularly the Paternò–Büchi reaction, photochemical electron transfer induced transformations, different kinds of catalytic reactions such as photoredox catalysis for organic synthesis and photooxygenation are discussed. Particular aspects such as the structure and reactivity of aryl cations, photochemical reactions in the crystalline state, chiral memory, different mechanisms of hydrogen transfer in photochemical reactions or fundamental aspects of stereoselectivity are discussed. Photochemical reactions are also investigated in the context of chemical engineering. Particularly, continuous flow reactors are of interest. Novel reactor systems are developed and modeling of photochemical transformations and different reactors play a key role in such studies. This research domain builds a bridge between fundamental studies of organic photochemical reactions and their industrial application.

1 Introduction

When compared to reactions at the ground state, photochemical transformations are characterized by the fact that they involve electronic excitation.[1] Thus, by light absorption the electron configuration of a molecule changes. Since the reactivity of a chemical compound is defined by its electron configuration, it is obvious that the photochemical reaction conditions considerably augment the number of transformations of a compound family. Often, photochemical reactivity is even complementary to ground state chemistry. More basically, this phenomenon may be described by potential-energy surface topology.[2,3] Applying photochemical methods to organic synthesis, products can be synthesized which are difficultly or not available with conventional methods.[4,5] Many catalytic reactions with organometallic compounds or enzymes are improved under these conditions. Since photochemical reactions can be performed under mild conditions, they further enable studying transformations in supramolecular structures or investigating particular phenomena of absolute chiral induction or chiral memory.[6] Photochemical transformations are also applied to the synthesis of unusual or strained hydrocarbons.[7] Such investigations contribute to a profound understanding of fundamental aspects of chemical structures and bonds. Electronic excitation, often avoids chemical activation with acids, bases, metals, and so on. Side reactions and waste products are thus limited. The photon is considered as a "traceless reagent".[8] Photochemical transformations provide a lot of perspectives for sustainable chemistry. They even belong to the standard methods of "green chemistry".[9] They can readily be optimized when performed in a microreactor or continuous flow systems. In many fields such as pharmaceutical or agricultural chemistry or in materials science photochemical reactions are therefore highly appreciated.

Traditionally, the study of organic photochemical reactions is strongly linked to physical chemistry. This intense cooperation between two research domains enables a profound and comprehensive understanding of reaction mechanisms and consequently a facile optimization of the reactions and application to industrial production. Also more general topics of chemistry are often elucidated by this research. It further facilitates interaction with other scientific domains such as materials science, medicinal and biochemistry, supramolecular chemistry, environmental science, *etc*. Although photochemical transformations are investigated in many different domains, we would like to focus the present contribution on some reactions possessing high interest in the

[a]*James Cook University, College of Science and Engineering, Townsville, QLD 4811, Australia. E-mail: michael.oelgemoeller@jcu.edu.au*
[b]*CNRS, Université de Reims Champagne-Ardenne, ICMR, Equipe de Photochimie, UFR Sciences, B.P. 1039, 51687 Reims, France. E-mail: norbert.hoffmann@univ-reims.fr*

context of organic synthesis. After a period of stagnation, activities in this field are increasing once again in academic and industrial research. The aim of this article is therefore to indicate and stimulate this fruitful interaction with some examples related to synthetic organic photochemistry.

2 Norrish Type II reaction and cyclizations

The Norrish Type II reaction and the competing Yang cyclization are classical photochemical reactions of carbonyl compounds.[10] After photochemical nπ*-excitation of the carbonyl function in **1**, intramolecular hydrogen abstraction takes place (Scheme 1). This reaction step occurs at both the singlet state and the triplet state. It requires specific orientations of the carbonyl group and the hydrogen atom which will be abstracted. The reactions were also performed in the solid state.[11,12] Under these conditions the structure is rigid and the orientation of the participating atoms is determined by X-ray structure analysis. Thus, it was found that the C=O···H–C dihedral angles Δ, ω and θ in **1** may vary greatly and that the O–H distance d is most relevant for the efficiency of this reaction step. Radical intermediates such as the resulting 1,4-diradical **2** play an important role in the outcome of many photochemical reactions.[13] Depending on the intersystem crossing (isc) rate, the 1,4-diradical **2** may either be formed at its singlet or triplet state. At the singlet state, the intermediate undergoes cleavage easily leading to the alkene **3** and the enol **4**. The latter product undergoes immediate tautomerization to the corresponding ketone. This overall reaction corresponds to the Norrish Type II reaction. This cleavage step is favored by entropy and it is not inhibited by intersystem crossing. At the triplet state, three reactions are in competition. Hydrogen back transfer may occur thus leading to substrate **1**. The Norrish Type II reaction may also be in competition with the Yang cyclization by intramolecular radical combination. The latter reaction leads to cyclobutanols **5**. In all these cases, intersystem crossing must occur since the final products possess singlet multiplicity. This step is therefore accelerated by efficient spin orbit coupling.[14] Such an efficient interaction is linked to a particular transition state in which the two radical carrying orbitals are orthogonally orientated (**6**).[15,16] As already mentioned, hydrogen abstraction can also occur at the singlet state. The quenching of the singlet state may even be faster than the corresponding triplet state. However, the hydrogen transfer is less efficient.[17]

Cyclizations of photochemically generated diradicals are of particular interest since they may be applied to organic synthesis. Therefore, details of the stereochemical influence on such reactions have been intensively investigated. Thus, the influence of the relative configuration on the competition between the Norrish Type II fragmentation and the Yang cyclization was studied. When the aromatic ketone **7** derived from isoleucine was irradiated, hydrogen abstraction in the γ position at the ethyl group took place leading to the 1,4-diradical **8** (Scheme 2).[18] Generally, in such aromatic ketones, intersystem crossing is fast and the nπ* triplet state is rapidly populated. Two main conformers **9** and **10** of the diradical are in equilibrium. Conformation **10** in which the two radical positions are orientated *syn* with respect to each other dominates in this equilibrium since it is 1.1 kcal mol^{-1} more stable than **9**. For

Michael Oelgemöller

Associate Professor Michael Oelgemöller received his Diploma from the University of Münster in 1995 and his Ph.D. from the University of Cologne in 1999. He was a researcher at the ERATO-JST Photochirogenesis project in Osaka (1999–2001) and at Bayer CropScience Japan in Yuki (2001–2004). From 2004–2008 he held the position of Lecturer in Organic and Medicinal Chemistry at Dublin City University. In February 2009 he joined James Cook University in Townsville as an Associate Professor in Organic Chemistry. His research activities include continuous-flow photochemistry, solar manufacturing of chemicals, photochemical synthesis of bioactive compounds and photochemical degradation of pollutants.[229]

Norbert Hoffmann

Norbert Hoffmann studied chemistry at the RWTH Aachen University, Germany and received his PhD degree in 1992 under the supervision of Hans-Dieter Scharf. In 1993, he obtained a permanent position (Chargé de Recherche) at the French National Center for Scientific Research CNRS in Reims, France. In 2004, he was appointed Research Director at the CNRS. His main research interests are in the field of organic photochemistry: electron transfer, photoinduced radical reactions, stereoselective reactions, cycloadditions of aromatic compounds, reactions in photochemical continuous flow reactors and application of these reactions to organic synthesis. Further research interests concern the production of fine chemicals from biomass and the synthesis of new organic semiconductor materials for microelectronics (chemistry of perylene derivatives).

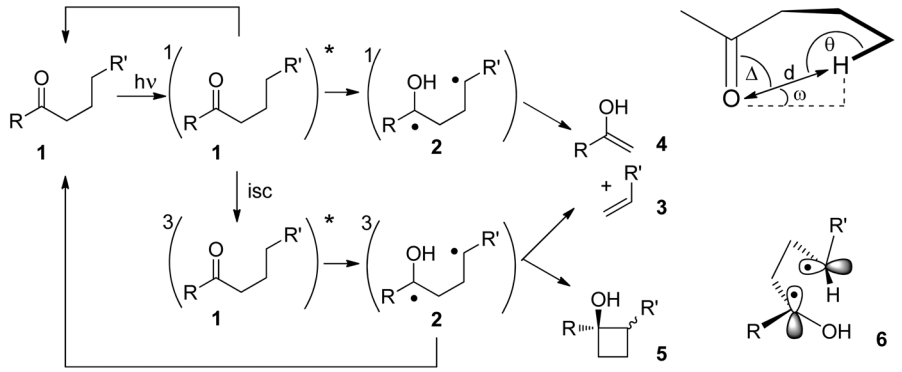

Scheme 1 Mechanism of the Norrish Type II reaction and the competing Yang cyclization.

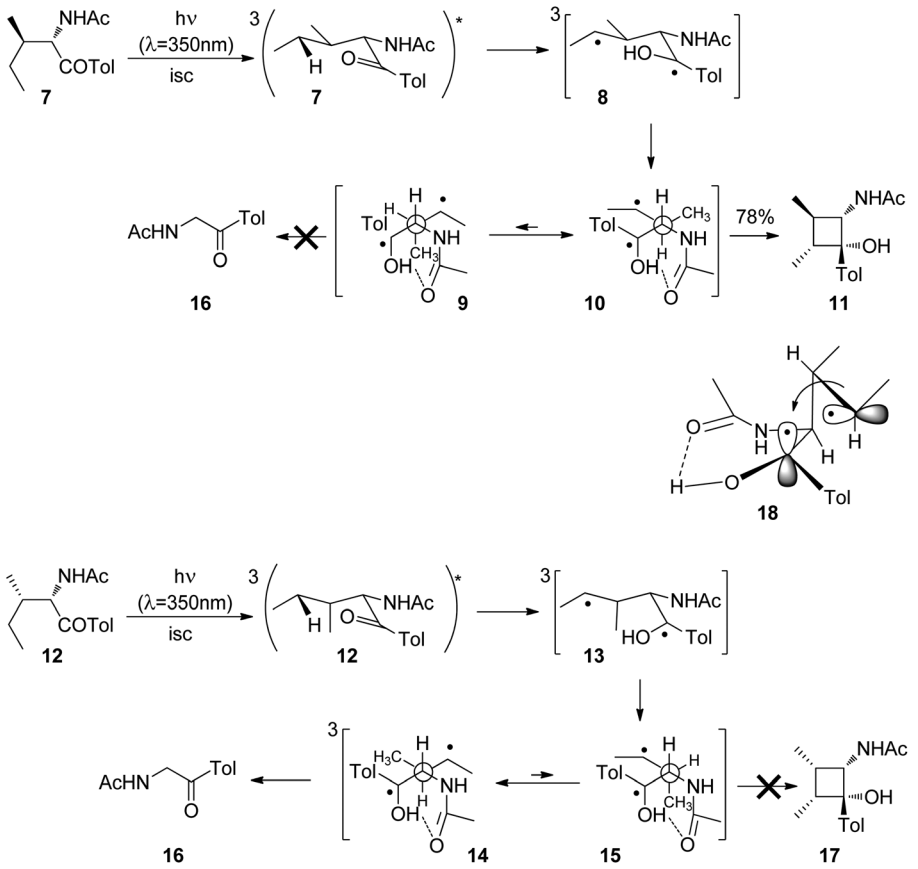

Scheme 2 Stereoselectivity of the Norrish Type II reaction and the competing Yang cyclization.

this reason, cyclization leading to the cyclobutanol derivative **11** is the only observed step. It must further be pointed out that a hydrogen bond between the newly formed hydroxyl function and the carbonyl group stabilizes these conformers. The corresponding diastereoisomer **12** after photochemical excitation, intersystem crossing and γ hydrogen abstraction is transformed into the 1,4-diradicals **13** with the main conformations **14** and **15**. The *anti* configuration of the methyl groups in the cyclobutanol derivative **11** is explained by the structure of the transition state **18** of the cyclization step. In this structure, the radical carrying orbitals are orthogonally orientated as a means to minimize steric hindrance and spin orbit coupling. In contrast to the previous case, the conformer **14** with *anti* orientation of the radical centers is more stable than the corresponding *syn* conformer **15**. The energy difference is 1.7 kcal mol^{-1}. In this case, exclusively, the fragmentation product **16** is formed. No corresponding cyclobutane product **17** was observed.

As already indicated, Yang cyclization has also been studied by irradiation of crystalline solids. In solution, conformational equilibria have a major influence on the competition between Norrish Type II fragmentation and Yang cyclization. The crystal lattice may also select and fix a conformation favoring the Yang cyclization thus inhibiting the fragmentation. High ee values are generally observed in photochemical reactions when they are performed with solids crystallizing in chiral space groups. In cases such as the present one, the crystal lattice selects conformations favorable for Yang cyclization in one enantiomeric form of the aromatic carboxylate. Photochemical reactions in chiral solids thus are an efficient method of asymmetric synthesis.[11,19]

Studies of such transformations in crystals also provide general and fundamental information on crystallography. The chiral salt of the aromatic keto acid **19** crystallized in space group $P2_12_12_1$. In these crystals, the oxygen of the carbonyl group is closer to H_x than to the enantiotopic H_y of the adamantane substituent (Scheme 3).[12,20] Upon irradiation, therefore, only the hydrogen atom H_x is abstracted and the diradical intermediate **20** is formed. Cyclization leads to the cyclobutanol **21**. Only this *endo* isomer is generated. Furthermore, this compound is obtained in high enantiomeric excess. It is particularly interesting to note that both the substrate **19** and the product **21** possess almost the same crystal structure (Fig. 1) in terms of space group, crystal system and cell constants. Thus, an X-ray crystal structure analysis of a mixed crystal containing 40% of the substrate **19** and 60% of the photoproduct **21** could be carried out.

The investigations of photochemical reactions in the solid state also enable a deeper understanding of how organic compounds crystallize depending on their structure. In a more detailed study, a large number of X-ray structure analyses were performed on single crystals containing substrate **19** and photoproduct **21** in different proportions (Fig. 2).[21] Although, the space group does not change when the conversion advances, the dimensions, in particular two cell constants of the orthorhombic crystal system vary (Fig. 3). During the first 20 min of the irradiation, the conversion rapidly advances and the percentage *P* of photoproduct increased until it reaches 80%. During this period, the value of cell constant *a* slightly

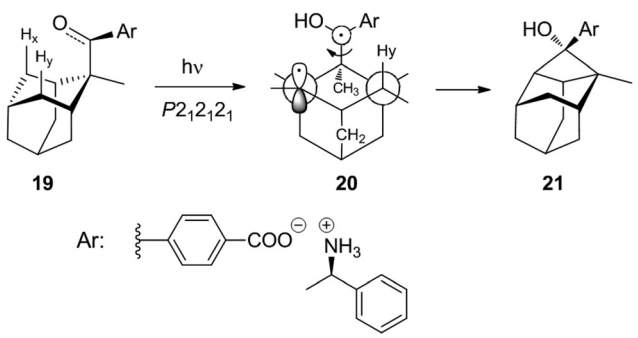

Scheme 3 Yang cyclization with an adamantane derivative in the solid state using a chiral salt for asymmetric induction.

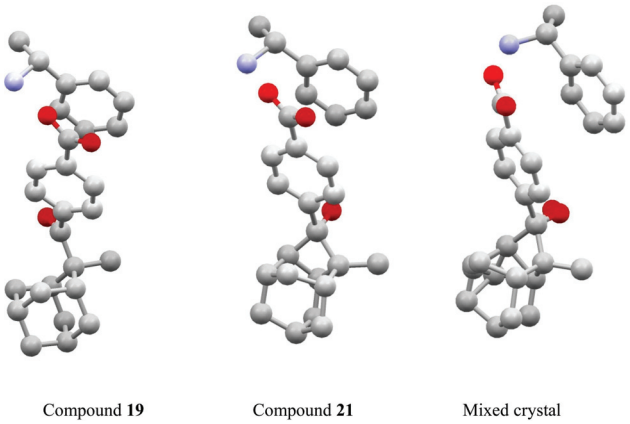

Fig. 1 Crystal structures during a Yang cyclization in enantiomorphous crystals.

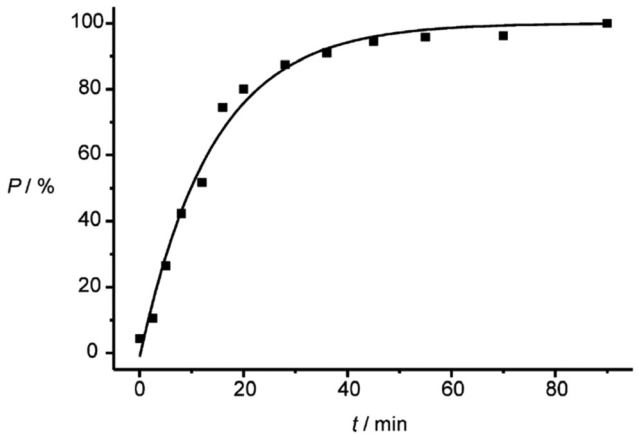

Fig. 2 Transformation of compound **19** into **21**. After 80% conversion, the reaction rate slows down. (Reprinted with permission from: I. Turowska-Tyrk, E. Trzop, J. R. Scheffer and S. Chen, *Acta Crystallogr., Sect. B: Struct. Sci.*, 2006, **62**, 128–134. DOI: 10.1107/S0108768105034014. Copyright (2006) IUCr.)

increases (Fig. 3(a)) while the value of constant *b* decreases (Fig. 3(b)). Cell constant *c* barely changes (Fig. 3(c)). During this period, the volume of the unit cell rapidly increases to a maximum of 2313 Å^3 (Fig. 3(d)). An additional 70 min of irradiation was necessary to complete the conversion. During this period, the changes of the cell constants *a* and *b* are much larger and the constant *c* decreases slightly. The cell volume drastically diminishes to reach a final value of about 2300 Å^3. All these changes are the result of the changes inside the cell which are monitored by atom distances as well as bond and dihedral angles. These parameters evolve in a very discontinuous manner. Some of them strongly change during the first period and remain constant during the final period of the conversion. Other parameters evolve in the opposite manner. Some parameters also change rapidly during the first period. They remain constant for the following period of conversion in order to evolve rapidly again at the end to attain their final values.

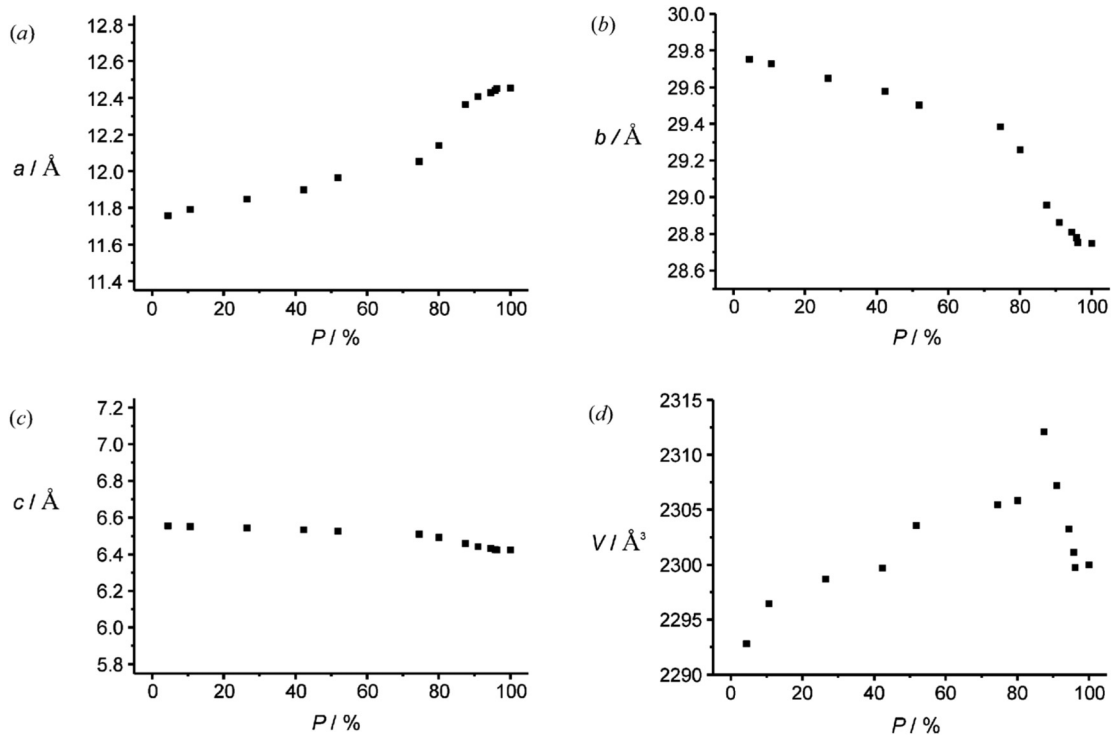

Fig. 3 Variation of cell constants during the transformation of compound **19** into **21**. (Reprinted with permission from: I. Turowska-Tyrk, E. Trzop, J. R. Scheffer and S. Chen, *Acta Crystallogr., Sect. B: Struct. Sci.*, 2006, **62**, 128–134. DOI: 10.1107/S0108768105034014. Copyright (2006) IUCr.)

Globally, the volume of the crystal structure increases because it must host a large variety of different molecular structures. In the anionic part, the adamantane moiety moves more than the remaining part since it is less engaged in hydrogen bonding. When the conversion comes to its end, the structure seems to collapse because the number of different molecular structures diminishes. Only the molecules of the final product need to be packed in a crystal structure. The final structural parameters of the cyclobutanol moiety are established during this period. Although the changes at the molecular level are very discontinuous, the changes of the cell parameter are nevertheless very ordered. Cell constant *a* increases, constant *b* decreases and cell constant *c* remains almost unchanged.

Crystal-to-crystal [4 + 4] photocycloadditions with anthracene moieties were used to synthesize regular two dimensional polymers.[22] In the present case, the crystal structures act as a template which orients three photoreactive centers of the monomers in the desired manner. These monomers possess D_{3h} or C_{3h} molecular symmetry. Thus layers are formed. Such polymers are of high interest, for example, in the domain of materials science as it has been frequently shown for the graphene prototype. Controlled two dimensional polymerization is particularly difficult.[23] The presented method provides access to a larger variety of such compounds. These results are also good examples for the use of particularly mild photochemical reaction conditions for the construction of supramolecular structures.

Several electron active substitutions on the tether separating the two radical positions may affect the competition between Norrish Type II fragmentation and Yang cyclization.[24] Such a competition has been observed in reactions of carbohydrate derivatives.[25] The presence of an additional ketone function in α-diketones generally favors the formation of hydroxycyclobutanones *via* Yang cyclization with respect to the Norrish Type II cleavage. Such structures are also of high interest for organic synthesis. For example, the glucose derivative **22** was efficiently transformed into the corresponding hydroxycyclobutanone derivative **23** (Scheme 4).[26] Only one anomer was obtained which was generated under retention of configuration. Furthermore, only one configuration was generated at the quaternary center carrying the hydroxyl function. The reaction was carried out with UV or sunlight with almost the same results. When the diketone moiety is placed in the former anomeric position of the glucose derivative **24**, a Norrish Type II reaction takes place.[27] After hydrogen abstraction in the γ position, in the resulting 1,4-diradical **25**, a C–O bond is cleaved. An enol and a ketone function are thus formed in the intermediate **26**. The final product **27** is then obtained by intramolecular aldol reaction followed by the formation of a half acetal.

Photochemically induced intramolecular hydrogen abstraction followed by cyclization may be carried out with a variety of chromophores.[24] Also macrocyclizations have been carried out.[28] Such reactions are valuable tools in organic synthesis. The photochemistry of α,β-unsaturated carbonyl or carboxyl

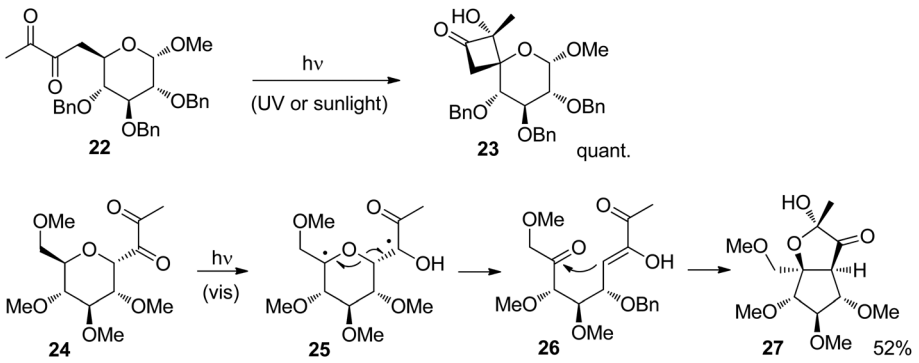

Scheme 4 Reactions similar to the Norrish Type II reaction and the Yang cyclization.

compounds resembles that one of the simple carbonyl compounds. Photochemical transformations of these compounds, particularly [2 + 2] photocycloadditions, were often applied to organic synthesis.[29] Most frequently, such reactions start at the $^3\pi\pi^*$ excited state which is the T_1 state. Intramolecular hydrogen abstraction may also occur at this electronically excited state.[30] Due to the high energy of the singlet state S_1,[31] such compounds are most frequently excited by sensitization, for instance by triplet energy transfer from acetone, when these reactions are applied to organic synthesis.

Such a reaction has been carried out with α,β-unsaturated lactones carrying a tetrahydropyranyl substituent on the site chain (Scheme 5).[32] Compounds **28a,b** are excited to their ππ* triplet state (**29**) by triplet energy transfer from the nπ* excited acetone. In this state, the π bond is suppressed and the spin density is particularly high in the β position (**29**).[33–35] For this reason, hydrogen abstraction occurs in this position and the diradical **30** is formed. Hydrogen is exclusively transferred from the anomeric center of the tetrahydropyranyl moiety. Radical combination leads to the final products **31a** and **31b** in a ratio of 1 : 1. When an alkyl substituent is present on the site chain between the tetrahydropyranyl and the furanone moiety as in compounds **32a,b**, only one spirocyclic product **33** was isolated possessing the *lk* relative configuration (*S**,*S**) at

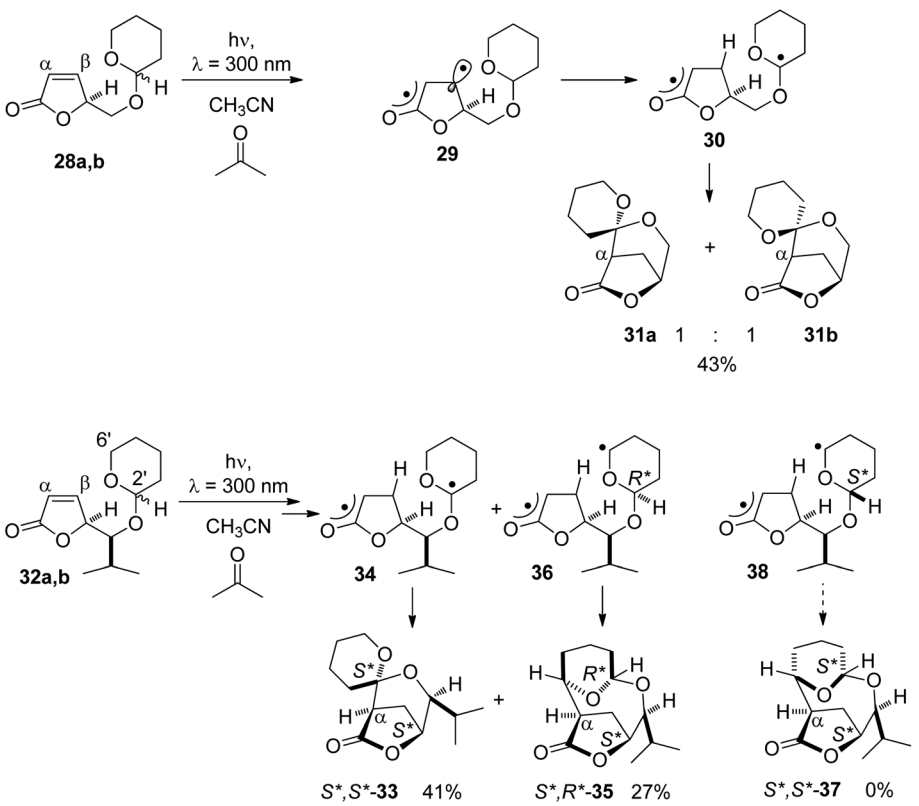

Scheme 5 Regio- and stereoselective hydrogen abstraction followed by radical cyclization in α,β-unsaturated lactones.

the anomeric center and the lactone ring. This results from hydrogen abstraction at the anomeric center (**34**) and radical combination. No stereoisomer possessing the *ul* relative configuration (*S**,*R**) was obtained. In the case of the substrate possessing the *ul* relative configuration (*S**,*R**), hydrogen abstraction also occurs in the 6′ position of the tetrahydropyranyl ring (**36**). Radical combination leads to the formation of the macrocyclic compound **35**. Product **37** resulting from a radical combination in intermediate **38** with a *lk* configuration (*S**,*S**) was not obtained.

The relative configuration at the tetrahydropyranyl (**39**) and the furanone moiety and the equilibrium between equatorial and axial conformations (Scheme 6) are the two structural elements which mainly control the regioselectivity of hydrogen abstraction. In order to determine the influence of each of these elements on the outcome of the reaction, the transformation was carried out with the glucose derivatives **40**, **41**, **42** and **43**. Due to the equatorial position of all further substituents in glucose derivatives, the equatorial (**40** and **41**) and axial orientations (**42** and **43**) at the anomeric center are locked.

Upon irradiation under sensitization conditions, compounds **40** and **42** possessing *R* configurations at the furanone moiety yielded the same spirocyclic compounds **44** and **45** in almost the same diastereomeric ratio (Scheme 7). These products result from hydrogen abstraction at the 1′ position, the anomeric center of the glucose moiety. The higher yield in the case of the transformation of the β anomer **42** is explained by the fact that hydrogen abstraction at the anomeric center is easier than in **40**.[36] When compound **43** possessing an *S* configuration at the furanone moiety and α-configuration at the sugar part was transformed, only the macrocyclic compound **46** was isolated in good yield. This product results from hydrogen abstraction at the 5′ position of the glucosyl substituent. When the corresponding β-anomer **41** was transformed under the same conditions, again spirocyclic compounds **47** and **48** were isolated. Moreover, the macrocyclic compound **46** was also formed. The latter compound can only be formed when an epimerization at the anomeric center takes place during the transformation. Studies on reactions with partial conversion confirmed this hypothesis. This epimerization is also photochemically induced.

All detected mechanistic steps of these reactions are present in the transformation of compound **41** (Scheme 8). After excitation and hydrogen abstraction, the intermediates **49a** and **49b** are generated. They are in equilibrium. Radical combination in the intermediates leads to the formation of the spirocyclic compounds **47** and **48**. In the case of the diradical intermediate **49b**, hydrogen transfer from the lactone moiety back to the glucosyl moiety may occur leading to the formation of the α-anomeric compound **43**. This compound was indeed detected in considerable amounts in the reaction mixture of **41** after 50% of conversion. As previously shown, under the same conditions *via* hydrogen abstraction in the 5′ position (**50**), compound **43** reacts selectively to yield the macrocyclic compound **46**. It must be pointed out that significant parts of this mechanism have been evidenced by a stereochemical analysis.

In order to get a deeper insight into the stereochemical requirements for hydrogen abstraction, DFT calculations have been carried out. The $^3\pi\pi^*$ excited and vibrationally relaxed state has been modeled with structure **51** (Scheme 9). Transition states for hydrogen abstraction in positions 2′ (acetal center) and 6′ have been calculated. Due to different nomenclature systems, the positions 2′ and 6′ of these tetrahydropyranyl structures correspond in glucose derivatives to the positions 1′ and 5′ respectively. Table 1 reports the calculated differences in the free enthalpy of activation for hydrogen abstraction in positions 2′ and 6′ in model structure **51**. These results confirm the experimental observation that in the case of **40** and **42** (*R* configuration at the furanone moiety, Scheme 9, model structures **51a,b**, Table 1), hydrogen abstraction is favored at the anomeric center **52** (Scheme 9). In the case of the model structure **51c,d** corresponding to the *S* configuration at the furanone moiety, only in the electronically excited α-anomer (**51c**), hydrogen abstraction in the 6′ position (**53**) is favored. Thus the computational results reproduce the experimental observations for the transformation of the glucosyl compounds **40**, **41**, **42** and **43** (Schemes 6 and 7). In particular

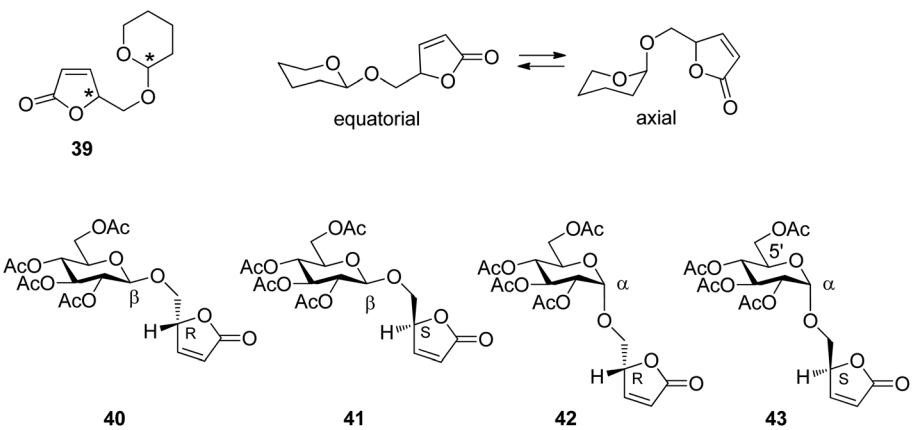

Scheme 6 Stereochemical elements in α,β-unsaturated lactone derivatives and the corresponding glucosyl compounds.

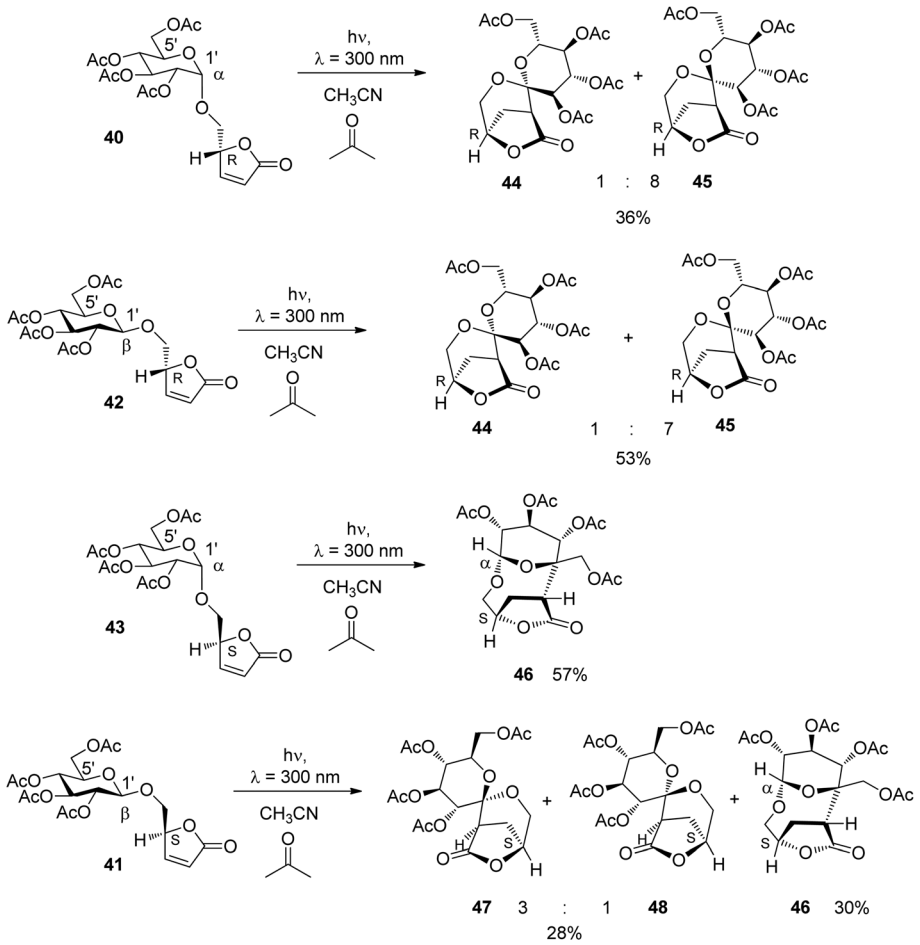

Scheme 7 Stereoselective triplet sensitized transformation of α,β-unsaturated lactone derivatives.

the high spin density in the β-position of the $^3\pi\pi^*$ excited and vibrationally relaxed state as modeled by structure **51** is essential for the observed regio- and stereoselectivity of the hydrogen abstraction step. Similar studies have been performed for the reaction of compounds **32a,b** (Scheme 5). These reactions have also been discussed in the more general context of hydrogen transfer.[32,37] The fact that the proton and the electron are transferred simultaneously leads to the formation of a C–C bond in the α position of the α,β-unsaturated lactone. A two-step mechanism (electron transfer followed by proton transfer) would have led to the formation of a C–C bond in the β position.

In such reactions, the phenomenon of the spin-center shift[38] is also observed. After photochemical excitation of the acetophenone derivative **54** hydrogen abstraction occurs in one of the diastereotopic γ positions leading to the diradical intermediates *R*-**55** and *S*-**55** (Scheme 10).[39] In contrast to the previously described reactions, in this case, the tosyl group in the α position is eliminated and the radical position is shifted in this position leading to the 1,3-diradical intermediates *R*-**56** and *S*-**56**. Radical combination generates the bicyclic final products *R*-**57** and *S*-**57**. The enantioselectivity of the overall reaction is mainly determined when the 1,4-diradical intermediates *R*-**55** and *S*-**55** are formed. The competition between hydrogen abstractions in the two diastereotopic γ positions depends on a ratio between conformers in an equilibrium. The enantioselectivity depends on the solvent and the reaction temperature. The latter is particularly interesting. When the reaction was carried out in methanol, the enantioselectivity decreases when the reaction temperature is diminished. When the reaction was carried out in methylene chloride, the ratio between *R*-**57** and *S*-**57** was 2.5 : 1 at −40 °C while it was 1 : 2.5 at −56 °C. Although often considered as unusual, such behavior is frequently observed.[40] From Eyring diagrams such as the one depicted in Fig. 4, enthalpy and entropy effects are deduced. An extensive discussion in this context has been performed, for example, in the context of the diastereoselective [2 + 2] photocycloaddition.[35] For an example of a photooxygenation see below.

Similar reactions have been carried out with aromatic ketones or aldehydes. The reaction depicted in Scheme 11 [41,42] can be carried out with numerous derivatives. After photochemical excitation of the benzophenone derivative **58** and intersystem crossing (isc), the triplet diradical intermediate **59** is generated by intramolecular hydrogen abstraction. The dienol

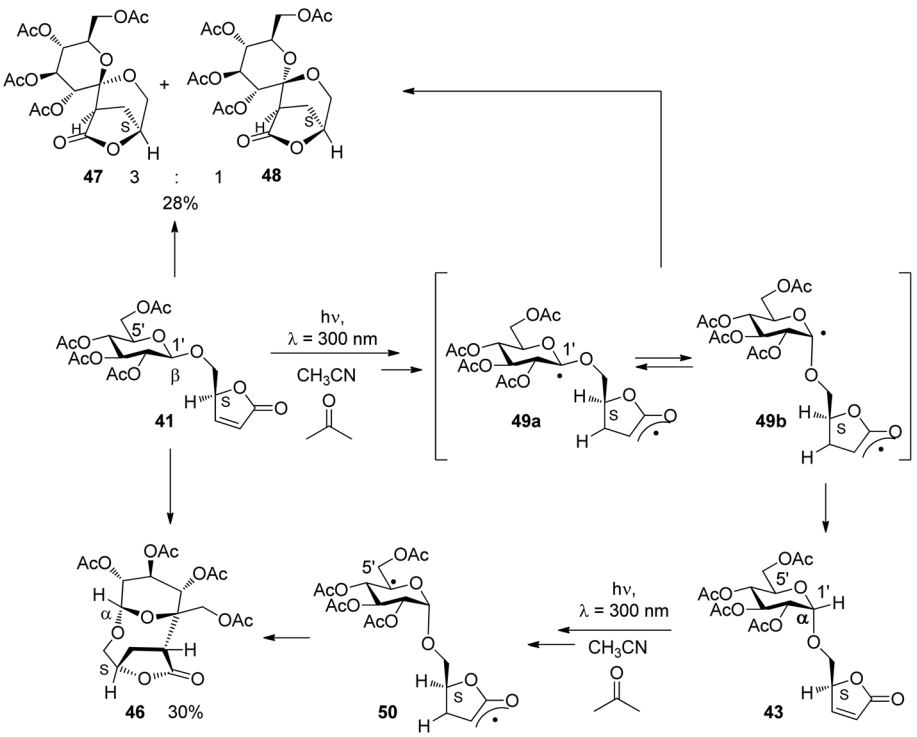

Scheme 8 Radical steps in the stereoselective triplet sensitized reaction of α,β-unsaturated lactone derivatives.

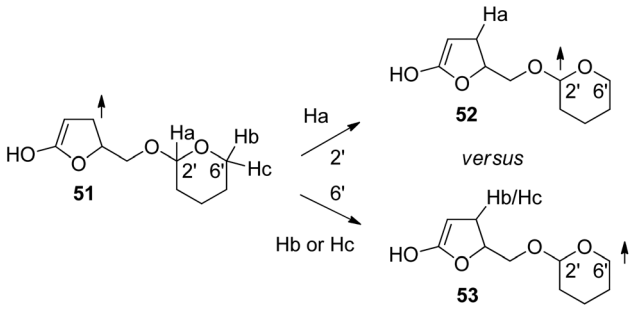

Scheme 9 Model structures for the computational study of regio- and stereoselective hydrogen abstraction in the triplet sensitized reaction of α,β-unsaturated lactone derivatives.

species **60** is then formed. Both intermediates **59** and **60** may be considered as the triplet and the singlet form, respectively, of one species, the photochemically generated enol tautomer. Intermediate **60** is placed on the singlet ground state potential energy surface. It easily undergoes [4 + 2] cycloaddition with alkenes such as **61**. The final product **62** was obtained in high yields in a stereospecific manner which is typical for a Diels–Alder reaction at the ground state. This reaction was frequently applied to the synthesis of organic compounds such as natural and other biologically active compounds or organic materials.[43] Similar reactions also play an important role in the photochemical removal of protecting groups.[44] Intermediates such as **60** are also called phototautomers.[42,45–47] Concerning the stability of tautomers, a complementary tendency between the ground state and electronic state is generally observed.[48,49] Tautomers which are less stable at the ground state can be generated *via* photochemical excitation. In this context, photochemically generated achiral enols have been transformed into the corresponding chiral ketone forms using asymmetric catalysis.[50] The determination of the enantioselectivity as a function of temperature was used to determine the influence of enthalpy and entropy on the stereoselectivity in such reactions.[51]

Table 1 Calculated energy differences for competing hydrogen abstraction in positions 2′ and 6′ (Scheme 9)

Compound	Configuration at the furanone moiety	Configuration at the anomeric center	Corresponding relative configuration of **51**	$\Delta\Delta G^{\neq a}$ (kcal mol^{-1})
51a	*R**	α	*lk*	−2
51b	*R**	β	*ul*	−13
51c	*S**	α	*ul*	0.1
51d	*S**	β	*lk*	[b]

[a] $\Delta\Delta G^{\neq} = \Delta G^{\neq}$ (position 2′) − $\Delta G^{\neq}$ (position 6′). [b] No value for $\Delta G^{\neq}$ (position 6′) reported.

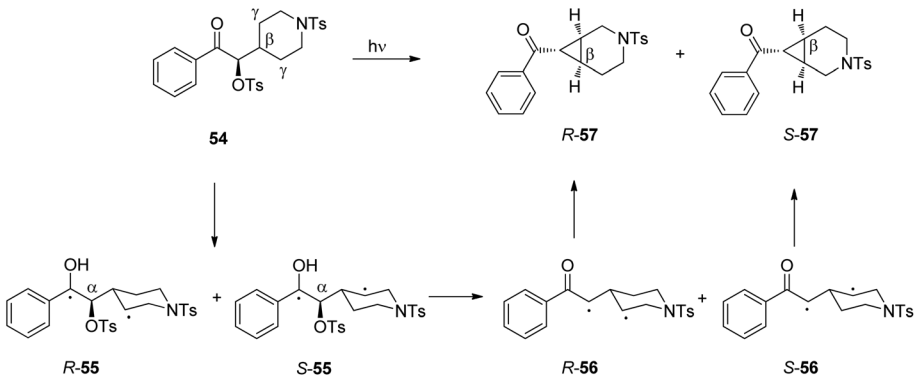

Scheme 10 Intramolecular stereoselective hydrogen abstraction involving a spin-center shift followed by cyclization.

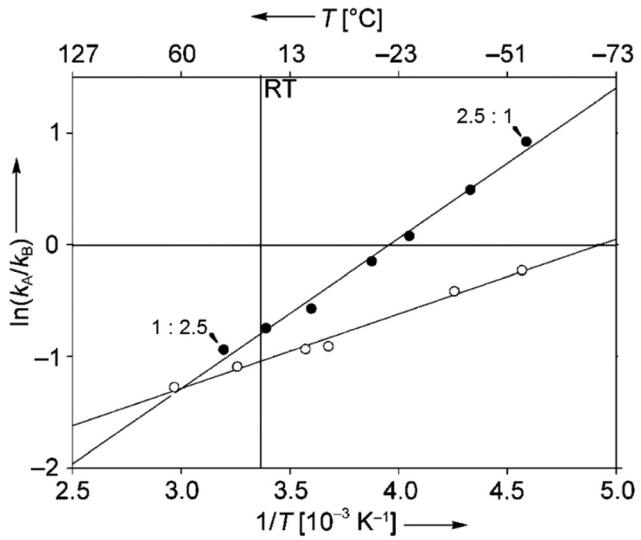

Fig. 4 Stereoselective hydrogen abstraction involving a spin-center shift (Scheme 10). Enantioselective formation of bicyclic derivatives *R*-**57** and *S*-**57**. k_A: overall rate of the formation of *R*-**57**, k_B: overall rate of the formation of *S*-**57**, ● CH_2Cl_2, ○ MeOH as the solvent. RT: room temperature. (Adapted with permission from: P. Wessig and O. Muehling, *Chem. – Eur. J.*, 2008, **14**, 7951–7960. Copyright (2008) John Wiley & Sons.)

Anthranilic acid derivatives have been transformed in a similar manner. A typical example is depicted in Scheme 12.[52] In the intramolecular photochemical reaction of compound **63**, the cycloaddition product **64** resulting from the [4 + 2] photocycloaddition and product **65** resulting from a [4 + 4] cycloaddition are formed. The formation of the latter compound indicates that the reaction mechanism is different from the one suggested in Scheme 11 for the transformation of a similar benzophenone derivative. In contrast to the [4 + 2] cycloaddition, a concerted [4 + 4] cycloaddition at the singlet ground state is forbidden according to the Woodward–Hoffmann rules.[53] In order to get a deeper insight into the mechanism, intensive photo-physical and theoretical studies have been carried out.[54] Based on the results the following mechanism has been suggested (Scheme 13). After photochemical excitation of **66**, a proton is transferred to the S_1 state and the corresponding imine–enol **67** is formed. Intersystem crossing (isc) occurs and the triplet diradical **68** is formed. This intermediate possesses lifetimes in the range of $\tau \approx$ 5.2–5.7 ns which is long enough to enable intramolecular trapping. The highly reactive nitrogen centered radical adds to the furan moiety which leads to the diradical intermediate **69**. Radical combination occurs in two competitive ways. Pathway a generates the major compound **70** (formal [4 + 2] cycloaddition) while pathway b leads to the minor product **71** (formal [4 + 4] cycloaddition). Depending on structural variation in the substrates, the corresponding triplet diradical intermediates of type **68** undergo typical side reactions such as trapping with triplet oxygen or intramolecular hydrogen abstraction. The isc step plays an important role in the outcome of the reaction. The influence of the substitution pattern in **66** on the quantum yield of the photocyclization has been discussed in this manner (Table 2). When a bromine atom is added the quantum yield considerably increased (entries 2 and 3). Thus the introduction of bromine in position 5 (entry 2) leads to the highest value measured in this series of substrates. This effect was explained by a higher spin orbit coupling (SOC) due to a heavy atom effect. The significantly stronger effect in the case of a substitution in position 5 (entry 2) when compared to the substitution in position 4 (entry 3) was explained by the higher spin density on the bromine atom in position 5 of the corresponding intermediate **68**. The spin densities have been determined by DFT calculations. As shown in the case of chlorine substitution (entry 4), electronegative atoms in the 5 position have also a favorable effect since they diminish the stability of the nitrogen centered radical in the intermediate **68**. Concomitantly, its reactivity is increased. However, the effect of SOC on a more efficient isc is stronger in the case of chlorine. The SOC is also influenced by the rotation of the hydroxyl alkyl radical position in intermediate **68**. It should further be noted that the quantum yield also depends on the R substituent. This should be small in the case of cyclic (tetralone) derivatives. A significant decrease of the quantum yield is also observed when hydrogen is replaced by a methyl group (entry 5).

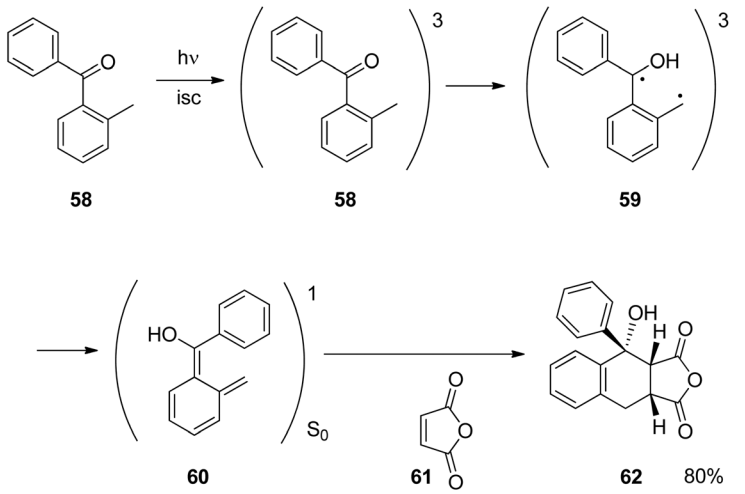

Scheme 11 Trapping of a photodienol by a [4 + 2] cycloaddition.

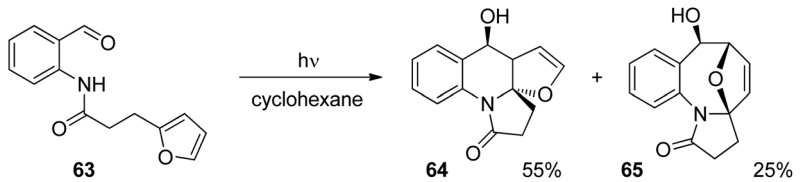

Scheme 12 Intramolecular photocycloaddition with an anthranilic acid derivative.

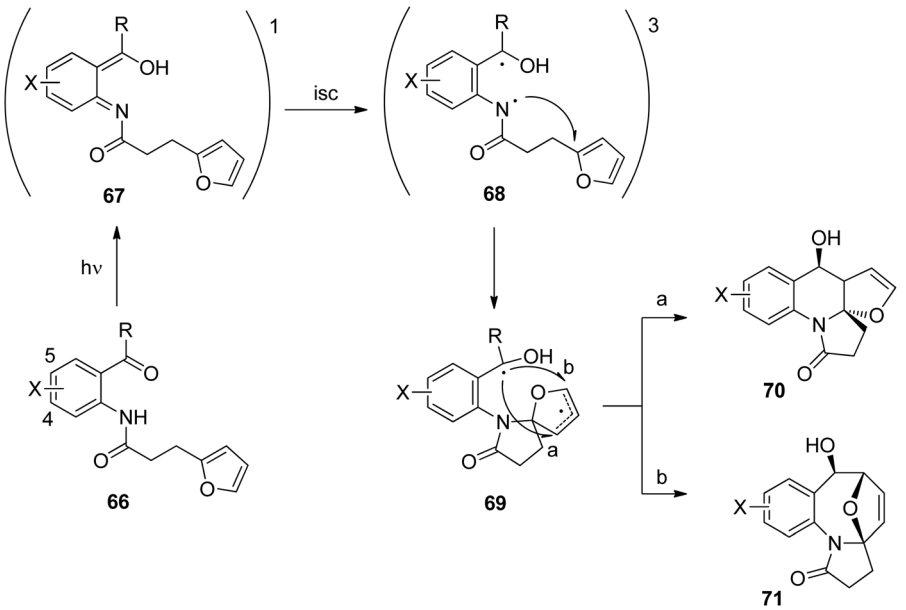

Scheme 13 Mechanism of the intramolecular photocycloaddition with an anthranilic acid derivative.

These photochemical reactions are now intensively investigated in the context of diversity oriented synthesis.[55] They provide an access to compound families which are not available or difficult to achieve by more conventional ground state reactions. The previous examples also nicely illustrate how the change of the addition of functional groups on the

Table 2 Quantum yields for photocyclization of compound **66** (Scheme 13)

Entry	Compound **66**	Quantum yield (Φ) of photocyclization
1	X = H, R = H	0.18
2	X = 5-Br, R = H	0.75
3	X = 4-Br, R = H	0.22
4	X = 5-Cl, R = H	0.32
5	X = H, R = Me	0.058

side chain of an acetophenone moiety modifies the reaction pathways and thus yield products of new compound families. Recently, this has been demonstrated for the transformation of epoxides.[56] The photochemical generation of radical species followed by hydrogen abstraction is also used for pharmaceutical applications such as cancer therapy. A typical example is the photo-Bergman reaction and related processes.[57]

3 Photochemical heterolytic cleavage – the structure and the reaction of aryl cations

Phenyl cations possess low stability. Only recently, the parent compound was generated and its reactivity was studied in cryogenic argon matrices.[58] When substituted with electron donor groups such compounds become more stable. They are generated from the corresponding halogen derivatives (**72**) by photolysis and can act as intermediates in photochemical reactions (Scheme 14).[59,60] The phenyl cation species possess singlet (**73**) or triplet spin multiplicity (**74**). Upon direct excitation by light absorption, the singlet state **73** is generated after release of the Cl^- ion. For phenyl cations possessing strong electron donor substituents such as amino functions, the triplet energy is generally lower. Thus the triplet state **74** is generated by intersystem crossing. In the case of the presence of weaker electron donors such as **75** the singlet state is less energetic (Fig. 5).[61] Nevertheless, some typical structural parameters for each spin multiplicity remain comparable. Thus the angle ∠(C3–C4–C5) for the singlet state (**75**) is larger than for the triplet state (**76**). In the first case, the partial structure is ketene-like while in the second case, it resembles a carbene.[62]

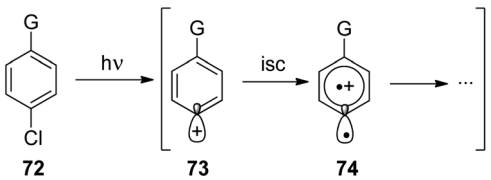

Scheme 14 Generation and structure of phenyl cation derivatives.

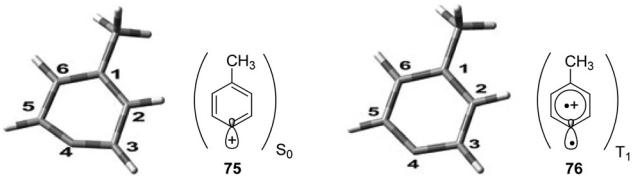

Fig. 5 Calculated structures for the singlet and the triplet state of the phenyl cation **75**, **76**. $E(T_1)$–$E(S_0)$ = 13.99 kcal mol^{-1}. Angle ∠(C3–C4–C5) = 147° for the S_0 and ∠(C3–C4–C5) = 127° for the T_1 state. (Adapted with permission from: H. Qrareya, C. Raviola, S. Protti, M. Fagnoni and A. Albini, *J. Org. Chem.*, 2013, **78**, 6016–6024. Copyright (2013) American Chemical Society.)

Various computational studies have been carried out on these structures.[63]

The phenyl cations easily react with a variety of nucleophilic species. In the case of a *p*-(*N*,*N*-dimethylamino)phenyl cation at the singlet state and the triplet state, rates for the reaction with different nucleophiles were determined.[64] The results have been discussed with the aid of Mayr's parameters for nucleophilicity and electrophilicity.[65]

The addition of such phenyl cations to nucleophilic species is of great interest in organic chemistry. The reaction of compound **77** with the pyrrole derivative **78** leading to the coupling product **79** resembles a Suzuki Miyaura reaction (Scheme 15).[66] However no palladium catalysis is needed. Furthermore, no borate substrates are involved which considerably facilitates the transformation. Only minor amounts of side products **80** and **81** are formed. The transformation of **82** with **83** resembles a Sonogashira reaction. Again the corresponding product **84** is formed avoiding any metal catalysis.[59] Various other nucleophiles have been successfully transformed under similar conditions. Thus the allyl silane compound **85** reacts with chloroanisole **86** (R = Me) yielding **87**.[67] Interestingly, the unprotected chlorophenol **86** (R = H) was also efficiently transformed and the corresponding products **87** were obtained in high yields. Enol ethers such as **88** were transformed into **89** without any Lewis acid catalysis. The resulting ketone **90** was isolated in high yields.[68] Reactions with alkenes possessing further functional groups such as 4-pentenoic acid **91** were successfully transformed, for example with chlorophenol **92**.[69] In an intramolecular trapping reaction, a butyrolactone derivative **93** is formed. It should be pointed out that this reaction was also carried out with phenol or aniline derivatives possessing other leaving groups such as chlorine. Thus triflates, phosphates or mesylates were transformed.

4 [2 + 2] Photocycloadditions

The photochemical reaction between carbonyl compounds and alkenes is certainly the most versatile method for the syn-

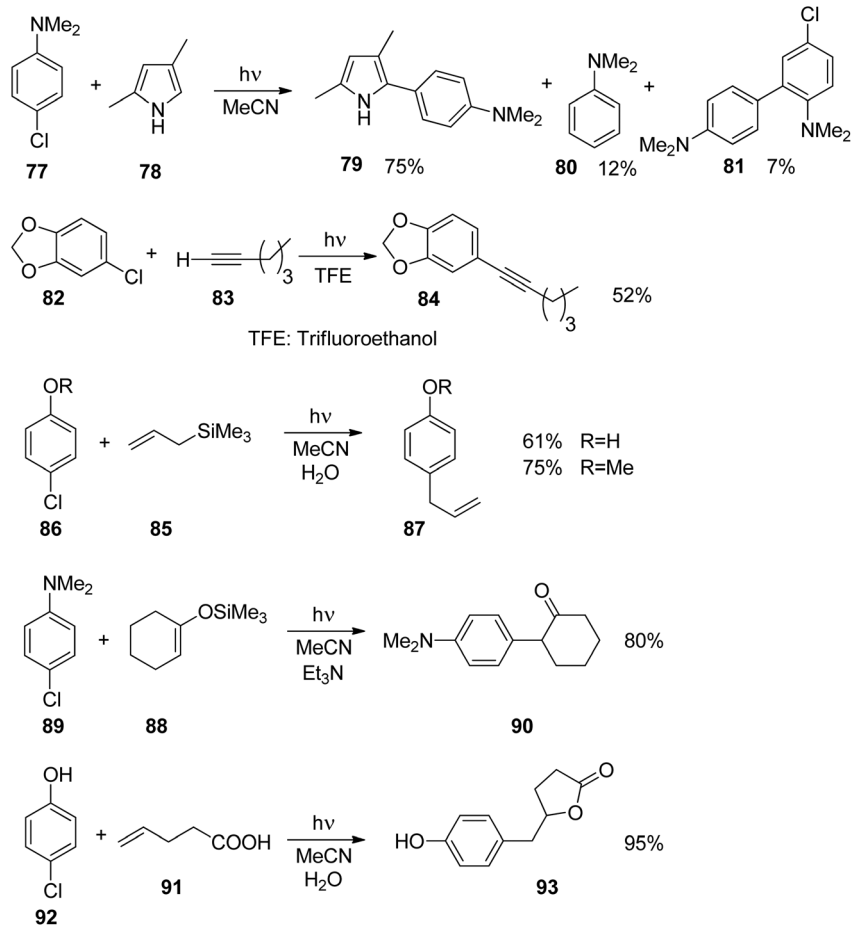

Scheme 15 Reactions involving phenyl cations with various nucleophilic species.

thesis of oxetanes.[70–72] These small heterocycles are encountered in some natural products. But they are also interesting synthesis intermediates. The generally accepted mechanism in most of these reactions is depicted in Scheme 16.[72,73] The reactions start with the excitation of the carbonyl compound **94** to the nπ* state. The Paternò–Büchi reaction may take place at the singlet state or the triplet state.[74] In the first case, the excited carbonyl function is added to the alkene leading to the formation of the biradical intermediate **95**. In the case of a triplet reaction, intersystem crossing (isc) takes place. This step is particularly fast in the case of aromatic compounds such as benzaldehyde or benzophenone ($k_{isc} \sim 10^{11}$ s^{-1}). Therefore, many of the chemical reactions start at the triplet state. The reaction with an alkene generates a 1,4-diradical intermediate **95** by the formation of a C–O bond. In order to get the final product at its singlet ground state, intersystem crossing must take place. Radical combination leads to the oxetanes **96**. Alternatively, the diradical **95** may generate the starting products. It must be pointed out that the second isc and the formation of the oxetane **96** or the formation of the starting products by cleavage of the newly formed C–O bond are strongly coupled (see below). Depending on the redox potentials of the substrates, photochemical electron transfer may also occur which leads to a radical ion pair **97**. In this case, the oxetane **96** is formed preferentially *via* the singlet diradical intermediates **95** or is directly generated. In such reactions the intermediate possesses zwitterionic character.[75,76] Unsaturated alcohols **98** are typical competitive products of this mechanism involving electron transfer. In this case, a C–C bond may also be formed. The two reaction pathways, involving electron transfer or not, have a different impact on the regioselectivity of the reaction.[77]

When electronically excited, the polarity of the carbonyl group is inversed with respect to the ground state. Thus the carbonyl oxygen becomes electrophilic and attacks an alkene at its most nucleophilic side. Therefore, the oxetanes **99a,b** are the only products isolated from the reaction of dihydrofuran **100** with benzaldehyde **101** (Scheme 17).[78] No electron transfer is involved in the formation of this isomer.[79] The formation of a solvent separated ion pair is endothermic (ΔG_{et} = +0.62 eV). The regioselectivity is again inversed when electron transfer is involved[76] as in the case of the transformation of benzaldehyde **101** with the more electron rich dihydrofuran derivative **102** possessing a ketenacetal moiety (Scheme 17).[80] A

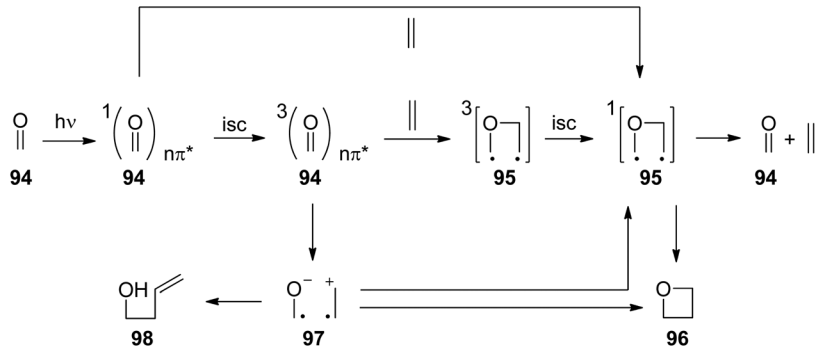

Scheme 16 Mechanism of the Paternò–Büchi reaction.

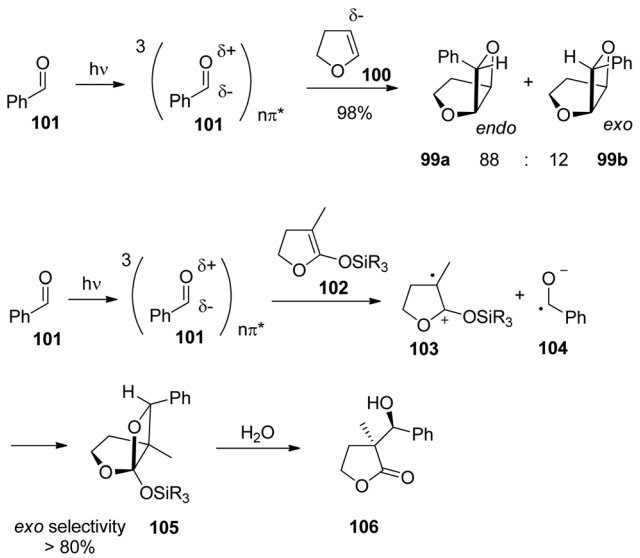

Scheme 17 Regioselectivity of the Paternò–Büchi reaction.

radical ion pair **103** and **104** is formed. This reaction step is exothermic by $\Delta G_{et} \sim -0.3$ eV (compare ref. 77). In the radical cation **103**, the positive charge is essentially localized on the carbon atom carrying the two oxygen atoms. This polarity determines the regioselective formation of product **105**. This orthoester is easily transformed into the butyrolactone derivative **106** by hydrolysis. It must further be pointed out that in the reaction of dihydrofuran **100**, the formation of the *endo* isomer **99a** is favored while in the case of the transformation of compound **102**, the thermodynamically favored *exo* diastereomer **105** is mainly formed. Concerning the understanding of the diastereoselection in the Paternò–Büchi reaction a lot of investigations have been carried out. Thus it has been evidenced that the 1,4-diradical intermediate **95** (Scheme 16) plays a key role in the diastereoselectivity of the reaction of α-ketoesters carrying a chiral auxiliary. The competition between the cyclization on the one hand and the formation of the starting materials (ketone and alkene) on the other hand contributes to the diastereoselectivity.[51,81] By measuring the temperature dependence of the stereoselectivity the contribution of the enthalpy and the entropy to the activation free enthalpy of each of the two steps have been determined and discussed.

The herein reported Paternò–Büchi reactions have been carried out with electron rich alkenes. The reaction was also carried out with carbonyl compounds at the S_1 state and electron deficient alkenes. In this case, an interaction between the alkene π system and the π* orbital of the carbonyl compound was discussed.[82] In such an interaction, the nπ* excited carbonyl function acts a nucleophile. In this context, an amphoteric nature was attributed to the excited carbonyl group.

The *exo*/*endo* selectivity was also investigated in detail. When derivatives of benzaldehyde **107** were transformed with dihydrofuran **100** the *endo* isomers of the oxetanes were formed in excess (Table 3 and Scheme 18) and high yields.[15,78,83] The *endo* isomers **108** are less stable than the corresponding *exo* isomers **109** due to their higher steric hindrance. By increasing the steric encumbrance by increasing the size of *R*, one should expect that *endo*/*exo* ratio is reduced. However, the opposite effect is observed. By increasing the size of this substituent (going from entry 1 to entry 3 in Table 3), the *endo*/*exo* selectivity is even improved while the product yield remains high. Increased steric hindrance on the olefinic reaction partner only slightly affects this selectivity.[84] In contrast, the corresponding naphthalene derivatives **113** yielded the *exo* isomers **114** selectively (entries 4 and 5). Unlike the benzaldehyde derivatives, the naphthylaldehydes react at the singlet state yielding the thermodynamically more stable *exo* products. In the triplet reaction, 1,4-diradicals such as **110**, **111** or **112** are formed themselves possessing triplet multiplicity also. In order to obtain the final products **108** or **109**,

Table 3 *endo*-Selective Paternò–Büchi reaction of aromatic aldehydes **106** and **113** with dihydrofuran **100** (Scheme 18)

Entry	R	*endo* : *exo*	Yield (%)
1	Phenyl	88 : 12	98
2	*o*-Tolyl	93 : 7	97
3	Mesityl	>98 : 2	90
4	1-Naphthyl	<2 : 98	55
5	2-Naphthyl	<2 : 98	87

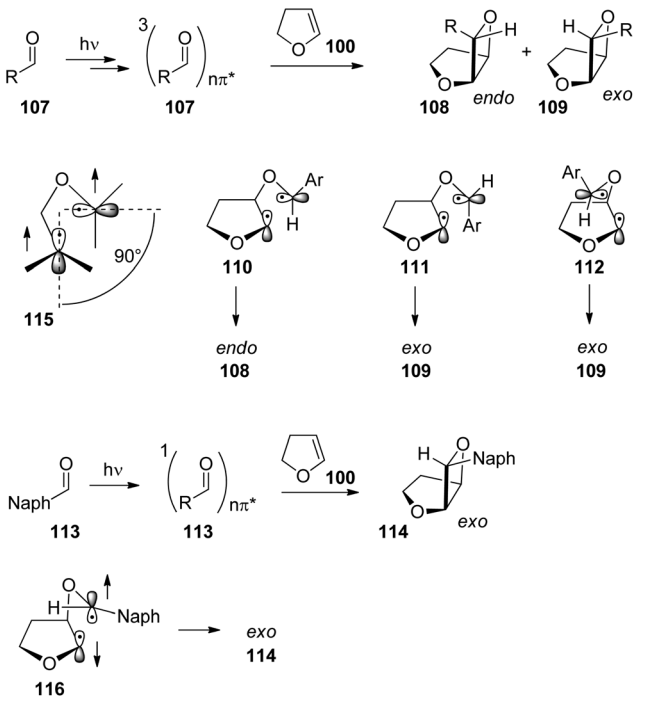

Scheme 18 Mechanisms of the *exo*/*endo* stereoselection in the Paternò–Büchi reaction.

an intersystem crossing must take place (Scheme 18). As discussed in the previous section on the Norrish–Yang reaction this process is favored by a strong spin orbit coupling.[14] Spin orbit coupling in such intermediates is increased when the two p orbitals carrying the unpaired electrons are orthogonally orientated (**115**). Among numerous possibilities, the three conformations **110**, **111** and **112** are significant. Due to low steric hindrance, conformer **110** is dominant in the conformational equilibrium. Cyclization leads to the formation of the thermodynamically disfavored *endo* product **108**. Cyclization of conformers **111** and **112** in which the two p orbitals carrying the unpaired electrons are also orthogonally orientated would lead to the *exo* products **109**. By increasing the steric hindrance by modification of the phenyl substituent R, the dominance of conformer **110** in the equilibrium is enhanced and therefore the formation of the *endo* portion of product **108** is increased. In the case of the transformation of the naphthylaldehydes **113** which react at the singlet excited state, the corresponding diradical intermediate **116** can react immediately. No change of the spin multiplicity is required. The cyclization step occurs at the conformation **116** in which the naphthyl substituent is placed in the sterically favored *exo* position. It should further be pointed out that the product yields are lower. The triplet multiplicity is advantageous for the Paternò–Büchi reaction. A detailed analysis of conformational equilibria and spin orbit coupling in these Paternò–Büchi 1,4-diradicals using high level *ab initio* methods has been recently performed.[85]

In the case of aliphatic aldehydes such as propionaldehyde **117** the *endo*/*exo* selectivity depends on the concentration of the alkene (dihydrofuran **100**) in the reaction mixture (Scheme 19 and Fig. 6).[16,86] At low concentrations, the *endo* product **118** is mainly formed while at higher concentrations both products are obtained in almost equal amounts. Obviously, singlet and triplet diradical intermediates are generated. The triplet diradicals are formed in a unimolecular process with k_{isc} ranging from 10^9 to 10^{12} s^{-1}. Thus diffusion has an influence on the competitive bimolecular formation of singlet or triplet diradicals. The fluorescence quenching rate of propionaldehyde **117** by dihydrofuran **100** is $k_q = 2.2 \times 10^9$ M^{-1} s^{-1} with a corresponding lifetime $\tau(S_1) = 1.8 \times 10^{-9}$ s.[87] In the case of high concentrations, singlet diradicals are generated leading to low *endo*/*exo* selectivity while at low alkene concentration, unimolecular inter system crossing is faster and **117** is transformed only at its triplet state in a bimolecular reaction with **100**. In the latter case, the thermodynamically disfavored product **118** was formed in large excess. A more detailed kinetic evaluation of the plot in Fig. 6 revealed that at a concentration of 0.05 M of alkene **100**, almost equal amounts of singlet and triplet excited propionaldehyde molecules are trapped in the bimolecular reaction leading to an *endo*/*exo* ratio of about 68 to 32. It must be pointed out that the transformation of benzaldehyde **101** with **100** under the same conditions (compare Scheme 18 and Table 3) yielded the corresponding *endo*/*exo* isomers with ratios around 88 : 12 regardless of the concentration of the alkene **100**. Aromatic aldehydes generally possess low singlet lifetimes and particularly high values of k_{isc} so that only triplet species of the carbonyl compound are trapped in the bimolecular reaction. The viscosity of the reaction mixture also has an influence on the *endo*/*exo* selectivity. At higher viscosity, diffusion and consequently the bimolecular trapping of the excited carbonyl species are slowed down. The formation of *endo* isomers resulting from triplet diradicals is thus favored.[87]

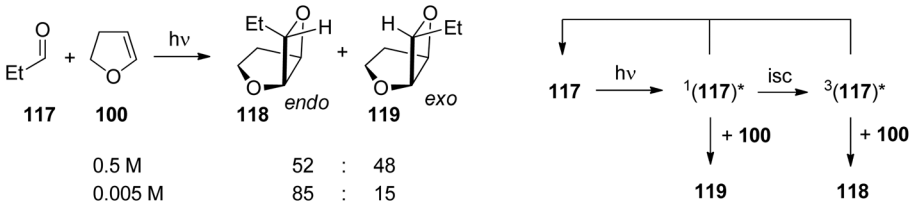

Scheme 19 Concentration dependence of the *exo*/*endo*-selectivity of the Paternò–Büchi reaction on aliphatic ketones.

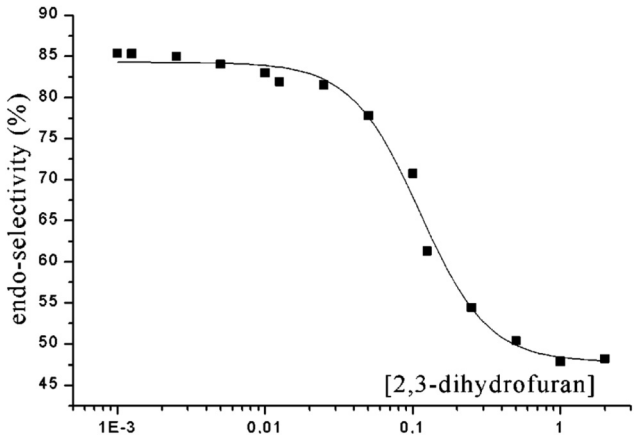

Fig. 6 Dependence of the *endo*/*exo* selectivity (ratio of *endo* to *exo* isomers) in the reaction of **117** with 2,3-dihydrofuran **100** on the concentration of **100** (compare Scheme 19). (Adapted with permission from: A. G. Griesbeck, M. Fiege, S. Bondock and M. S. Gudipati, *Org. Lett.*, 2000, **2**, 3623–3625. Copyright (2000) American Chemical Society.)

The viscosity is also influenced by the temperature. Thus it was possible to change from a singlet reaction in a reaction medium with low viscosity and favored formation of the *exo* isomer to a triplet reaction in the same reaction medium with high viscosity and favored formation of the *endo* isomer by decreasing the temperature. Therefore, at a particular temperature, a sudden change of the temperature dependence of the *endo*/*exo* selectivity occurs. Nonlinear Eyring plots are observed. Such a phenomenon has frequently been observed in stereoselective reactions.[16,51] In the present case, it is related to a change in mechanism induced by the reaction medium.[88,89] Often such changes of selectivities in chemical reactions depending on the temperature are linked to enthalpy–entropy compensation.[89,90]

Nonlinear Eyring plots are also observed for the regioselectivity of benzophenone with methylfuran.[91] Two cases are discussed. In the first one, the regioselectivity is determined by the approach of the triplet excited carbonyl compound to the furan derivative. In the second one, the regioselectivity also depends on the conformation equilibrium in the 1,4-diradical intermediates. Conformations leading to oxetanes *via* cyclization are in equilibrium with conformers leading to the starting products *via* fragmentation of the newly formed C–O bond. Although there is no photochemical electron transfer involved and in contrast to the reaction with dihydrofuran, the carbonyl oxygen of benzaldehyde is added in position 2 to furan derivatives such as in the case of 2-methylfuran **120** (Scheme 20).[72,91] This regioselectivity is explained by the higher HOMO coefficient in position 2. Furthermore, and also in contrast to the same reaction with dihydrofuran, the thermodynamically more stable *exo* isomers **121** and **122** are formed in excess.[16,72,91] This particular *exo*/*endo* selectivity is explained by the fact that the conformational equilibrium of the 1,4-diradicals is shifted to the structures **123** and **124**. The benzyl radical is located above the furan moiety. This sterically less favored arrangement is induced by an anomeric effect[92] which is caused by the interaction of an n-orbital of the initial oxygen atom with the σ*-orbital of the C–O bond of the furan moiety as indicated in structures **123** and **124** (compare also

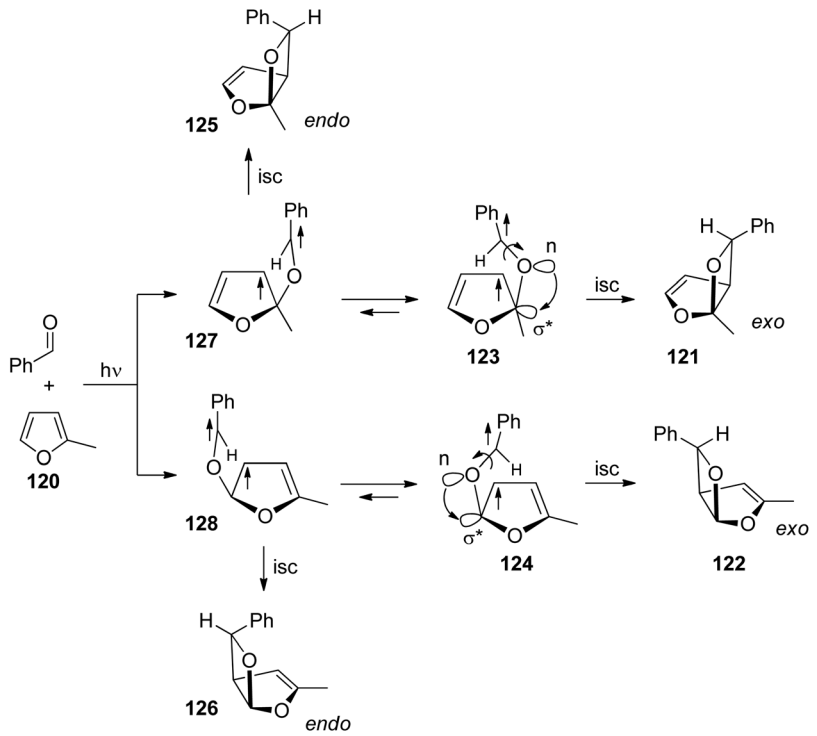

Scheme 20 Electronic effects influencing the *exo*/*endo*-selectivity of the Paternò–Büchi reaction.

ref. 85). The *endo* isomers **125** and **126** are formed from the corresponding diradical intermediates **127** and **128** respectively.

Hydrogen bonding is a powerful directing element also in photochemical reactions. Hydrogen bonding of the carbonyl group has also an impact on the regio- and stereoselectivity of the Paternò–Büchi reactions.[93] It orients the substrates with respect to each other. The effect was successfully applied, for example, to the asymmetric Paternò–Büchi reaction.[94] For further examples of photocycloadditions see ref. 95. Concerning hydrogen bonding at the $^3n\pi^*$ excited carbonyl function, it must be pointed out that such an interaction should be significantly weaker than a hydrogen bond at the corresponding ground state carbonyl function.[96] Due to the inversion of polarization at the excited state, the carbonyl oxygen is electrophilic, the energy of the hydrogen bond and its influence on the regio- and stereoselectivity in the Paternò–Büchi reaction should therefore be low.[3,97,98] A recent and very detailed investigation provides deep insight into the different influences of hydrogen bonding of an electronically excited carbonyl function in the Paternò–Büchi reaction. When the bicyclic furan derivative **129** was transformed with benzophenone **130**, only *trans* adducts **131** and **132** were formed (Scheme 21).[99] These products result from the addition of $^3n\pi^*$ excited benzophenone **130**. The reaction was carried out in toluene as a non-polar and aprotic solvent. The regioselectivity slightly depends on the temperature. At low temperature, the sterically less hindered regioisomer **131** is formed in somewhat higher quantities. Nevertheless, it remains the minor product. The privileged formation of compound **132** may be explained by the higher electron density at the higher substituted C=C bond of the furan moiety. No major influence of the alkene (**129**) concentration on the product ratio was detected. The stereoselectivity is essentially controlled by the steric hindrance of the methoxy substituent.

When the same reaction was carried out with the unprotected alcohol **133** in toluene as the non-polar and aprotic solvent, both *cis* (**134a,b**) and *trans* products (**135a,b**) were formed (Scheme 22 and Table 4).[99] These products were obtained in yields between 63% and 91%. Benzpinacol was a major side product. The formation of considerable amounts of the *cis* products **134a,b** was attributed to a directing effect caused by hydrogen bonds. The stereoselectivity and the regioselectivity are influenced in a characteristic manner by the temperature and

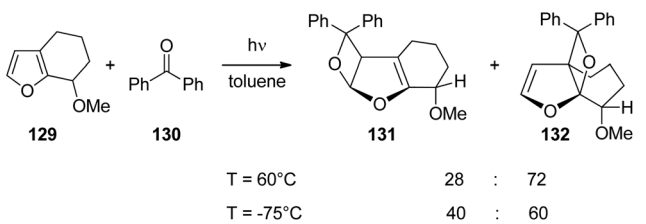

Scheme 21 Temperature dependence of the regioselectivity of the Paternò–Büchi reaction.

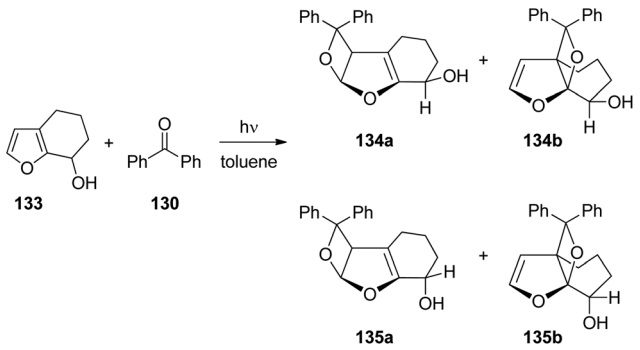

Scheme 22 Regio- and diastereoselective Paternò–Büchi reaction by a hydroxyl function.

the concentration of the alkene **133**. Since the hydrogen bond between the electronically excited benzophenone **130** and the hydroxyl function of **133** is of low energy, its effect on the regio- and stereoselectivity is reduced and hydrogen bond formation with the reaction medium also becomes relevant. This competition is nicely shown by the present results. When the reaction is carried out in DMSO as the solvent (Table 4, entry 7), only *trans* products **135a,b** were isolated as in the case of the reaction of the methyl ether **129** (Scheme 21). The hydroxyl function in **133** is thus "protected" from complexation by the electronically excited benzophenone. Furthermore, it has been shown by NMR studies that the complexation of benzophenone at the ground state with compound **133** by hydrogen bonds depends on the temperature and the concentration of **133**.[99] Significant complexation in dry d_8-toluene was observed at −60 °C and an alkene concentration of 100 mM. At higher temperatures or at lower alkene concentrations, hydrogen bond formation was considerably reduced. In light of these additional studies, the results reported in Table 4 may be interpreted as follows. At high temperature (entries 1–3), no significant influence of the alkene concentration on the stereo- and the regioselectivity is detected. Formation of hydrogen bonds between molecules of the alkene **133** is low. Therefore hydrogen bond formation between the substrates, the electronically excited benzophenone and the hydroxyfuran **133** becomes competitive at the transition state of the reaction. In the case of the regioisomers **134b** and **135b**, the formation of the *cis* isomer **135a** dominates. In the case of the regioisomers **134a** and **135a**, this effect is weaker and the formation of the *trans* isomer is favored **135a**. Hydrogen bonding also strongly directs the ketone into a sterically disfavored position leading to the formation of the regioisomers **134b** and **135b** in large excess. At low temperature (entries 4–6), hydrogen bond formation between the hydroxyl functions of molecules of alkene **133** becomes competitive to the complexation of electronically excited benzophenone. At low alkene concentration (entry 6) this effect is still weak and the product ratio still resembles those at high temperature. However, at a high alkene concentration (entry 4), the influence of hydrogen bonding between alkene **133** and the excited benzophenone is low. Due to the presence of larger amounts of the hydroxyl compound **133**, the

Table 4 Temperature and concentration of stereo- and regioselectivity in the Paternò–Büchi reaction induced by a hydroxyl function (compare Scheme 22)

			Stereoselectivity[a]		Regioselectivity[a]	
Entry	Temp (°C)	[**133**] (mM)	*trans*/*cis* (**135a**/**134a**)	*trans*/*cis* (**135b**/**134b**)	*trans* (**135a**/**135b**)	*cis* (**134a**/**134b**)
1	60	1000	70/30	41/59	22/78	8/92
2	60	100	67/33	41/59	21/79	7/93
3	60	10	67/33	42/58	21/79	8/92
4	−75	1000	85/15	81/19	53/47	47/53
5	−75	100	81/19	63/37	47/53	26/74
6	−75	10	79/21	51/49	45/55	19/81
7[b]	20	340	>97/3	>97/3	31/69	—

[a] The selectivities are normalized to 100%. [b] The reaction was performed in a dry and degassed DMSO solution.

reaction medium can't be considered anymore as an aprotic one. In all cases, the formation of the *trans* isomer is dominant (entries 4–6). This result may be compared to the results obtained from the transformation of the methylether derivative **129** (Scheme 21). Also, the formation of the sterically hindered regioisomers **134b** and **135b** becomes less favorable. Although, its influence has been reduced, hydrogen bonding between the electronically excited benzophenone and the hydroxyfuran derivative **133** remains important in the control of the stereo- and the regioselectivity of this Paternò–Büchi reaction.

In order to better characterize the unexpectedly strong hydrogen bonding at the $^3n\pi^*$ excited benzophenone, comprehensive computational studies were carried out. Early studies estimated the stabilization energy of hydrogen bonded $^3n\pi^*$ excited formaldehyde with water to be 0.2–0.4 kcal mol^{-1} while the corresponding interaction at the ground state was estimated to be 3.5 kcal mol^{-1}.[96] Recent studies of the stabilization energy of hydrogen bonded $^3n\pi^*$ excited formaldehyde with methanol was calculated to range between 0.5 and 0.7 kcal mol^{-1} and the corresponding interaction at the ground state was found to be 4.68 kcal mol^{-1}.[99] Somewhat higher stabilization energies were calculated for the hydrogen bonds with benzophenone. Values between 2.1–3.2 kcal mol^{-1} for the $^3n\pi^*$ excited state and values between 4.5–6.0 kcal mol^{-1} for the ground state were found. To get further information on the interaction between $^3n\pi^*$ excited carbonyl compounds and furan derivatives, the Mulliken charge at the carbonyl oxygen atom was determined during the addition of the photochemical excited formaldehyde or benzophenone **130** to the furan **136**. The benzophenone case is depicted in Fig. 7. The approach occurs *via* transition state **TS1** leading to the formation of an exciplex. The diradical intermediate **137** is then formed *via* transition state **TS2**. At the beginning of this reaction step, the Mulliken charge on the oxygen is around −0.13. This increases until reaching a maximum of −0.26 near the transition state **TS2**. In the diradical intermediate **137** the Mulliken charge of the initial carbonyl oxygen was calculated to be −0.13. These results clearly show that this oxygen is particularly basic at **TS2** and at this stage, hydrogen bonding is most efficient in controlling the stereoselectivity. The effect is less pronounced before **TS1** and, more importantly, in the 1,4-diradical **137**.

The hydrogen bonding influence on the *cis*/*trans* selectivity in the reaction is described in Scheme 23 and Table 4. It is particularly strong at the exciplex and at its irreversible transformation into the 1,4-diradical intermediate. A computational study was carried out on the reaction of $^3n\pi^*$ excited benzophenone with the bicyclic hydroxyl furan derivative **133**. The results for the formation of the diastereoisomers **134b** and **135b** are depicted in Scheme 23.[99] A considerable energy difference of 1.4 kcal mol^{-1} due to hydrogen bonding has been calculated for the *cis*-**TS** and the *trans*-**TS**. For the corresponding diradical intermediates *cis*-**DR** and *trans*-**DR** the energy difference is only 0.2 kcal mol^{-1} in favor of the *cis* isomer. These two intermediates undergo either cyclization leading to the final products or they undergo fragmentation leading to the starting products **130** and **133**. The intermediates are also in equilibrium with the *anti* conformers *cis-anti*-**DR** and *trans-anti*-**DR**. The energy difference between the *cis-anti* and *trans-anti* conformer is large (2.1 kcal mol^{-1}) in favor of the *trans* isomer. This high energy difference is essentially caused by steric hindrance in the case of *cis-anti*-**DR**. No influence of hydrogen bonding is detected for the *anti* conformers. Apart from the equilibrium with the *syn* conformers, the *anti* conformers may only undergo fragmentation. Thus the tendency to form oxetanes from the *cis*-approach of the electronically excited benzophenone to **133** is enhanced by hydrogen bonding at the stage of the exciplex and its transformation to the diradical intermediate. This tendency is also increased by the relatively high energy of the corresponding *cis-anti*-**DR** which reduces fragmentation of the diradical intermediate to the starting material.

The [2 + 2] photocycloaddition of α,β-unsaturated carbonyl compounds is frequently applied to organic synthesis.[100] For this reason, the stereoselectivity is particularly studied. More recently, particular asymmetric catalysis was applied to these reactions.[101] Chirality may be induced by complexation of the substrate to a template *via* hydrogen bonds or Lewis acid complexation.

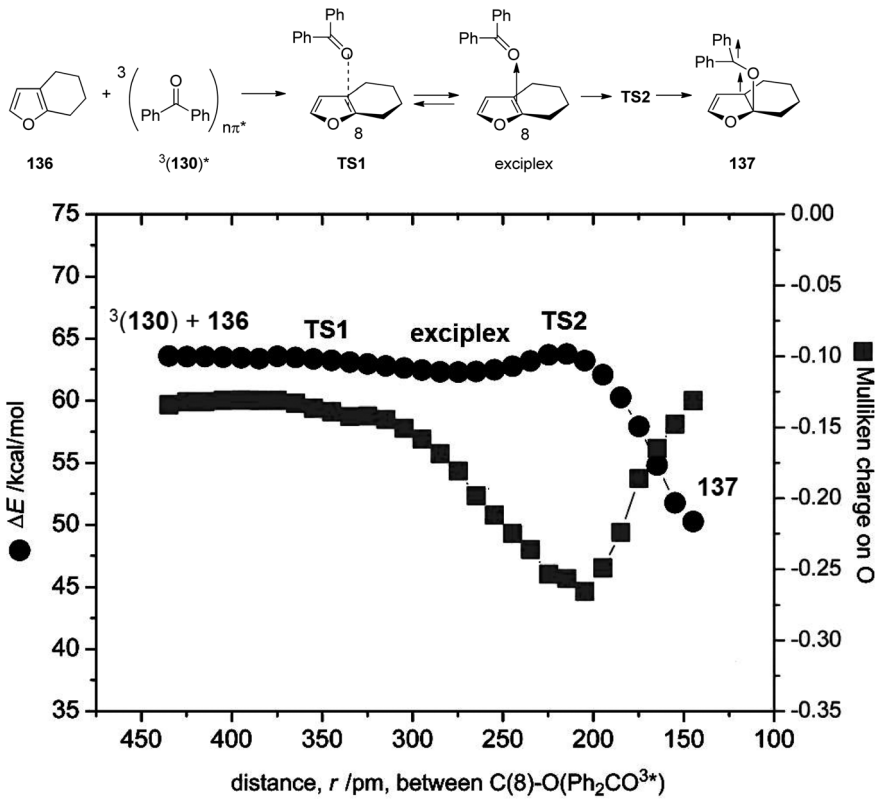

Fig. 7 UB3LYP/6-31+G(d) analysis of the energy profile and the distance dependent Mulliken charge of the carbonyl oxygen during the approach of $^3n\pi^*$ excited benzophenone to **136** and the C–O bond formation between the two species. (Adapted with permission from: Y. Yabuno, Y. Hiraga, R. Takagi and M. Abe, *J. Am. Chem. Soc.*, 2011, **133**, 2592–2604. Copyright (2011) American Chemical Society.)

Also UV absorption of such nitrogen containing heterocycles can also be shifted towards the visible (bathochromic) when efficient Lewis acid complexation takes place. In Fig. 8, UV spectra of compound **136** (Scheme 24) are depicted.[102] In the absence of a Lewis acid, an absorption maximum is observed around λ = 290 nm. This maximum is shifted to $\lambda \approx$ 345–350 nm. The photochemical reactivity of compounds such as **136** is generally low when they are electronically excited by direct light absorption. This is due to the fast internal conversion from the first excited singlet state S_1 to the ground state S_0. Lewis acid complexation increases the life time of the S_1 state.[103] Intersystem crossing to the T_1 state becomes competitive which favors [2 + 2] photocycloaddition. Complexation with the chiral Lewis acid **137** was used in the intramolecular asymmetric [2 + 2] photocycloaddition of the cyclic enone **136** (Scheme 24). Chiral induction was efficient when 0.5 equivalent of the Lewis acid was used. The formation of the enantiomer **138** is explained by structure **139**. Recently, a computational study on the effect of Lewis acids on the mechanism of such [2 + 2] photocycloadditions has been published.[104]

Enantioselective [2 + 2] photocycloaddition with visible light and Lewis acid activation was also carried out using photoredox catalysis with $[Ru(bpy)_3]^{2+}$ complexes.[105] An intramolecular reaction with two different α,β-unsaturated carbonyl compounds was studied. Eu^{3+} complexes with peptide ligands were used as Lewis acids. Dimerization of cinnamates *via* [2 + 2] photocycloaddition is difficult when it is carried out in solution. However, when such compounds are complexed by thiourea derivatives, this reaction becomes efficient, especially when it is carried out in a continuous flow reactor.[106] In this case, the reactivity is increased by two hydrogen bonds between the thiourea compound and the carboxyl group of the cinnamate.

5 Photochemical electron transfer induced reactions

Photoinduced electron transfer reactions play a dominant role in the chemistry of life.[107] Despite this, their application to organic synthesis started only a few decades ago.[108] The understanding of electron transfer in general and of photoinduced electron transfer (PET) processes in particular developed relatively late in the middle of the twentieth century.[109,110] Before that time, many PET reactions were originally thought to proceed *via* homolytic steps.

Upon electronic excitation of a compound, its redox properties may become enhanced, either as an electron donor (D) or an acceptor (A). The possibility of a subsequent electron

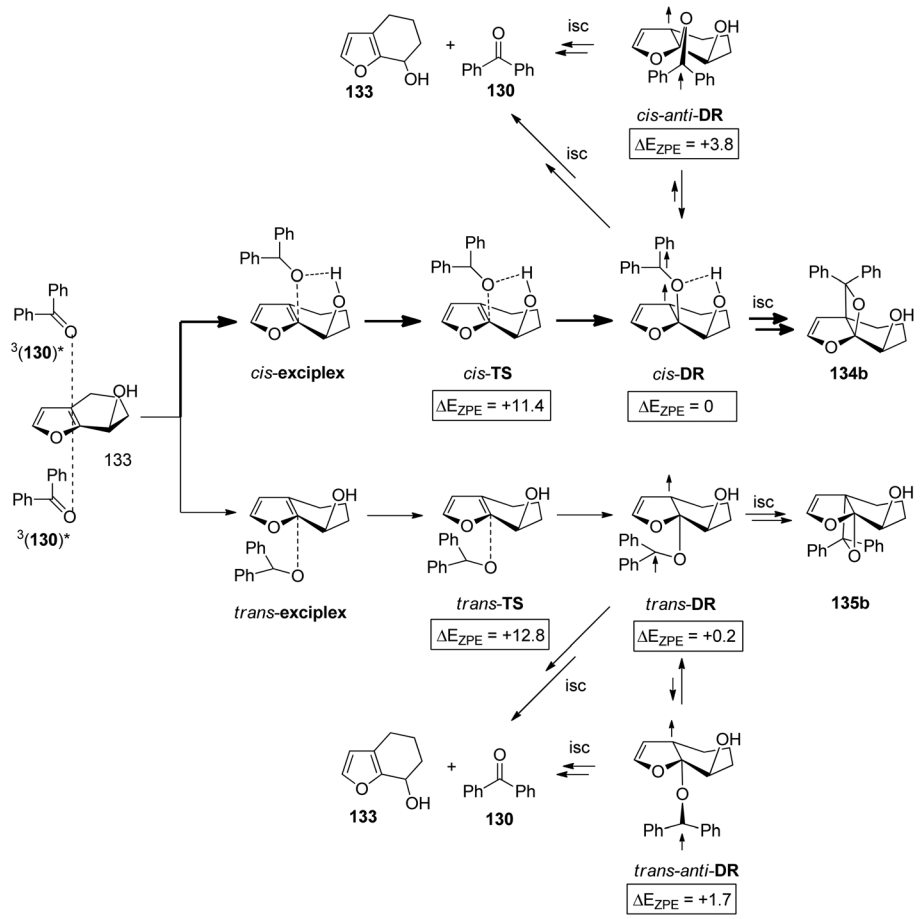

Scheme 23 Energies (ΔE_{ZPE} values are given in kcal mol^{-1}) for the reaction of ^{3}nπ* excited benzophenone with the furan derivative **133** leading to oxetanes **134b** and **135b** calculated at the UB3LYP/6-31+G(d) level.

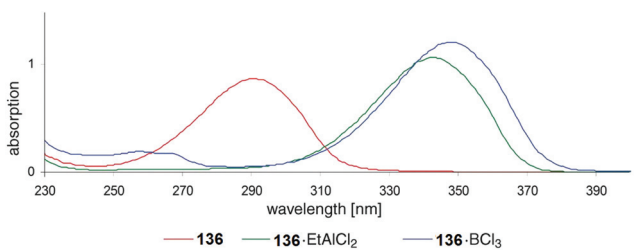

Fig. 8 Bathochromic shift of absorption maxima by Lewis acid complexation. (Reproduced with permission from: R. Brimioulle and T. Bach, *Science*, 2013, **342**, 840–843. Copyright (2013) The American Association for the Advancement of Science.)

transfer process can be estimated from the Rehm–Weller approach (eqn (1)).[111] Only for exergonic processes ($\Delta G < 0$), a PET process is considered thermodynamically favorable.

$$\Delta G = [E^{Ox}_{1/2}(D) - E^{Red}_{1/2}(A)] - \Delta E_{excit} + \Delta E_{coul} \quad (1)$$

where $E^{Ox}_{1/2}(D)$ and $E^{Red}_{1/2}(A)$ are the oxidation and reduction potential of the donor or the acceptor; ΔE_{excit} represents the electronic excitation energy of the chromophore; ΔE_{coul} indicates the coulombic interaction energy of the products, most commonly radical ions.

In intermolecular PET reactions, radical ions are formed either as close pairs or as free species from neutral molecules (Scheme 25).[110] These species can undergo a variety of subsequent follow-up processes, for example, an addition (or recombination) reaction of a radical or radical ion or a nucleophilic capture of a cation or radical cation, respectively.

In intramolecular PET processes, a donor and an acceptor are connected *via* a linker (donor–bridge–acceptor molecules). The photochemical behavior of these has been described as "a bug that opens its mouth when struck by light, can hold it open for only a short time, and during that time can swallow anything within striking range of its open mouth including its own tail".[112]

Rapid back electron transfer (BET, also called return electron transfer RET) commonly limits the efficiency of the PET process, resulting in low yields and prolonged irradiation times.[113] Consequently, various strategies have been developed to circumvent this energy-inefficient process, among these PET-sensitization, co-sensitization and salt effects.[110,114,115]

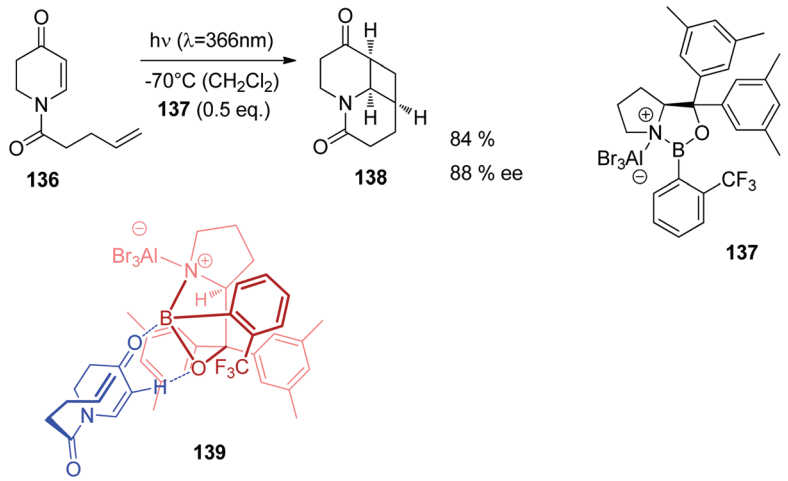

Scheme 24 Asymmetric Lewis acid catalyzed [2 + 2] photocycloaddition of the dihydropyridone derivative **136**.

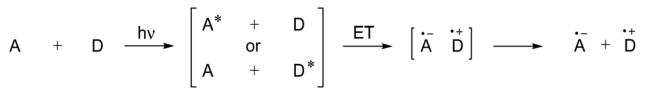

Scheme 25 Photoinduced electron transfer between neutral donor and acceptor molecules.

5.1 Cyclization and addition reactions

Due to its favorable photophysical and electrochemical properties,[116,117] the phthalimide chromophore has been intensively utilized for PET studies.[118] From this data, the limiting oxidizing power of phthalimides for an exergonic electron transfer is *ca.* 2.4 V (*vs.* SCE) for the first excited singlet state (E_{00} = 3.8 eV) and *ca.* 1.7 V (*vs.* SCE) for the first excited triplet state (E_{00} = 3.1 eV). In some cases, electron transfer from the spectroscopically non-detectable second triplet state (E_{00} = 3.6 eV) has been suggested, thus increasing the oxidizing power to *ca.* 2.3 V (*vs.* SCE).

Thioethers (Me_2S: $E_{Ox.}$ = *ca.* 1.25 V *vs.* SCE[119]) are easily oxidized by excited phthalimides. For example, irradiation of the simple alkylthio-substituted phthalimide derivatives (**140**) in acetone furnished the corresponding unbranched azathiacyclols (**141**) as major products in moderate to good yields (Scheme 26).[120] The branched products **142** were obtained in smaller amounts, if at all, thus demonstrating the higher kinetic acidity of the primary *vs.* secondary α-CH group. Solely the butylene-linked substrate exclusively gave the branched product **142** and this was explained by a geometrically favored ε-CH_2-activation.

The phthalimide/methylthioether system was successfully utilized for the synthesis of medium to macrocyclic products with a ring size of up to 38 atoms, among these sulfur containing amines, lactams, lactones, and crown ether analogues (Scheme 27).[120,121]

Due to the very low oxidation potential of tertiary amines (R_3N: $E_{Ox.}$ = 0.7–1.3 V *vs.* SCE[119]), photoinduced electron transfer reactions of aminoalkyl-substituted phthalimides are highly exergonic. However, since amines are potent hydrogen donors, photoreductions and photopinacolizations are commonly observed side reactions. As a result, yields and selectivities are generally low.[122] For dibenzylated aminoalkyl-substituted derivatives, higher conversions and yields of up to 39% were obtained.[122c]

Efficiencies and selectivities of the above mentioned cyclization reactions could be significantly improved by incorporating a suitable leaving group in the α-position to the electron donor. The trimethylsilyl, trialkylstannyl or carboxylate function has been successfully utilized for this strategy.[123]

Intramolecular PET reactions involving alkenyl phthalimides show a remarkable solvent dependence.[124] When irradiated in MeCN, [$\pi^2 + \sigma^2$]-addition to the C(O)–N bond takes place and benzazepinediones are isolated. In contrast, irradiation in alcohol furnished alcohol-trapping products. Their formations were explained by an anti-Markovnikov trapping of the intermediary generated radical cations by the

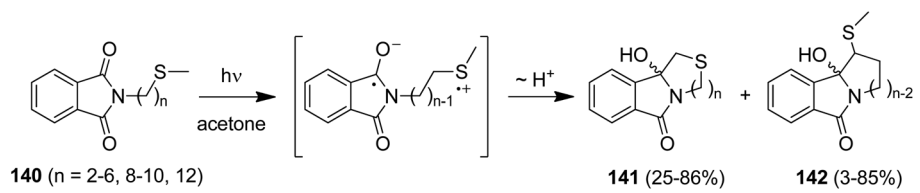

Scheme 26 PET-cyclizations of simple alkylthio-substituted phthalimide derivatives.

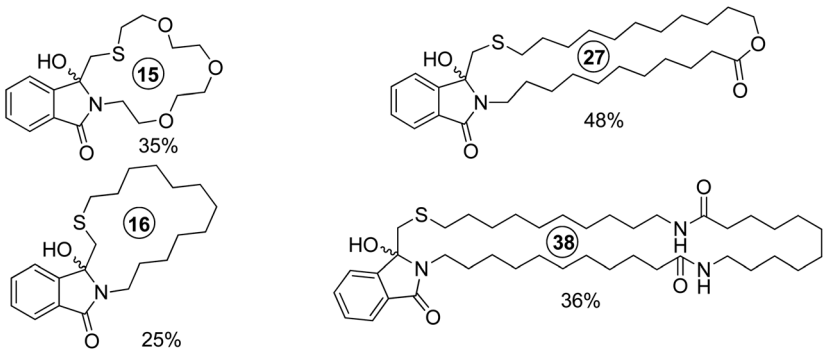

Scheme 27 Examples of sulfur containing medium to macrocyclic products.

nucleophilic solvent.[125] In an extension of this reaction, the tetrachlorophthalimide (**143**) with a remote hydroxyalkyl substituent furnished the macrocyclic lactone **144** in 50% yield when irradiated in the presence of α-methylstyrene (Scheme 28).[126]

Despite their relatively high oxidation potentials (*e.g.* acetate:[127] $E_{Ox.}$ = 1.54 V in MeCN, 2.65 V in H_2O *vs.* SCE), carboxylates can be efficiently decarboxylated under PET conditions. Due to the irreversible exclusion of carbon dioxide, these decarboxylation reactions operate with high quantum yields of up to 0.6 and enable short irradiation times.[116] Using this mechanistic feature, a range of phthalimido ω-alkylcarboxylates (**145**) have been successfully converted to ring systems (**146**), among these medium and macrocyclic amines, polyethers, lactams, lactones, as well as cycloalkynes and arenes (Scheme 29).[128,129] Examples of photodecarboxylations were also realized in macro- and micro-formats.[130,131]

The photodecarboxylation was furthermore applied to the diastereoselective synthesis of [1,4]benzodiazepines and pyrrolo[1,4]benzodiazepines (Scheme 30).[132] Irradiation of the chiral, α-amino acid-derived substrates **147** showed high diastereoselectivities and the *trans*-diastereoisomers **148** were

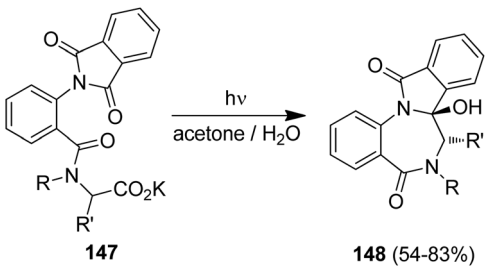

Scheme 30 Memory-of-chirality in photodecarboxylative cyclizations.

solely formed. Using proline and the proline-analogue, a remarkably high memory of chirality effects was furthermore determined with ee values of 86% and >98%, respectively. The memory-of-chirality concept has been recently expanded to adamantane-type dipeptides.[133]

The intermolecular photodecarboxylative addition protocol has been used for the synthesis of known and potentially bioactive 3-(alkyl and aryl)methylene-1*H*-isoindolin-1-ones as target compounds.[134] As an example, the phthalimide derivative **149** was converted in two simple steps and in overall yields

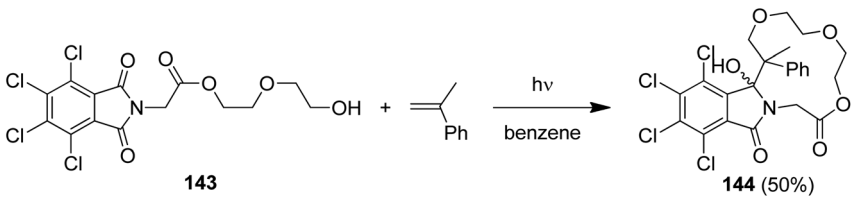

Scheme 28 α-Methylstyrene trapping and macrocyclization of tetrachlorophthalimide **143**.

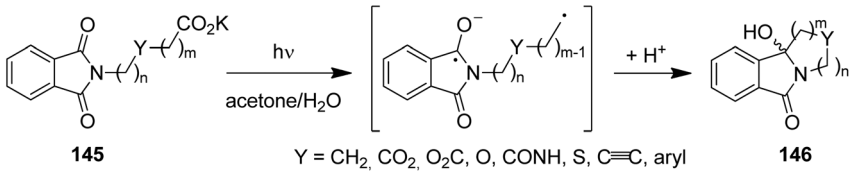

Scheme 29 Photodecarboxylative cyclizations of phthalimido ω-alkylcarboxylates.

of 19–65% into the corresponding products **150** (Scheme 31). Some representatives of **150** have documented cardiovascular activity.[134b] This transformation was furthermore realized in series in an advanced continuous-flow reactor.[134c]

At the ground state, electron transfer between naphthylamine derivatives such as **151** and α,β-unsaturated lactones or furanones such as **152** (Scheme 32) is not possible.[135] However, when irradiated with UV light an efficient transform-

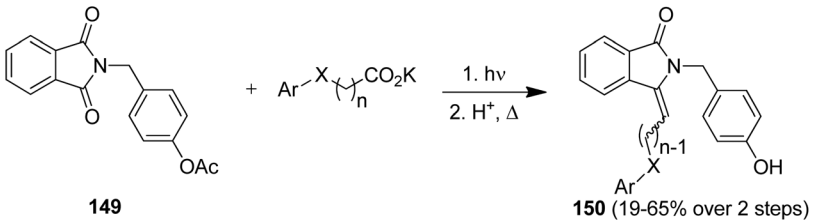

Scheme 31 Photodecarboxylative alkylations and dehydrations cascade.

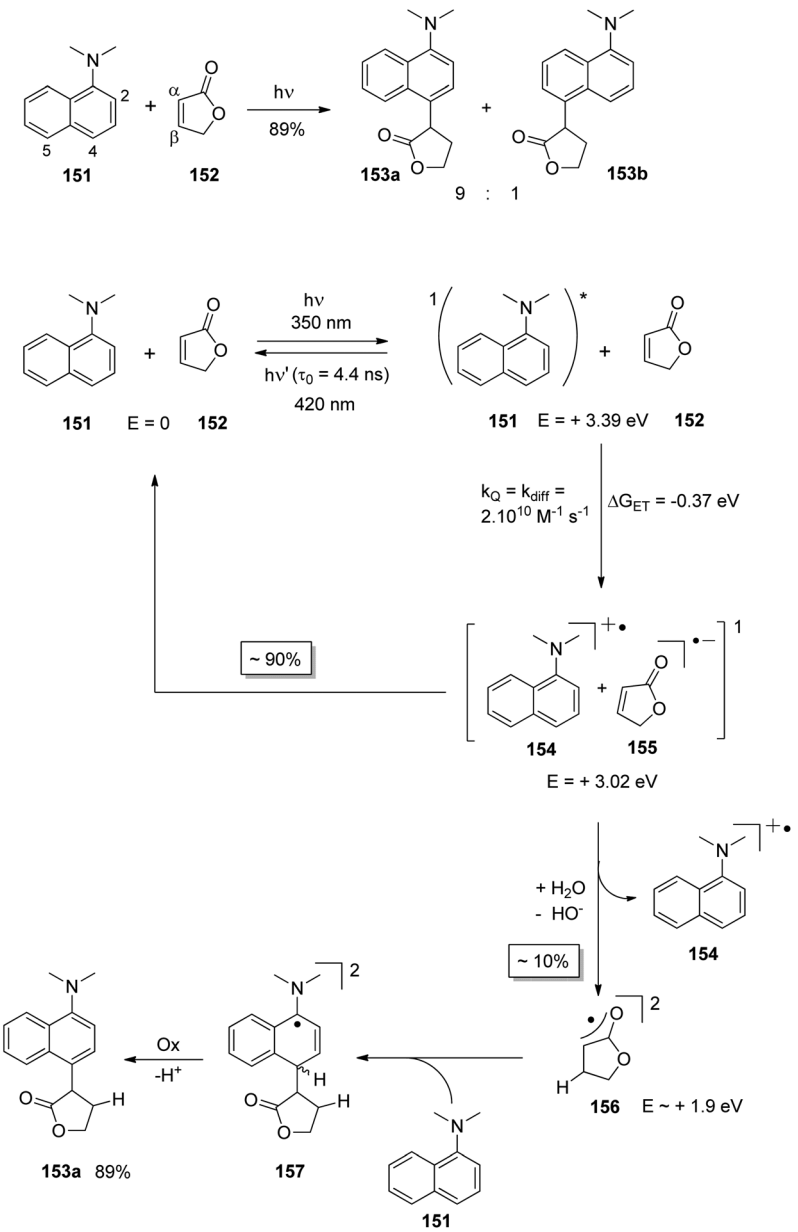

Scheme 32 Photochemical electron transfer induced addition of a naphthylamine derivative to an α,β-unsaturated lactone.

ation was observed and products **153a,b** were isolated in high yields. When the 1-naphthylamine derivative **151** is electronically excited by irradiation λ = 365 nm, fluorescence is efficiently quenched (diffusion control) by electron transfer and a radical ion pair **154** and **155** is formed. This process is endothermic by −0.37 eV. From product quantum yield determination of the overall reaction, it was concluded that about 90% of these radical ion pairs undergo back electron transfer leading to the substrates at their ground state. However, in the presence of a proton donor (water was added to the reaction mixture), the radial anion **155** is trapped by protonation in the β position of the furanone and the electrophilic neutral radical **156** is formed. This regioselectivity is unusual since the basic center of such a radical anion is generally located at the carbonyl oxygen as is also the case for enolates. Based on previous results, this observation was explained by different charge densities in the radical anion depending on whether it is free in solution or attached to another species. In the present case, such an arrangement in a contact ion pair would induce an unusual charge distribution on the anion part. The resulting neutral radical **156** is electrophilic and thus added easily to the naphthalene derivative **151** which is used in excess. Thus the intermediate **157** is formed and after oxidation, the final product **153a** is obtained. The protonation of the radical anion in the β position of **155** induces the unusual addition of a nucleophile in the α position of an α,β-unsaturated carboxylic compound (**153a,b**). The unusual regioselectivity of the protonation was additionally proven by isotopic labeling experiments.

Electrophilic substitutions in 1-naphthylamine derivatives generally take place in positions 4 and 2 of the naphthalene system. It is therefore surprising that the addition of an electrophilic species was observed in position 5 as in the formation of compound **153b**. In order to explain this observation, a two-step process for the addition of the radical intermediate **156** was proposed (Scheme 33). First an electron transfer occurs from the naphthylamine compound **151** to the electrophilic radical **156** leading to the radical cation **154** and the enolate **158**. Charge combination then yields the radicals **157a,b**. The overall electron distribution in the radical cation **154** has been calculated and the results indicate particularly low negative charge in position 4. They also show low densities in positions 5 and 8 while the negative charge density is high in position 2. Thus the addition of the enolate **158** by charge combination occurs preferentially in positions 4 and 5. The reaction in position 8 is sterically hindered. In this context, it must be mentioned that electrophilic neutral radicals may also add directly to 1-naphthylamine derivatives without previous electron transfer. Thus, the addition of electrophilic trifluoromethyl radicals to 1-naphthyl amine occurs in one step and only in positions 2 and 4.[136] Both regioisomers were obtained in a 1 : 1 ratio. This latter result is in line with the regioselectivities observed in a large number of electrophilic aromatic substitutions. Compounds such as **153a** possess a variety of pharmaceutical activities. Conventionally they are synthesized using methods of organometallic chemistry or organometallic catalysis.[137]

In a similar reaction, perfluoroalkylations of 1-naphthylamine derivatives have been carried out (Scheme 34).[138] After photochemical excitation, electron transfer from the excited naphthylamine derivative **151** to the perfluoroalkyliodide **159** becomes exothermic (ΔG_{ET} = −1.78 eV). Very fast release of iodide leads to the neutral perfluoroalkyl radical **161** which adds to the naphthalene derivative **151**. The intermediate **162** is generated. Attempts to quench the reaction by trapping of the radical anion by addition of dinitrobenzene failed which indicates the formation of the neutral perfluoroalkyl radical **161** is fast. α-Aminoalkyl radicals such as **162** are easily oxidized. In the present case, the perfluoroalkyliodide **159** is reduced by a corresponding electron transfer from **162**. This procedure also allows the formation of perfluoroalkyl radicals **161** after release of iodide. The resulting cation **163** is a typical Wheland intermediate of an electrophilic aromatic substitution which yields the final product **160** after deprotonation. The electrophilic radicals **161** add easily with the electron rich

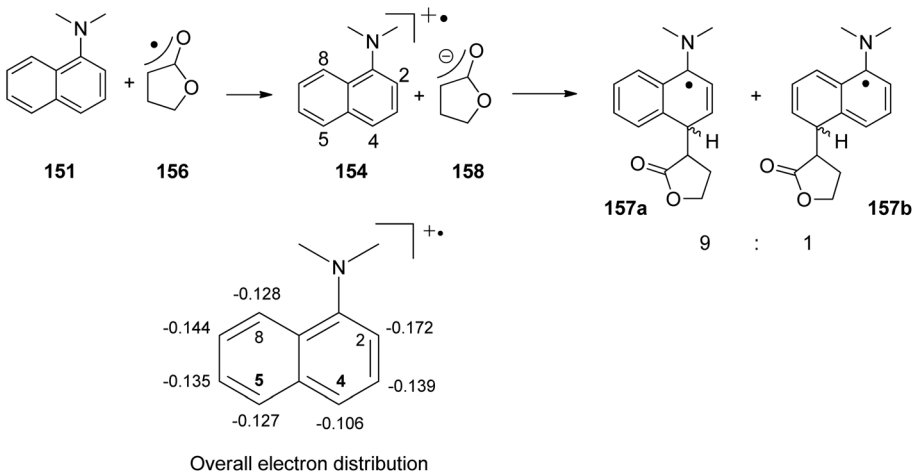

Scheme 33 Regioselectivity of the photochemical electron transfer induced addition of a naphthylamine derivative to an α,β-unsaturated lactone.

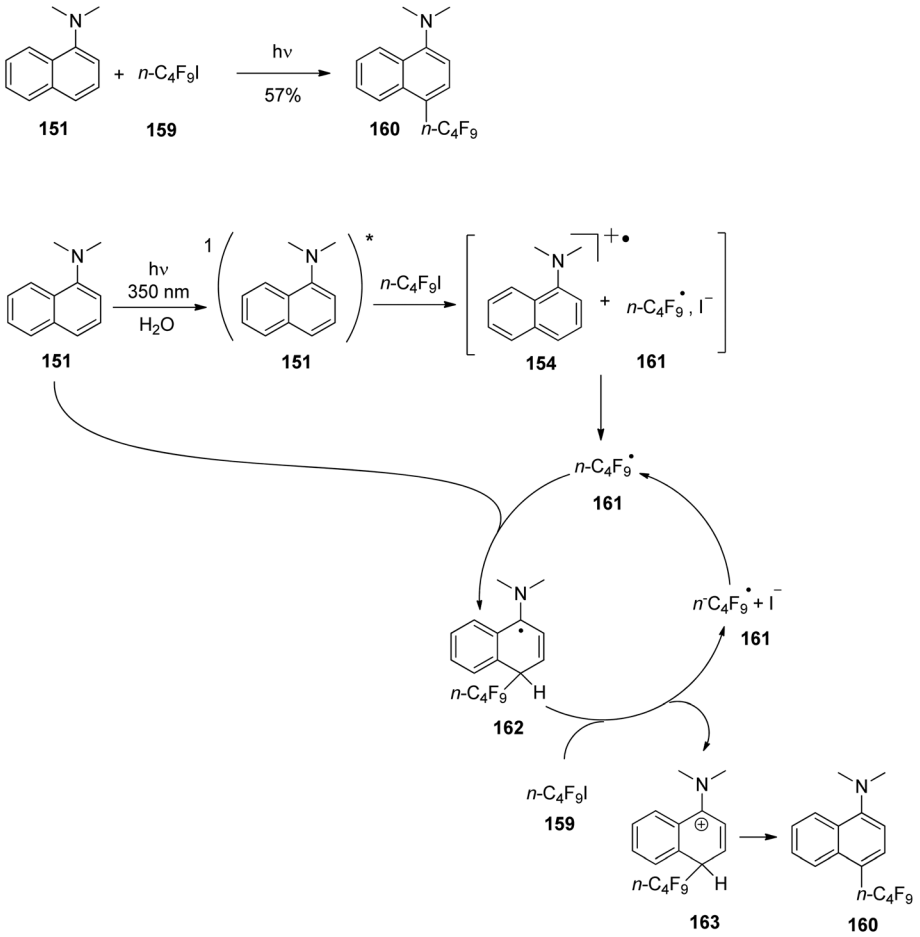

Scheme 34 Photochemical electron transfer induced addition of a fluoroalkyl radical to a naphthyl amine derivative involving a chain mechanism.

1-naphthylamine derivative **151**. Thus a radical chain process is established. The high product quantum yields of around 200 clearly indicate the efficiency of this process. The reaction was also carried out with aniline derivatives. Depending on the substrate structure and the precise reaction conditions, product yields up to 88% have been observed.

5.2 Catalytic reactions

Catalytic reactions play an important role in synthetic chemistry. In particular, catalytic conditions accelerate transformations with high activation energies. This effect is based on the formation of energetically low reaction intermediates between the substrate and the catalyst. In many catalytic processes no activation with chemical reagents used in stoichiometric amounts is necessary. Thus the formation of side products is considerably reduced. As already pointed out, photochemical reaction conditions significantly alter the reactivity of organic compounds. They also have an impact on the elementary steps of catalytic reactions. It is therefore obvious that the combination of both domains, catalysis and photochemistry, should enable synergy effects.[139,140] Many photochemical reactions are induced by sensitization in which an additive (sensitizer) transfers its excitation energy on a substrate.[141,142] This process may be compared to catalysis and indeed definitions for a sensitizer and a photocatalyst are often very similar. The next procedure well illustrates the proximity of these terms. It deals with the radical addition of simple tertiary amines to electron deficient alkenes. Recently, an efficient methodology has been developed to perform this transformation.[143] Thus the *N*-alkylpyrrolidines such as **165** were added efficiently to α,β-unsaturated lactones or furanones such as **164** (Scheme 35) when electron donor substituted aromatic ketones were used as sensitizers such as 4,4′-dimethoxybenzophenone **167**.[144] Product (**166**) yields up to 94% and quantum yields up to 4 have been observed. However, reactions with many acyclic tertiary amines such as triethylamine were less efficient. Similar reactions have also been carried out with unsubstituted benzophenone and this sensitizer has also been used in this case. When comparing these two types of sensitizers, it was observed that in the case of electron donor substituted aromatic ketones as sensitizers such as **167**, the reactions were particularly fast. The sensitizer was used in catalytic amounts and was recovered up to 80% after the reaction. However, in the case of benzophenone for example, large amounts, often more than one equivalent of the sensitizer, were used and considerable decomposition *via* photoreduction

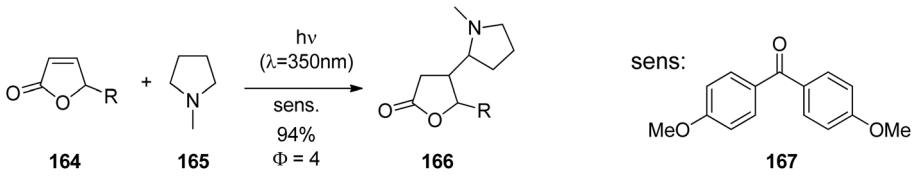

164 165 166 167

Scheme 35 Photochemically sensitized addition of tertiary amines to electron poor double bonds using electron donor substituted aromatic ketones as sensitizers.

and photopinacolization were observed.[145] These are typical reactions of these ketones in the presence of amines.[146] Electron donor substituted aromatic ketones undergo such transformations less efficiently. The difference in reactivity was attributed to different excited states. While benzophenone possesses an nπ* configuration for the T_1 state, compounds such as 4,4′-dimethoxybenzophenone **167** possess a ππ* configuration at this triplet state. In order to check whether these different excited states have an influence on the reaction, among other parameters, the triplet quenching rates k_q with the reactive amine **165** and the unreactive triethylamine (TEA) and the lifetime $t_{1/2}$ of the corresponding ketyl radicals have been determined (Table 5).[147] The luminescence quenching occurs *via* electron transfer. Concerning these photophysical steps, no significant difference between the two types of aromatic ketones on the one hand and between the reactive tertiary amine **165** and the unreactive TEA on the other hand have been detected.

Based on these observations the mechanism depicted in Scheme 36 is discussed. After light absorption of the sensitizer, electron transfer occurs from the tertiary amine **165** to the sensitizer **167** and the radical ion pair **168** and **169** is generated. Proton transfer between the ions leads to the neutral radicals **170** and **171** which enter into the radical chain reaction. The nucleophilic α-aminoalkyl radical **171** easily adds to the electron deficient double bond of the furanone **164** and the electrophilic oxoallyl radical **172** is thus formed.[148] After hydrogen transfer from the tertiary amine **165** to **172** the final product **166** is formed and an α-aminoalkyl radical **171** is also generated. Such photochemically induced radical chain reactions often afford very high quantum yields. In the present case, the relatively low quantum yield $\Phi = 4$ indicates that the termination step is also efficient. Thus the oxoallyl radical **172** may react with the ketyl radical **170** of the sensitizer leading to the final product **166** and the sensitizer **167** is regenerated. Due to the efficiency of this second radical cycle, the sensitizer becomes an efficient photocatalyst. As the difference in efficiency between the electron donor substituted aromatic ketones such as **167** and unsubstituted aromatic ketones such as benzophenone cannot be explained by the photophysical primary processes, the observed effects must be linked to the reactivity of the different ketyl radicals. Thus, the reaction of ketyl radicals such as **170** with electrophilic radicals such as **172** must be particularly efficient. Perhaps, an electron transfer is also involved in this step.

The same reaction was carried out with inorganic semiconductors such as TiO_2 and ZnS as photochemical electron transfer sensitizers.[149] Thus heterogeneous photocatalysis was applied for this transformation.

In the context of asymmetric catalysis, the reaction has also been carried out in an intramolecular manner with a chiral sensitizer.[150] In such reactions, the tertiary amine partner is present in stoichiometric amounts with respect to the olefinic partner and no radical chain process is possible. However due to the proximity of the oxoallyl radical and the ketyl radical, an efficient regeneration of the sensitizer is also possible and the productiveness of the overall reaction is thus guaranteed.

Due to the fact that no further optimization of the reaction seemed to be possible by modifying the structure of the aromatic ketone as a sensitizer or a photocatalyst, particular interest was paid to the radical mechanism. The complex interplay of different neutral radical intermediates may be affected by the addition of thiocarbonyl derivatives. The addition of these compounds to radical species is reversible[151] and this behavior has been applied in polymer chemistry in order to control the radical polymerization.[152] In the present case of the photochemically induced radical addition of amines to electron deficient alkenes, it was found that the addition of thiocarbonyl compounds such as the thiocarbamide **173** to the reaction mixture increases the reactivity of the tertiary amine (Scheme 37).[153] Thus, the addition of triethylamine (TEA) to furanone **174** became possible and the adduct **175** was isolated in high yield. As previously discussed, α-aminoalkyl radical **176** generated by a two-step hydrogen transfer forms the tertiary amine to the photochemically excited sensitizer (compare also Scheme 36). The addition of such radicals to furanones is reversible. The equilibrium depends on the structure of the

Table 5 Rate constant for triplet quenching by amines and half-life of the ketyl radicals

Ketone	Amine	k_q (10^9 M^{-1} s^{-1})	$t_{1/2}$ (ms)
Benzophenone	**165**	3.6	0.1–0.2
	TEA	3.5	0.1–0.2
4,4′-Dimethoxybenzophenone **167**	**165**	1.5	0.1–0.2
	TEA	0.8	0.1–0.2
Xanthone	**165**	5	0.1–0.2
	TEA	4.4	0.1–0.2
Acetophenone	**165**	2	0.1
	TEA	2.4	0.1
4-Methoxyacetophenone	**165**	1	>0.05
	TEA	0.28	>0.05

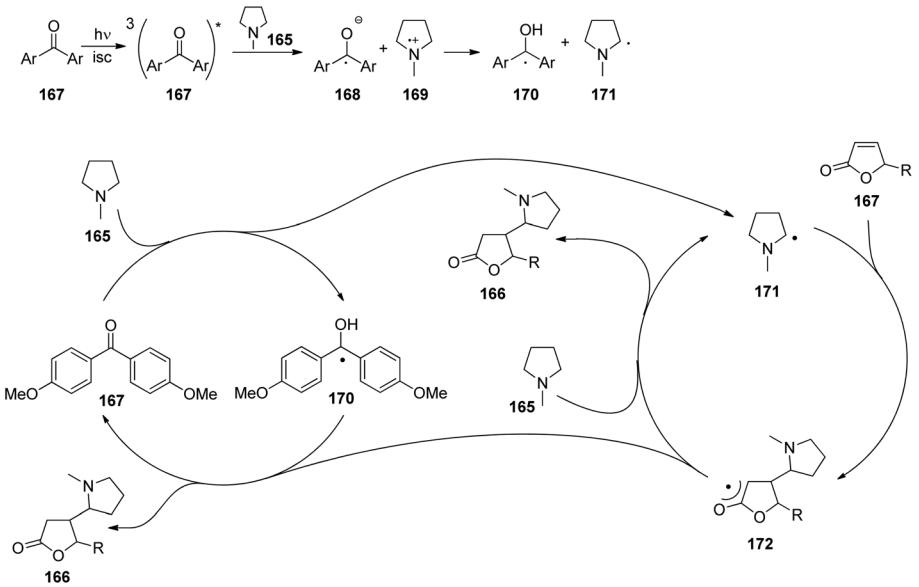

Scheme 36 Mechanism of the photochemically sensitized addition of tertiary amines to electron poor double bonds.

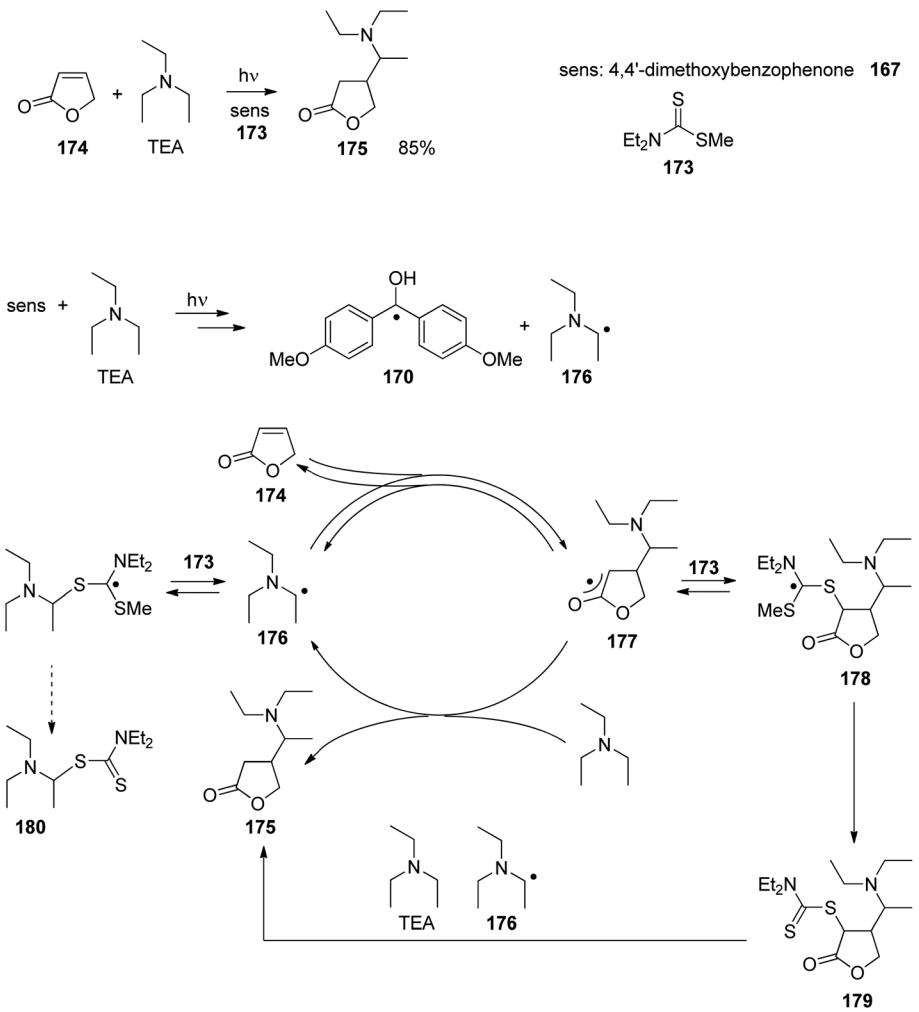

Scheme 37 Photochemically induced radical addition of unreactive amines to electron deficient alkenes in the presence of thiocarbonyl compounds.

tertiary amine. In the case of TEA, either the formation of the intermediate **177** is less favorable or this intermediate is less efficiently trapped by the reaction with a TEA molecule. In the presence of thiocarbamide **173**, the equilibrium is shifted to the product side by efficient addition of **173** to the oxoallyl radical **177** leading to the intermediate **178.** The latter intermediate also forms the thiocarbamide adduct **179.** In the presence of TEA and the corresponding α-aminoalkyl radicals **176**, this adduct yields the final product **175** by release of the thiocarbamide group. Thus, a second reaction channel to the final product is opened. The thiocarbamide adduct **179** was detected by mass spectroscopy. The corresponding signal intensities and thus the stationary concentration of **179**, depend on the excess of TEA in the reaction mixture. When the excess of TEA is diminished, the stationary concentration of **179** increases and *vice versa*. The transformation of **179** into the final product **175** is induced by such an addition. Under these modified reaction conditions, a variety of less reactive tertiary amines were successfully added to electron deficient double bonds.[153,154] The addition of thiocarbamate **173** to nucleophilic radicals, α-aminoalkyl radicals, **176** is less efficient. Nevertheless, a corresponding adduct **180** was also detected by mass spectroscopy.

In this context, it should be mentioned that photochemistry generally provides a large variety of methods to generate radical species and induce radical tandem or domino reactions as they are often observed in radical chemistry.[155] The presented method of the photochemically induced radical addition of tertiary amines to alkenes was also applied to related tandem addition cyclization reactions. Particularly interesting transformations have been performed with aniline derivatives. When a solution of *N*,*N*-dimethylaniline **182** and the chiral furanone **181** was irradiated in the presence of the electron donor substituted aromatic ketone **184** as the sensitizer, the two diastereomers **183a,b** of a tetrahydroquinoline were isolated (Scheme 38).[156] However, considerable amounts of the side products **185** and **186** were also obtained. These products result from partial reduction of the furanone **181.** Using isotopic labeling, it was shown that this side reaction is coupled to the formation of tetrahydroquinolines **183a,b.** When the reaction was performed with the aniline derivative **187** carrying deuterium atoms in the *ortho* and *para* positions, deuterium was detected in the α-position of the lactone **188** and in one of the α-positions of the coupling product **189** (Scheme 39). When this reaction was carried out with the derivative **190** carrying deuterium atoms on the methyl groups, deuterium was detected in the β-position of the lactone **191** and again in one of the α-positions of the coupling product **189.** The incorporation of one deuterium atom in the side products was between 45 and 60%. The results obtained from these experiments are explained by the mechanism depicted in Scheme 40. Photochemical electron transfer from the aniline derivatives to the excited sensitizer **184** leads to α-aminoalkyl radicals **192.** They readily add to the electron deficient double bond of the α,β-unsaturated lactone **181** and oxoallyl radicals **193** are formed. After cyclization, the resulting tricyclic radical **194** needs to be oxidized in order to generate the final product **195.** In this step, deuterium is transferred from the intermediate **194** to the furanone **181.** Most probably, this reaction occurs in two steps. First, electron transfer occurs and in the second step, a proton follows. This sequence explains well the formation of the deuteroxyallyl radical intermediate **196.** After hydrogen abstraction in the β-position from one of the methyl groups of the aniline derivative **187**, and tautomerization the reduction side product **188** carrying a deuterium atom in the α-position is obtained. Intermediates such as **196** are nucleophilic and may therefore be added easily to the α,β-unsaturated carbonyl or carboxyl functions. Thus the oxoally radical **197** is formed and after hydrogen abstraction, the second side product **189**, carrying a deuterium in one of the α-positions is obtained. In the case of the aniline derivative **190**, the deuterium transfer occurs one step later in the mechanism. Deuterium is transferred from the CD_3 group to the hydroxyallyl intermediate **198.** After tautomerization, the lactone side product is obtained with deuterium in the β-position (**191**). This mechanistic investigation was necessary to optimize the process. In this reaction, the furanone substrate acts as an oxidant in the rearomatization step when the

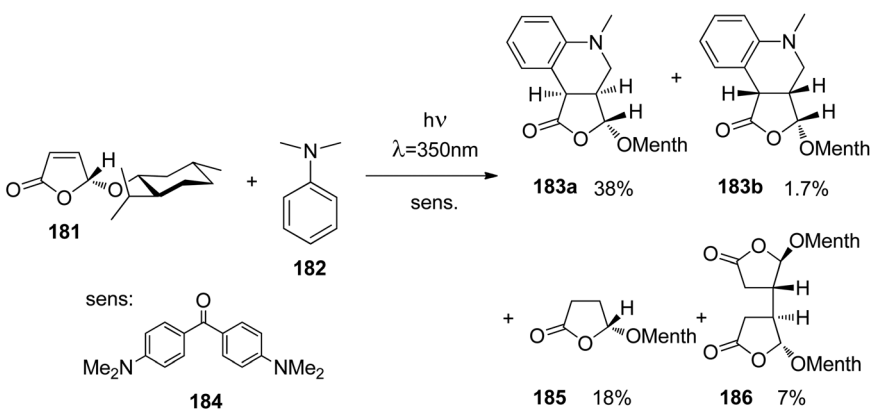

Scheme 38 Radical addition cyclization reaction of aromatic tertiary amines with a furanone.

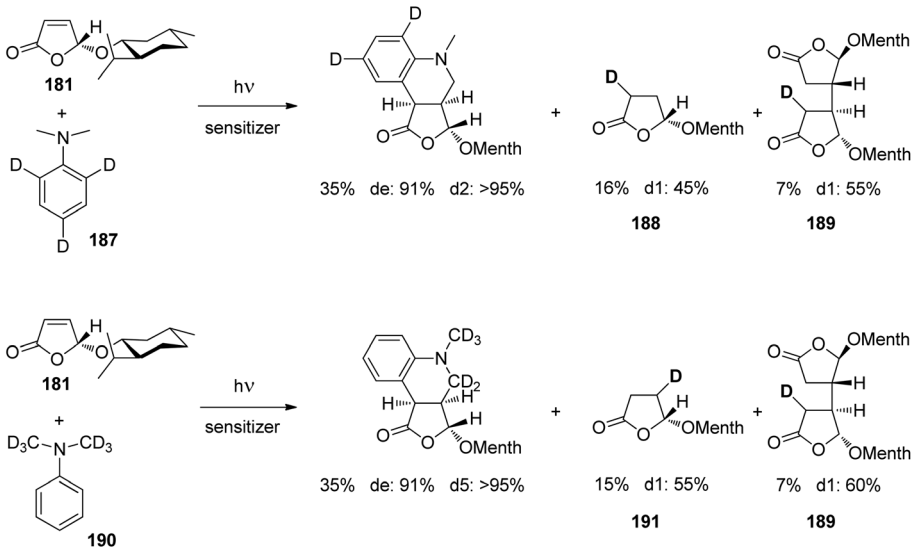

Scheme 39 Isotopic labeling in the radical addition cyclization reaction of aromatic tertiary amines with a furanone.

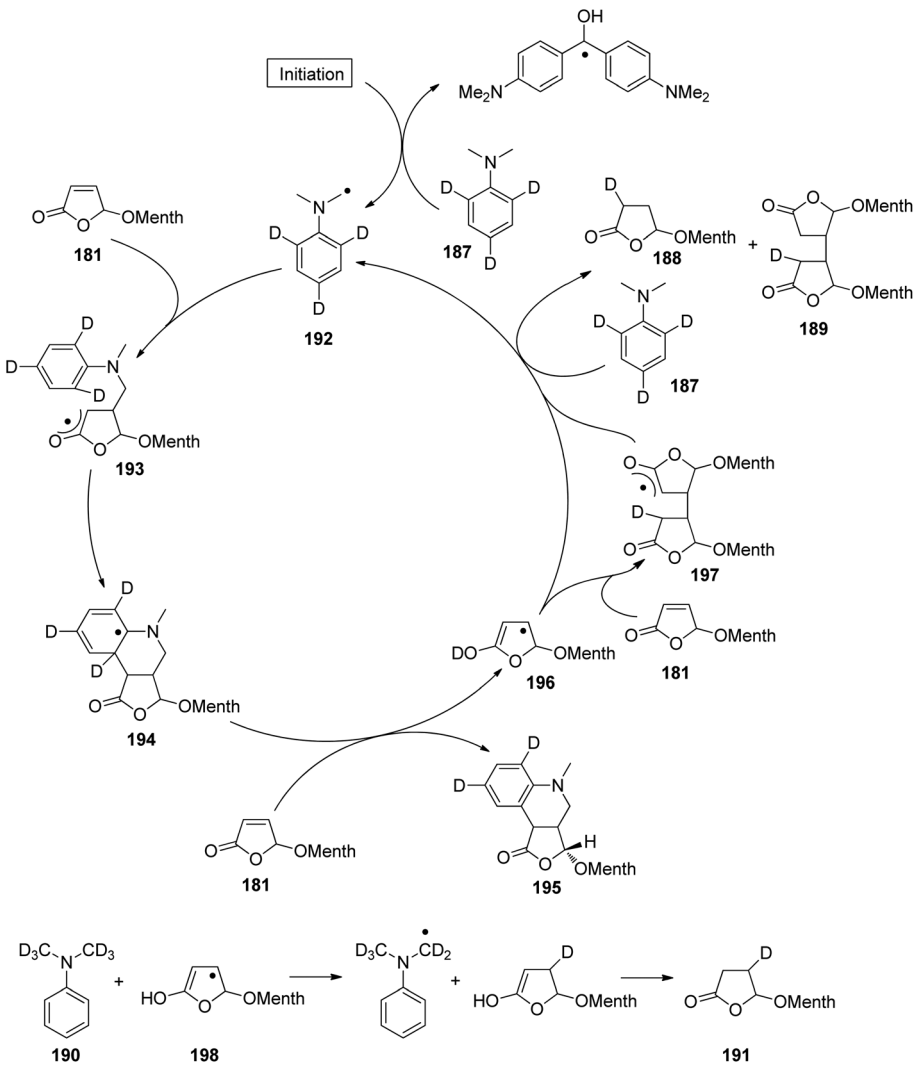

Scheme 40 Proposed mechanism of the radical addition cyclization reaction of aromatic tertiary amines with a furanone based on isotopic labeling.

tricyclic radical intermediate (**194**) is transformed into the final product **195** or **183a,b**. It was therefore concluded that the furanone **181** needs to be replaced by another oxidant in order to stop the consumption of this substrate in the side reaction. This was achieved when simple ketones such as acetone was added to the reaction mixture. Consequently, the yield of the desired tetrahydroquinoline compounds **183a,b** was doubled and the formation of the undesired side products **185** and **186** was completely suppressed. Under the optimized conditions, the reaction was successfully performed with a variety of aniline derivatives.

The diastereoselectivity of addition reactions in the β-position of the chiral furanone **181** at its ground state is almost always complete. The presented tandem addition cyclization reaction with *N*,*N*-dimethylaniline **182** is somewhat less selective. Due to this fact, the transformation was used to investigate in detail the chiral induction in transformations with such alkoxyfuranones.[157]

The tandem addition cyclization reaction of aniline derivatives with furanones was also performed with inorganic semiconductors such as TiO_2 or ZnS as the photochemical electron transfer sensitizer thus applying heterogeneous photocatalysis.[158,159] As in the case of homogeneous photocatalysis, the corresponding isotopic labeling experiments gave a deep insight into some mechanistic steps of the reaction.

Most of the previously discussed photoredox catalytic reactions use UV light.[142,160] These conditions were quite efficient since a lot of chemical reactions of interest for application to organic synthesis have been developed. For example, sophisticated systems of photochemical co-catalysis have been developed. Photoredox catalysis using visible light is now frequently applied to organic synthesis.[140,161] Coordination compounds[162] such as ruthenium trisbipyridine complexes or similar derivatives play a central role in this domain.[163] Very often $[Ru(bpy)_3]^{2+}$ salts are used. The energetically lowest electronic excitation possesses a MLCT character. By light absorption the corresponding singlet state is populated. The values given in Scheme 41 have been determined for aqueous solutions. Intersystem crossing is very efficient and the triplet state is reached. The luminescence quantum yield of this lowest excited state is low and its lifetime is high. Thus many intermolecular quenching processes are possible. Among them reductive and oxidative electron transfers are efficient. Photochemical excitation facilitates both processes. Due to the MLCT character of the excited state, electron transfer from the ligand to the quencher takes place in the oxidative quenching cycle. Consequently, in the reductive quenching cycle, an electron is transferred from the quencher to the metal center. Similar properties are also reported for iridium complexes and many applications to organic synthesis of photoredox catalysis

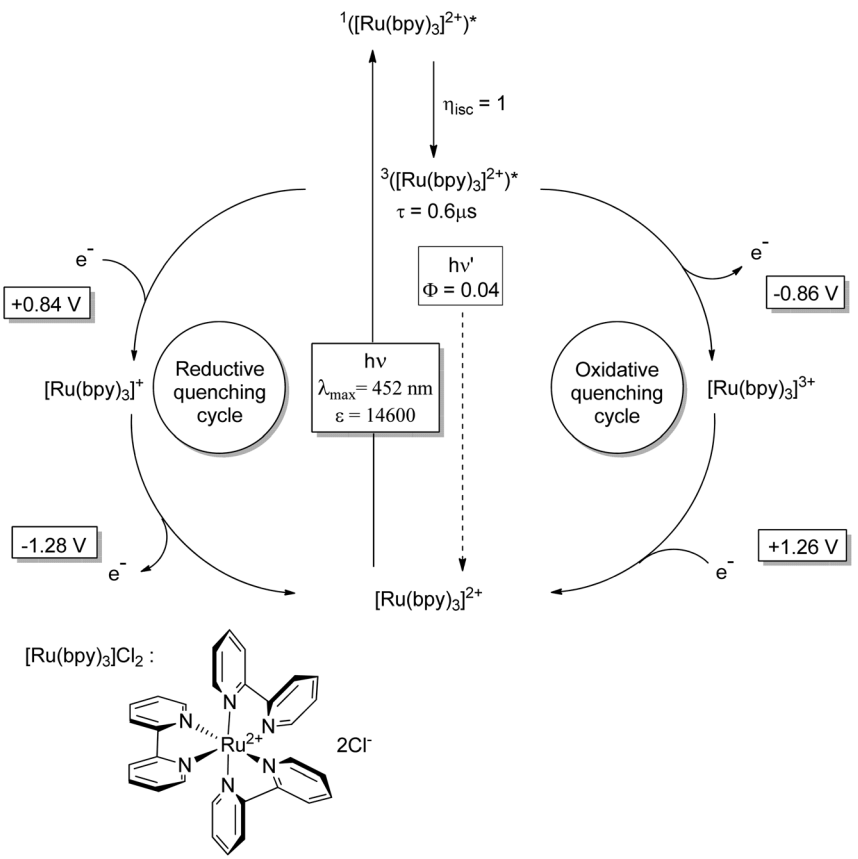

Scheme 41 Redox potentials of $[Ru(bpy)_3]^{2+}$ salts at the ground and excited states.

are also reported with such catalysts. The redox potentials also depend on the substitution pattern of the ligands. A lot of such compounds, in particular from ruthenium, are available and the redox properties of the catalyst can easily be adapted to the requirements of the organic reaction.

Although known for a long time,[164] photoredox catalysis with organometallic and coordination compounds was only recently developed in a systematic manner by many research groups. In particular the photoredox systems involving ruthenium or iridium complexes are very robust and thus a lot of different reactions can successfully be performed. Furthermore, these systems can be combined with other types of catalysis such as organocatalysis. A prominent recent example is the asymmetric alkylation of aldehydes. Combining asymmetric organocatalysis involving enamine intermediates with $[Ru(bpy)_3]^{2+}$ based photoredox catalysis with visible light, phenacyl bromide **199** was added to aldehydes such as **200** (Scheme 42).[165] The mechanism depicted in Scheme 43 has been proposed. The organocatalytic cycle starts with the addition of the organocatalyst **201** to octylaldehyde **200** leading to the enamine **202**. Phenacyl bromide **199** is not electrophilic enough to be added to the enamine **202**. However, the corresponding radical **203** possesses higher reactivity and its addition to **202** yields the α-aminoalkyl radical **204** with high enantiomeric excess. In order to join the normal organocatalytic cycle this intermediate needs to be oxidized to an iminium ion **205**. The latter yields the final product **206** and the catalyst **201** by hydrolysis. This oxidation is performed by the photochemically excited $[Ru(bpy)_3]^{2+}$. The oxidation potentials of α-aminoalkyl radicals such as **204** range between −0.92

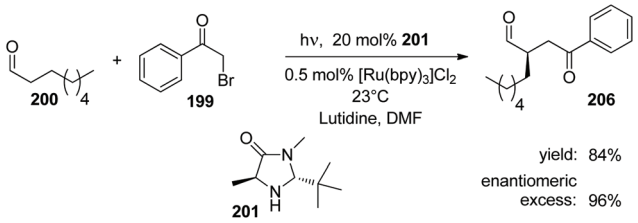

Scheme 42 Photoredox catalysis combined with asymmetric organocatalysis.

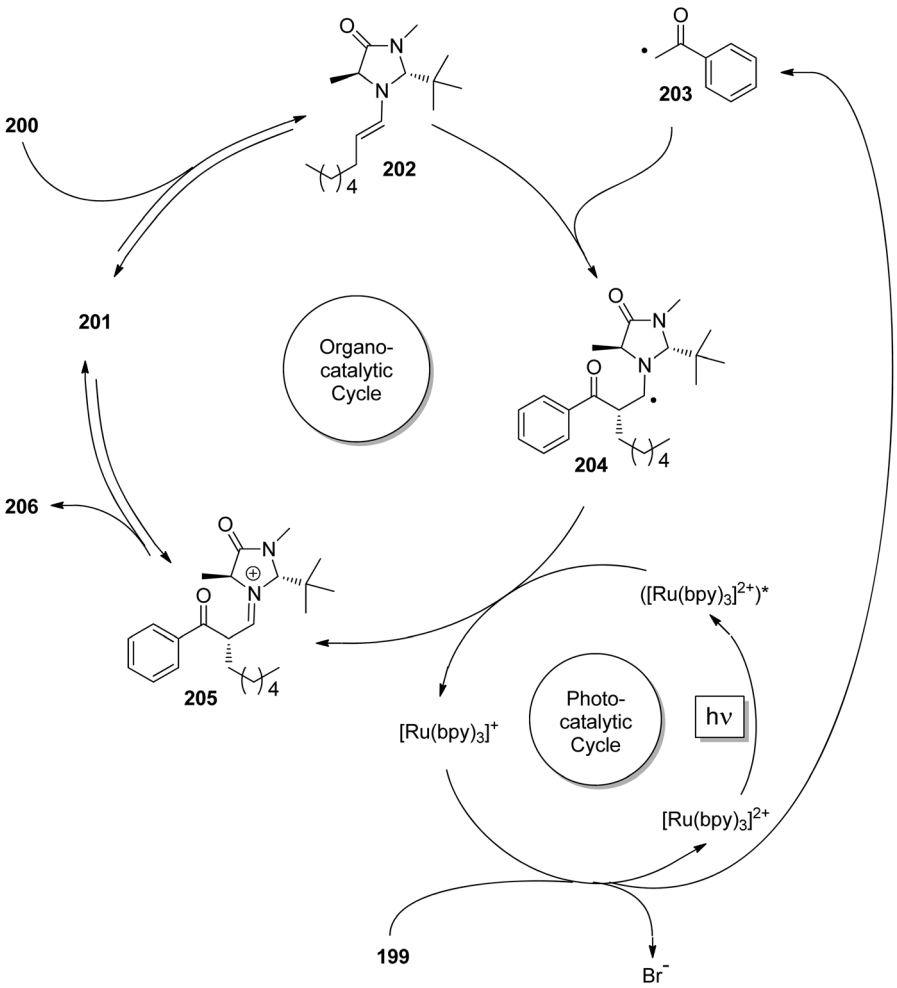

Scheme 43 Mechanism of photoredox catalysis combined with asymmetric organocatalysis.

and −1.12 V (SCE in acetonitrile).[166] The temporary participation of open shell intermediates in catalytic cycles which otherwise only involve closed shell intermediates is also called SOMO catalysis. During the oxidation of **204**, a ruthenium(I) species is generated. This intermediate is a strong reductant (−1.33 V *versus* SCE in acetonitrile).[167] It is therefore capable of reducing phenacyl bromide **199** which has an oxidation potential of −0.49 V (SCE in acetonitrile).[168] The electrophilic phenacyl radical **203** is formed after release of bromide.

The mechanism as is depicted in Scheme 43 needs an initiation step. Most probably, the reaction starts with an electron transfer from sacrificial enamine **202** to the excited ruthenium complex. Once, the first and more reactive α-aminoalkyl radicals **204** are formed, the oxidation of the enamine intermediate does not play an important role any more in the overall reaction. It must be pointed out that in the present example, both the oxidation and the reduction of the ruthenium complex are involved in the formation of the final product. A lot of other photoredox catalytic reactions have been reported in which only one of these redox processes is involved. In such cases, a stoichiometric amount of a sacrificial electron donor or acceptor is needed.

Similar reaction conditions have been applied to the asymmetric fluoro alkylations.[169] In this case, somewhat better results were obtained when the iridium complex $[Ir(ppy)_2(dtb\text{-}bpy)]^+$ was used instead of $[Ru(bpy)_3]^{2+}$. This difference may be explained by the fact that the corresponding $[Ir(ppy)_2(dtb\text{-}bpy)]$ intermediate of the photoredox catalytic cycle is a stronger reductant (−1.51 V *versus* SCE in acetonitrile).[170] Furthermore, such asymmetric alkylation combining photoredox catalysis and organocatalysis is also performed with organic dyes as photoredox catalysts with the same efficiency.[171] Thus the whole catalytic system is organic and one may now distinguish in the catalytic cycles a part with closed shell steps and a part with open shell steps. Inorganic semiconductors such as photoredox catalysts have also been successfully applied.[172]

Interesting reactions have recently been performed with perylenetetracarbox-3,4:9,10-disimides. These dyes are particularly stable especially when electron transfer is involved. For this reason, many studies have been performed with such compounds.[173] The photochemical and electrochemical properties have been intensively studied.[174] Using the perylene derivative **207** as a photoredox catalyst, a cross-coupling reaction between *ortho*-chlorocyanobenzene **208** and pyrrolidine **209** was carried out (Scheme 44).[175] The coupling product **210** was obtained in good yields. Under similar conditions, efficient hydrodehalogenation was also carried out. In such a reaction, the trifluoromethyl pyridine derivative **211** was transformed in high yields into **212**. It must be pointed out that in these reactions aryl chlorides must be reduced and visible light irradiation in combination with the corresponding photo redox catalysts does not provide sufficient energy for such reaction steps. Thus such reaction conditions cannot be applied.

The mechanism depicted in Scheme 45 was suggested to explain the results. After photochemical excitation of the perylene derivative **207**, electron transfer from the sacrificial electron donor trimethylamine (Et_2N) takes place. The resulting radical anion is not capable of reducing substrates such as **208** or **211** in Scheme 44. The reduction redox potential for the formation of this radical anion is −0.88 V (*vs.* Fc^+/Fc). In particular, in the absence of oxygen, such radical anions are remarkably stable and they have been well characterized.[176] Possessing a blue color (characteristic absorption at $\lambda \sim 700$ nm), these species are capable of absorbing a second photon in the visible spectrum range. The electronically excited radical ions reduce the arylchloride thus regenerating the photocatalyst. The resulting radical anion **213** of the arylchloride releases chloride and the aryl radical Ar$^\bullet$ reacts either by hydrogen abstraction or by addition to pyrrole **209** leading to the coupling product **214**. Under more standard photochemical reaction conditions, only UV light provides sufficient energy to generate intermediates for the cleavage of the C–Cl bond. In the present reaction, such a UV photon is replaced by two visible photons. This strategy might considerably increase the application of visible light in organic photochemical reactions.

A further process using two visible photons to generate a higher excited species is photon upconversion.[177] Several types

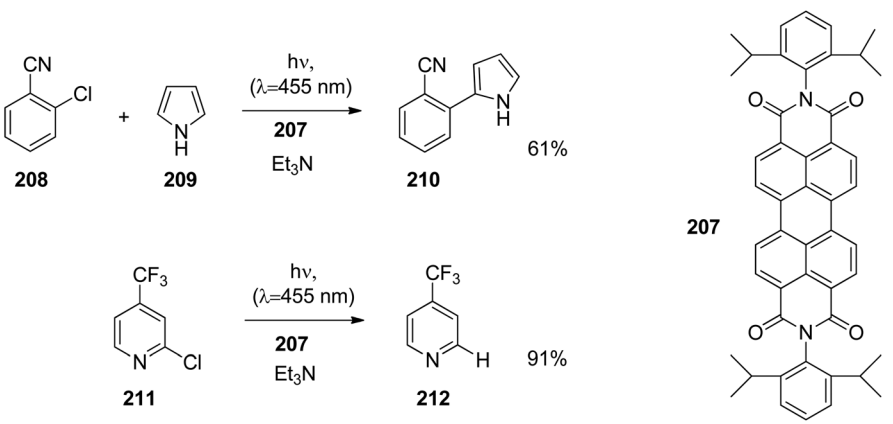

Scheme 44 Photoredox catalytic reactions using perylenetetracarbox-3,4:9,10-disimides as catalysts.

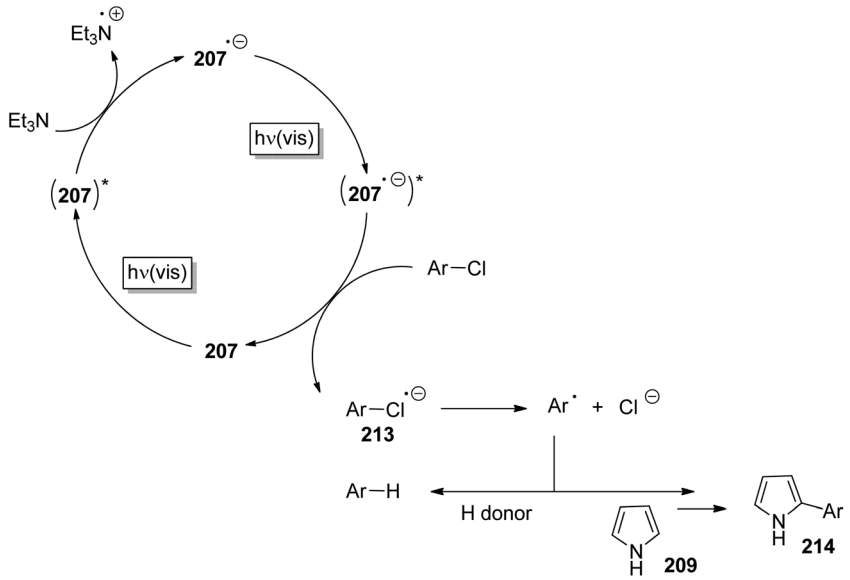

Scheme 45 Mechanism of photoredox catalytic reactions using the perylenetetracarbox-3,4:9,10-disimide **207** involving two visible photon activation.

of processes have been reported. In one of them two triplet excited molecules interact with each other thus generating one molecular at its singlet ground state and a second one at its higher energetic first excited singlet state. Recently, this process has been applied to photoredox catalysis using metal free sensitizers.[178]

The previously discussed examples of photochemically supported or induced catalytic reactions involving organometallic or coordination compounds are based on electron transfer. In another type of metal catalysis, ligand exchange plays a key role. These steps are also affected by photochemical reaction conditions. A typical example is the Vollhardt reaction with inexpensive cobalt catalysts.[179] Three acetylene moieties are combined in a [2 + 2 + 2] cycloaddition to form an aromatic compound. This reaction is an important method to synthesize a large variety of such compounds. Although the reaction occurs occasionally under thermal conditions, the best results are obtained when the reaction mixture is irradiated with visible light. The same reaction is also used to synthesize pyridines by combining two acetylene moieties with a nitrile.[180] In this case, detailed investigations have been carried out in order to characterize the significant influence of light[181] on the outcome. The enantiopure nitrile **215** was transformed with two equivalents of acetylene to yield the corresponding pyridine derivative **216** (Table 6).[182] Under photochemical reaction conditions (irradiation with visible light) and when compared to thermal reaction conditions,[183] the catalyst concentration was reduced. The reaction was carried out at room temperature and atmospheric pressure instead of high temperature and high pressure. The reaction was faster and the yields were increased. It must further be pointed out that in this particular example, heating of the acetylene containing reaction mixture under pressure causes

Table 6 Comparison between thermal and photochemical conditions for the [2 + 2 + 2] cycloaddition of acetylene to the chiral pyridine **216**

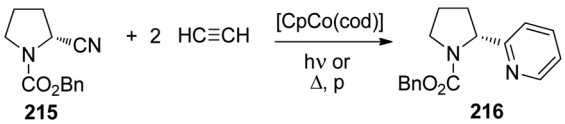

	Conditions				
Method	CpCo(cod) (mol%)	T (°C)	p (atm)	t (h)	Yield (%)
$h\nu$	0.5	25	1	4	90
Thermal	3.2	110	14	22	82

an explosion risk. Under these soft photochemical reaction conditions, efficient asymmetric catalysis was also performed.[184] As visible light is used to promote this catalysis, a similar reaction was performed with sunlight on an industrial scale.[185]

In order to characterize the influence of light on this catalytic reaction, detailed kinetic investigations have been carried out.[186,187] The reaction starts with the generation of the catalytically active species $CpCo^{I}$ by release of cyclooctadiene from the cobalt complex **217** (Scheme 46). The addition of two molecules of acetylene generates the cobalacyclopentadiene intermediate **218**.[188] The addition of a nitrile molecule leads to the formation of the intermediate **219** and then to the final product **220**. Under thermal reaction conditions the formation of the cobalacyclopentadiene intermediate **218** is the rate limiting step. The reaction is of zero order kinetics in nitrile consumption and of second order in acetylene consumption. Under photochemical conditions, first order kinetics is observed for the consumption of the nitrile. That means that

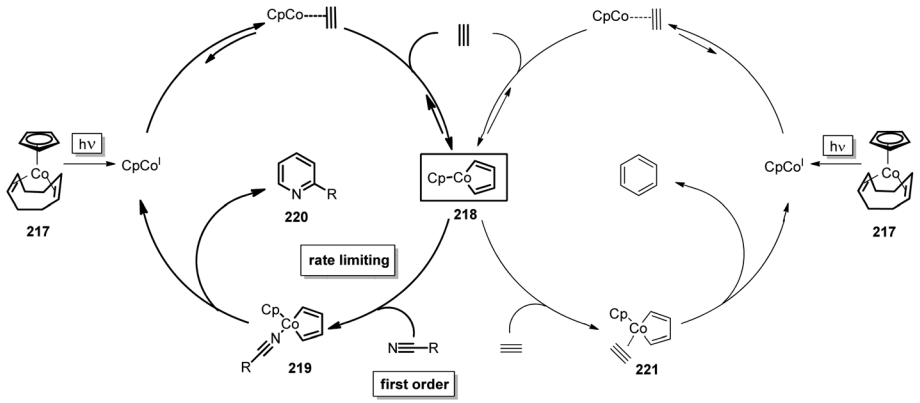

Scheme 46 Mechanism of the photochemically supported [2 + 2 + 2] cycloaddition leading to pyridines.

the formation of the metallacyclic intermediate **218** is accelerated and the addition of the nitrile to **218** leading to the intermediate **219** has become the rate limiting step. Irradiation with visible light accelerates the generation of the catalytically active species $CpCo^{I}$ from the cobalt complex **217**. Most probably, other mechanistic steps are also affected by the photochemical conditions. The formation of benzene is a competing reaction. In this case acetylene is added to the metallacyclic intermediate **218** leading to the intermediate **221**. Due to the higher reactivity of the nitrile with intermediate **218**, this side reaction generally plays only a minor role. However, due to the high acetylene pressure needed when thermal reaction conditions are applied, the formation of benzenes may become very disadvantageous. Using photochemical reaction conditions, the concentration of acetylene may be kept low which reduces the formation of benzene derivatives. Thus the transformations may also be carried out in solvents such as water in which the acetylene solubility is low.[189]

Enzymatic catalysis may also be affected by photochemical reaction conditions. Recently, a number of investigations have been performed with peroxidases. Thus the chloroperoxidase (CPO) isolated from *Caldariomuces fumago* is capable of oxidizing thioethers such as thioanisole **222** (Scheme 47 and Table 7).[190] The corresponding sulfoxide **223** is formed in high

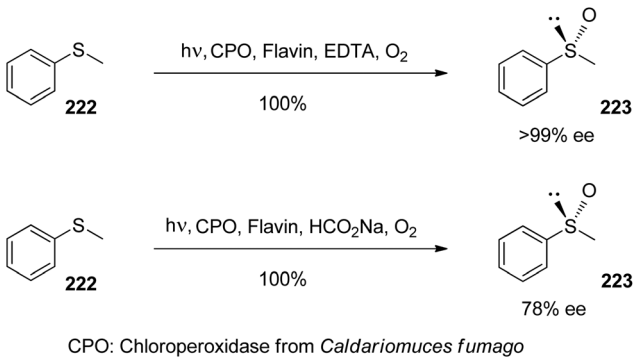

Scheme 47 Photochemical co-catalysis in an enzymatic CPO catalyzed oxidation.

Table 7 Effect of photochemical co-catalysis on an enzymatic CPO catalyzed oxidation of **222** (Scheme 47)

	Conversion (%)	Turnover number (CPO)
H_2O_2	30	6720
$h\nu$/flavin/O_2	100	22 400[a]

[a] Turnover number of the cocatalytic system: 1250.

yield and high enantioselectivity when a photochemical redox reaction is involved as a co-catalytic process and when oxygen is used as the oxidant. Furthermore, no overoxidation is observed. Under normal conditions, this enzyme employs hydrogen peroxide as the oxidant. When the reaction is performed under these standard conditions with stoichiometric amounts of H_2O_2, conversion and turnover number (for CPO) remain low (Table 7). These observations are explained by the mechanism depicted in Scheme 48. In a photochemical redox reaction, flavin **224** is reduced. EDTA or HCO_2Na are used as sacrificial electron donors. The reduced flavin derivative **225** is oxidized by molecular oxygen which leads to the formation of hydrogen peroxide. The advantage of this process using a photoredox process as co-catalysis is that the stationary concentration of H_2O_2 is kept low which prevents the enzyme from decomposition. Thus the high turnover numbers may be explained.

The particularly difficult activation of a C–H bond is involved in the highly enantioselective oxidation of tetrahydronaphthalene to tetrahydronaphthalen-1-ol which was accomplished with *Agrocybe aegerita* aromatic peroxygenase (AaeAPO).[191] Using the same photoredox co-catalysis with flavin derivatives, a turnover number of 17 520 and a turnover frequency of 366 min^{-1} (both values for the enzyme) were determined. Using the same catalytic system, alkenes are oxidized to epoxides. In biological systems, some of these oxygenases use a natural redox reaction based on enzyme fixed flavin derivatives to produce hydrogen peroxide. In this case, the reduced flavin derivative can be generated by NADPH which itself is generated from $NADP^{+}$ by a dehydrogenase, for

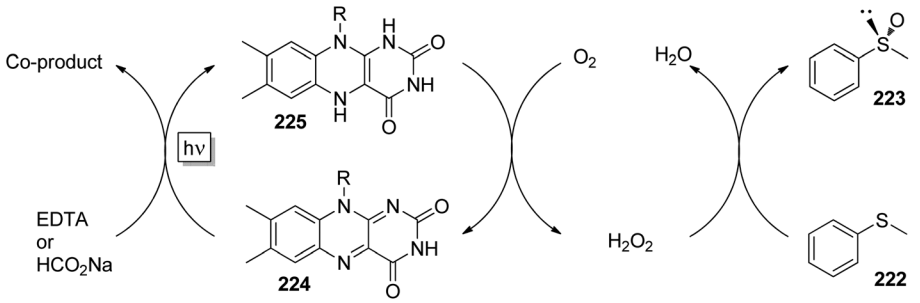

Scheme 48 Mechanism of photochemical co-catalysis in an enzymatic CPO catalyzed oxidation.

example glucose dehydrogenase. Thus, two enzymes are involved in the oxidation process. In the case of a phenyl acetone monooxygenase mutant, the NADPH cofactor system was replaced by an additional flavin based photoredox co-catalytic system.[192] In such a system, the enzyme bound flavin is reduced by the added free flavin. Thus the expensive and inconvenient dehydrogenase co-catalysis is avoided.

6 Photooxygenation with singlet oxygen

In contrast to most organic molecules and many inorganic molecules, the ground state of oxygen possesses triplet spin multiplicity (Scheme 49).[193,194] Two antibonding π orbitals are occupied by one electron. Two configurations are possible for energetically low singlet excited states. In the S_1 state, one of the antibonding π orbitals is occupied by two electrons while the other is unoccupied. At this state, the oxygen is particular polarizable. Most of the reactions of singlet oxygen occur at this state. In the S_2 state, the two antibonding orbitals are occupied, each by one electron with opposite spin. Despite its low electronegativity and due to spin forbidden interactions between triplet and singlet species, the chemical reactivity of oxygen at the ground state is reduced.[194] Also for this reason, biomolecules along with many other molecules at a singlet ground state are stable in an oxygen containing atmosphere and most of the known living organisms could evolve under these conditions (for some recent studies on these properties see ref. 195). Reactions of triplet oxygen are often characterized by radical intermediates. In contrast to this, singlet oxygen should possess a much higher reactivity and polar intermediates should also play an important role in the reaction mechanism. Photochemically, singlet oxygen is most conveniently produced by sensitization (Scheme 50). Since the excitation energy is low (22.4 kcal mol^{-1} for the S_1 state), dyes absorbing visible light are most frequently used.

Photooxygenation with singlet oxygen considerably enriches the oxidation methodology in organic synthesis.[196–198] Furthermore, the simple and cheap oxidants, air or molecular oxygen, are used to perform sophisticated oxidations. In this context, the reactions with alkenes are of particular interest. A certain number of intermediates are involved in such transformations. First, exciplexes are formed (Scheme 50). Depending on the redox potentials of the reaction partners and the reaction medium more or less stable ion radicals **226** are formed. Formation of σ-bonds leads to intermediates such **227a,b,c** depending on the structure of the alkenes (Scheme 50). In order to explain the outcome of organic photooxygenation, these intermediates are of particular interest.[198,199] In particular, the regio- and stereoselectivity of many transformations

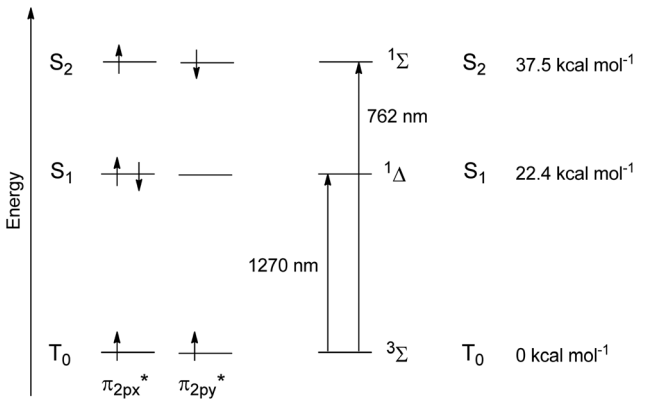

Scheme 49 Electron configurations and energy levels of oxygen.

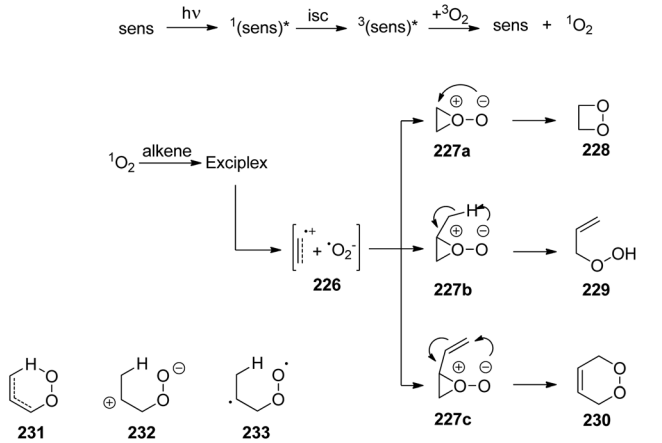

Scheme 50 Intermediates of photooxygenations.

may be explained when considering these structures. Three reactions of singlet oxygen and alkenes are most frequently observed. The tricyclic intermediate **227a** may rearrange to form a dioxetane, the product of a [2 + 2] cycloaddition (**228**). The same type of intermediate (**227b**) also may undergo rearrangement leading to a hydroperoxide **229**. In the case of dienes the corresponding intermediate (**227c**) leads to endoperoxides such as **230**. Intermediates of transition states such as **231**, **232**, or **233** are also discussed.

Asymmetric synthesis with photochemical reactions is particularly interesting since highly energetic states and intermediates are involved.[6,200,201] In the past, photochemical reactions were often considered as inherently unselective since it was supposed that the loss of the activation energy excess could only occur in an uncontrolled way *via* numerous reaction channels. It was concluded that photochemical reactions are only of little interest for application to organic synthesis. However in the large majority of photochemical reactions, the loss of the high electronic excitation energy occurs in a very controlled or defined way and the reactions become highly selective. This has already been shown by the previously discussed reactions. This topic is also well illustrated by the following example of an asymmetric photooxygenation of encarbamates.[201] In this case, two processes, the ene reaction and the formal [2 + 2] photocycloaddition (dioxetane formation), are in competition (Scheme 51).[202] In the case of *Z*-**234**, the dioxetane **235** is the major product. The ene product **236** is only formed in minor amounts. The ratio varies between 75 : 25 and 87 : 13 in favor of **235** depending on the substituent R. In the case of *E*-**234**, the formation of the ene product **236** is favored with respect to **235**. The product ratios range between 64 : 36 and 92 : 8 in favor of **236**. This product selectivity was mainly explained by frontier orbital interactions as depicted in structures **237** and **238** of the transition states for the approach of singlet oxygen. Other directing effects have been identified later. The nitrogen atom of **234** conducts the oxygen to the alkene. In the case of *Z*-**234**, hydrogen transfer from the distant methyl group is thus inhibited. In the case of *E*-**234** the methyl group is close to the approaching singlet oxygen. Hydrogen transfer is facilitated and the ene reaction is favored. In the case of the ene reaction and the reaction of *Z*-**234**, the diastereoselectivity ranges from 53 : 47 (R = Me) to 95 : 5 (R = *t*Bu) in favor of the *ul* attack. In the case of the reaction of *E*-**234**, it ranges from 56 : 44 (R = iPr) to 91 : 9 (R = *t*Bu). In contrast to the diastereoselectivity of the ene reaction, that one of dioxetane formation is very high, around 99 : 1 and does not depend on the nature of R. Transition states of both reactions and their impact on the stereoselectivity resemble the corresponding epoxy like structures as depicted in Scheme 50 (**227a,b**).[203]

Further remarkable effects were observed concerning the stereoselectivity. This topic was studied in detail for the formal [2 + 2] addition of singlet oxygen to ene carbamates leading to dioxetanes. Compounds *Z*-**239** and *E*-**239** carrying an additional chiral phenethyl substituent in position 2 have been transformed (Scheme 52). The absolute configurations of the dioxetanes **240** and **241** have been determined by chemical correlation transforming them into diols **242**. In many cases in particular in the reactions of *E*-**239**, the resulting dioxetanes are not stable and decompose into diphenylpropanone **243** and the oxazolidinone derivative **244**. As already pointed out and in contrast to the corresponding ene reaction, the diastereoselectivity in this transformation is very high and does not depend on the substituent R (Table 8). When R = Me (entry 1) the same diastereoselectivity is observed than in the cases of higher encumbering substituents such as R = iPr (entries 2 and 3), R = *t*Bu (entry 5) or R = Ph (entry 6). This is surprising because the oxygen molecule is small and the stereodifferentiation of the attack in both diastereotopic half spaces should not be very different as is the case for the corresponding ene reaction. Only in the case of the deuterated substituent, the diastereoselectivity is lower. This effect will be discussed later. The configuration at the center 3 or the relative configuration of both stereo-centers has no influence on the diastereoselectivity (entries 2 and 3). At this stage, no effect of double induction[204] is detected. Furthermore, it was found that the *E*-**239b** reacts with the same diastereoselectivity than the corresponding *Z*-**239b** which means that the chiral center

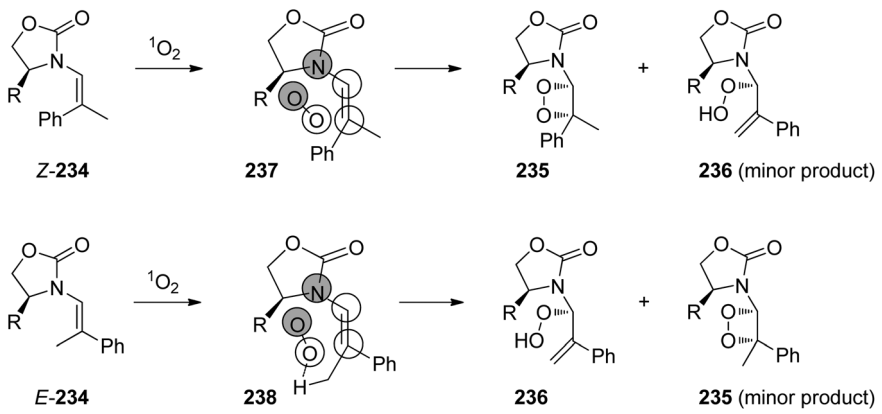

Scheme 51 Photooxygenation of ene carbamates.

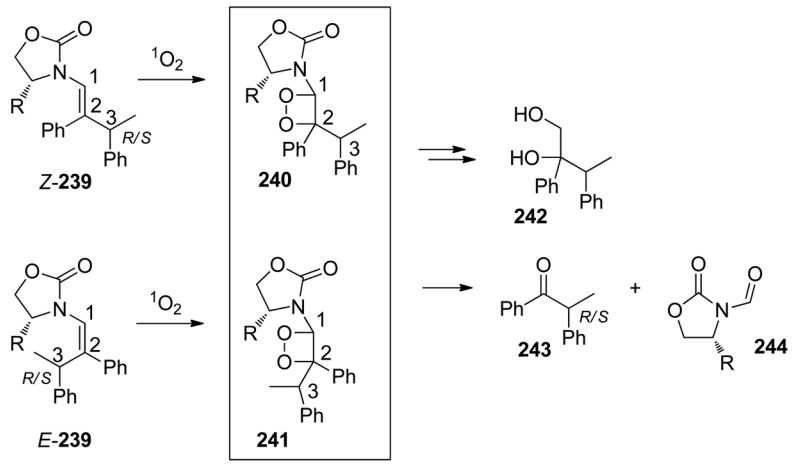

Scheme 52 Chemical correlation for the determination of the chiral induction in the photooxygenation of ene carbamates, cleavage of dioxetanes leading to diphenylpropanone **243** and the oxazolidinone derivative **244**.

Table 8 Diastereoselectivity of the photooxygenation[a] of encarbamates **239** (Scheme 53)

		Configuration		Diastereomeric ratio
Entry	Substrate	R	C-3	(1*S*,2*S*)/(1*R*,2*R*)
1	*Z*-**239a**	(*R*)-Me	(*S*)	99 : 1
2	*Z*-**239b**	(*R*)-iPr	(*S*)	99 : 1
3[b]	*Z*-**239c**	(*S*)-iPr	(*S*)	1 : 99
4[b]	d_8-*Z*-**239c**	d_7-(*S*)-iPr	(*S*)	10 : 90
5	*Z*-**239d**	(*S*)-*t*Bu	(*R*)	1 : 99
6	*Z*-**239e**	(*S*)-Ph	(*S*)	1 : 99
7[b]	*E*-**239b**	(*R*)-iPr	(*S*)	99 : 1[c]

[a] The transformations were carried out at −32 °C in $CDCl_3$ until complete conversion. No competing ene reaction was detected. [b] The reactions were carried out in CD_2Cl_2 as the solvent. [c] The corresponding diastereomeric ratio is (1*S*,2*R*)/(1*R*,2*S*).

in position 1 in **240** or **241** of the dioxetane ring is formed with the same relative configuration with respect to the chiral center of the carbamate ring (entries 7 and 2). Concerning the stereochemistry of the singlet oxygen approach to the enamine moiety, X-ray structure analytical data were discussed and it was assumed that similar privileged conformations exist in solution.[201,202,205] It was found that in the case of the *Z*-isomer, the oxazolidinone ring is placed almost in the plane of the enamine moiety (Scheme 53). For steric reasons, the attack of the singlet oxygen occurs *anti* with respect to the R substituent of the oxazolidinone ring. In the case of the *E*-isomers, the oxazolidinone ring is almost orientated orthogonally with respect to the enamine plane. The singlet oxygen approaches preferentially from the same side leading to a dioxetane with the same relative configuration with respect to the

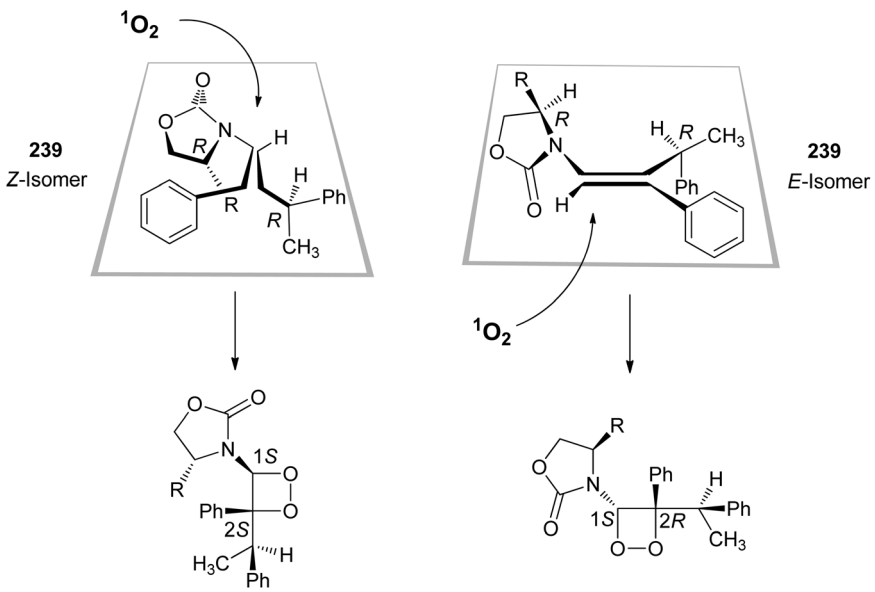

Scheme 53 Diastereoselective photooxygenation of *Z* and *E*-ene carbamates **239**. Structures of the substrates are based on X-ray structure analysis.

chiral center in the oxazolidinone ring. In this case, the singlet oxygen is further conducted in this diastereomeric half-space by an interaction with the carbonyl group of oxazolidinone.[206]

As has already been pointed out, the chiral center in position 3 of compounds such as **239** (Scheme 52) has no influence on the diastereoselectivity of dioxetane formation and consequently, the decomposition product 1,2-diphenylpropan-1-one **243** was obtained as a racemic mixture. A closer look at this transformation revealed however that the two diastereoisomers react with different rates.[205,207,208] Consequently and depending on the difference of these two rates, the ketone **243** is obtained in an enantiomeric excess when the reaction is stopped before conversion is complete. For example, when a 1 : 1 mixture of the diastereoisomers *E*-**239f** and *E*-**239b** is photooxygenated, in CD_3OD as the solvent, at 50 °C and when the reaction is stopped at a conversion of 30%, **243** is isolated with 70% ee in favor of the *R* enantiomer (Scheme 54).[207] When the same mixture of diastereoisomers is photooxygenated in CD_3CN as the solvent, at 50 °C and when the reaction is stopped at a conversion of 23%, **243** is isolated with 64% ee in favor of the *S* enantiomer. In view of the asymmetric synthesis of the chiral ketone **243**, this transformation is a kinetic resolution.[209] In such reactions the enantiomeric excess (ee) depends on the progress of the conversion *C*. The product ratio results from the rate ratio k_R/k_S which determines the stereoselectivity *s* of the reaction. These parameters are combined in eqn (2).

$$s = \frac{k_R}{k_S} = \frac{\ln[1 - C(1 + \mathrm{ee}(\mathbf{243}))]}{\ln[1 - C(1 - \mathrm{ee}(\mathbf{243}))]} \quad (2)$$

Based on this equation, the selectivity *s* or the rate ratio k_R/k_S can be calculated when the conversion and enantioselectivity of a transformation are determined as is usually the case. In Fig. 9, this relation is depicted. In particular when the selectivity is high, best ee values are observed for conversions around 50%.

To get a deeper insight into the mechanistic details of the stereoselectivity, the selectivity *s* or the rate ratio k_R/k_S was determined at different temperatures using different solvents.[205] For the *E* isomeric substrates (Chart 1), a high dependence of the enantioselectivity of **243** from these parameters is observed. This is not the case for the corresponding *Z* isomers.[207] Using the Eyring relation (eqn (3)) and a corresponding plot, the enthalpy and the entropy contribution to the free enthalpy $\Delta\Delta G^{\neq}$ of the diastereoselectivity are determined.

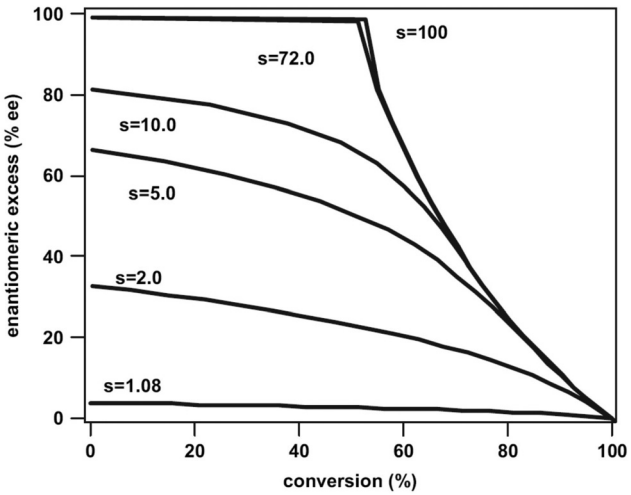

Fig. 9 Dependence of enantiomeric excess of **243** on the conversion in the photooxygenation of ene carbamates (compare Scheme 54). (Reprinted with permission from: J. Sivaguru, M. R. Solomon, H. Saito, T. Poon, S. Jockusch, W. Adam, Y. Inoue and N. J. Turro, *Tetrahedron*, 2006, **62**, 6707–6717. Copyright (2006) with permission of Elsevier.)

$$\ln\frac{k_R}{k_S} = \frac{-\Delta\Delta G^{\neq}_{R-S}}{RT} = \frac{-\Delta\Delta H^{\neq}_{R-S}}{RT} + \frac{\Delta\Delta S^{\neq}_{R-S}}{R} \quad (3)$$

When *s* or the rate ratio $\ln(k_R/k_S)$ is plotted against T^{-1}, linear relationships are observed and $\Delta\Delta H^{\neq}$ and $\Delta\Delta S^{\neq}$ values can be determined from the slope and the intersection with the *y*-axis respectively. Fig. 10 shows such plots for the photooxygenation of *E*-**245a** in different solvents and for *E*-**245b** in CD_2Cl_2. The highest enantioselectivity is observed in CD_3OD at low temperatures. Particularly when the reaction is carried out in CD_3CN or in CD_2Cl_2, it was observed that by increasing the temperature, the formation of *R*-**245** is favored no more and instead that of *S*-**243** is. According to the Eyring equation, at higher temperature, the entropy contribution increases and

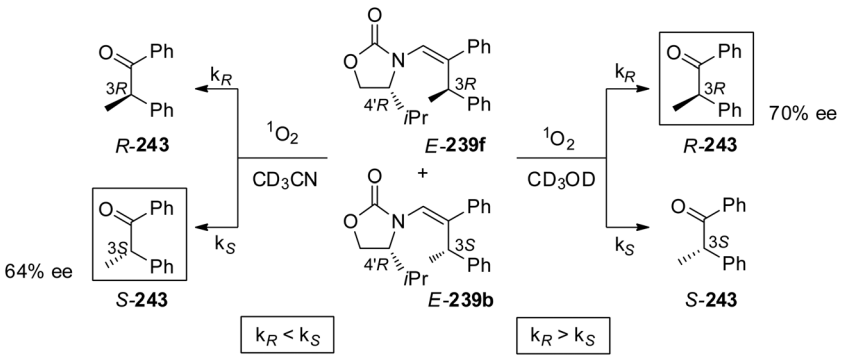

Scheme 54 Kinetic resolution by photooxygenation of ene carbamates.

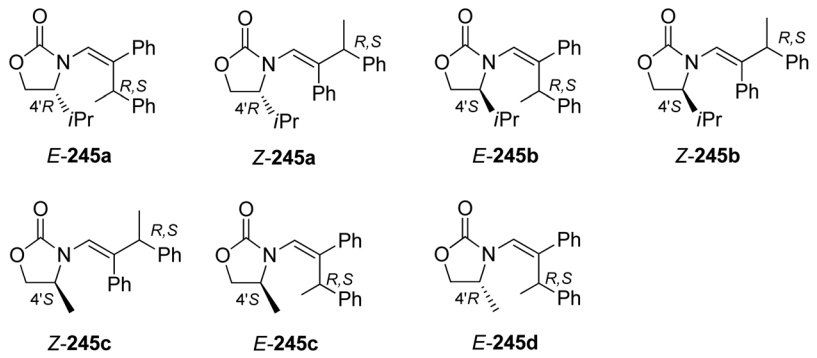

Chart 1 Compounds used to determine the influence of the reaction temperature and the solvent on the stereoselectivity.

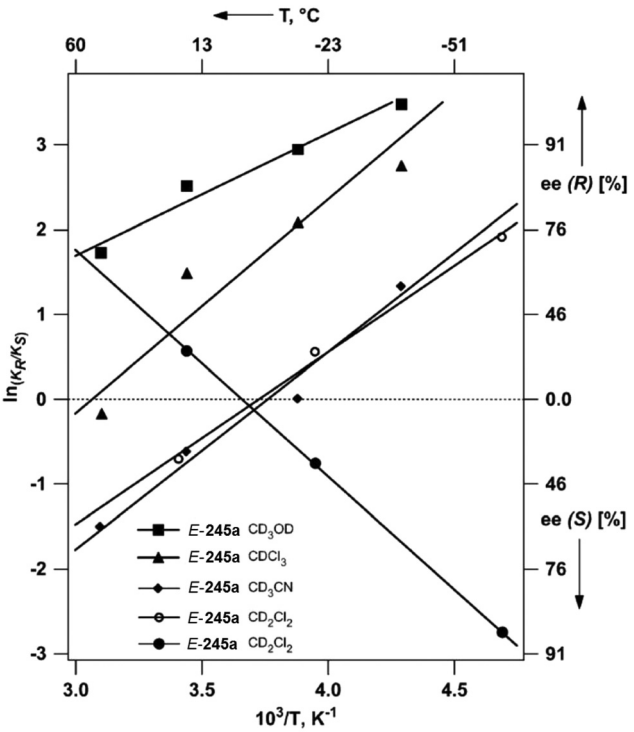

Fig. 10 Photooxygenation of *E*-**245a** and *E*-**245b** (Chart 1) in different solvents. (Adapted with permission from: J. Sivaguru, M. R. Solomon, H. Saito, T. Poon, S. Jockusch, W. Adam, Y. Inoue, N. J. Turro, *Tetrahedron*, 2006, **62**, 6707. Copyright (2006) with permission of Elsevier.)

may become dominant. Thus the privileged formation of the *S*-**243** is favored by the entropy while the privileged formation of *R*-**243** is favored by the enthalpy. Such behavior is generally observed when conformational mobility plays a more important role than simple steric hindrance (in rigid structures). Indeed, these observations are in contrast to the more rigid structure of *Z*-**245b** or *Z*-**245c** for which the $\Delta\Delta H^{\neq}$ and $\Delta\Delta S^{\neq}$ are small and the temperature dependence of the enantioselectivity is low. Due to the fact that the chiral center at the oxazolidone moiety is changed in *E*-**245b** with respect to *E*-**245a** the corresponding lines for the photooxygenation in CD_2Cl_2 are mirroring. Their intersection is close to the *x*-axis and the corresponding $\Delta\Delta H^{\neq}$ and $\Delta\Delta S^{\neq}$ values have opposite signs.

As pointed out above, the entropy ($\Delta\Delta S^{\neq}$) and the enthalpy contribution ($\Delta\Delta H^{\neq}$) to the free enthalpy ($\Delta\Delta G^{\neq}$) of the enantioselectivity is different for each system (molecular structure, solvent). It is further observed that the difference of the enthalpy contribution between two systems is proportional to the corresponding difference of entropy contribution which means that there exists a linear relationship between $\Delta\Delta H^{\neq}$ and $\Delta\Delta S^{\neq}$. A change in entropy contribution is compensated by a change in enthalpy contribution. When activation enthalpies and activation entropies are involved such compensation phenomena are called isokinetic or isoselective relationships.[51,81,88–90,210] The observation of such a relationship in the present case indicates that the photooxygenations of investigated enecarbamates[205,207] possess the same reaction mechanism. In Fig. 11, the isoselective relationship is

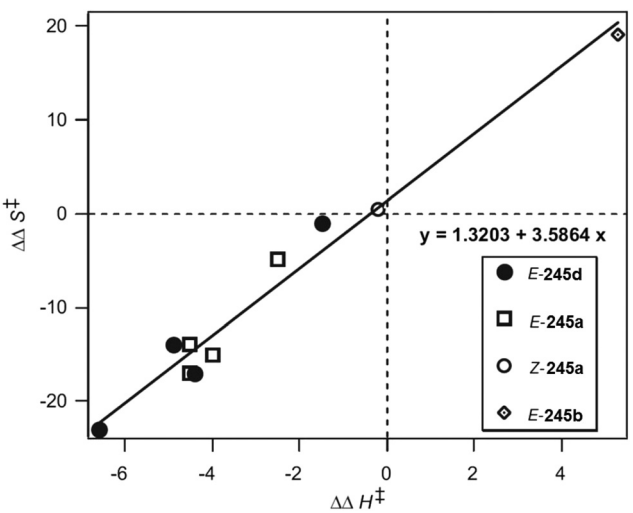

Fig. 11 Isoselective relationship for the photooxygenation of various enecarbamates. (Adapted with permission from: J. Sivaguru, M. R. Solomon, H. Saito, T. Poon, S. Jockusch, W. Adam, Y. Inoue, N. J. Turro, *Tetrahedron*, 2006, **62**, 6707. Copyright (2006) with permission of Elsevier.)

depicted. The photooxygenation of compounds *E*-**245d** and *E*-**245a** have been performed in 4 different solvents as indicated above while *Z*-**245a** and *E*-**245b** have been transformed only in CD_2Cl_2.

It is surprising that the interaction of a small particle such as singlet oxygen can cause such high enantioselectivities, even in conformationally labile systems as just outlined above. In fact, $^1O_2$ is the smallest oxidation reagent commonly used in organic synthesis. Oxidations of chiral ene carbamates with the somewhat more encumbering ozone were much less selective.[208] Therefore, reasons other than only steric interactions have been suggested in order to explain the stereoselectivity increase of the photooxygenation of ene carbamates. In particular, deactivation of singlet oxygen has been discussed in this context. It is well known that the lifetime of the singlet oxygen is much higher in deuterated than in the corresponding non-deuterated solvents.[197,211,212] Vibrations of a C–H bond more efficiently quench singlet oxygen than C–D bonds. This effect has an impact on the diastereoselectivity. In fact, the stereoselectivity of the photooxygenation of *Z*-**239c** is higher than that of d_8-*Z*-**239c** (Table 8). The photooxygenation in a diastereotopic half-space containing a lot of C–H bonds is less efficient than the one in a diastereotopic half space with only few of such bonds since in the first case vibrationally induced deactivation of singlet oxygen is more efficient. Or, a diastereoisomer is slowly oxidized when it assembles a large number of C–H bonds in the volume element in which the singlet oxygen approaches the substrate. A competing diastereoisomer that assembles a lower number of C–H bonds in this volume element is rapidly oxidized. These effects have been discussed in the photooxidation of *E*-**245c** (Scheme 55 and Table 9).[205] When carried out in acetonitrile as an aprotic solvent, the 3*S*-*E*-**245c** epimer was more rapidly transformed ($k_R < k_S$) at higher temperature (18 °C) while at low temperature (−40 °C) *R*-**243** was preferentially formed ($k_R > k_S$). A closer inspection of the X-ray structures revealed that in the case of the 3*R*-*E*-**245c** epimer, the methyl group of the oxazolidone moiety and the phenyl substituent of the phenethyl moiety are oriented opposite to each other in two diastereotopic half-spaces. In the case of the 3*S*-*E*-**245c** epimer, the methyl groups of the oxazolidone and the phenethyl moieties are in the same diastereotopic half-space. When it is assumed that the crystalline structure resembles the privileged conformation in solution at low temperature, the reactive center of the epimer 3*S*-*E*-**245c** is better protected by C–H bonds and consequently the deactivation of singlet oxygen is more efficient. The photooxygenation of this stereoisomer is slower and the formation of *R*-**243** from 3*R*-*E*-**245c** is faster. At higher temperatures, other conformations may be favored inducing the opposite stereoselectivity as was indeed observed at higher temperatures (18 °C). Furthermore, steric hindrance may become more important with respect to the deactivation rates of singlet oxygen.

Table 9 Photooxygenation of *E*-**245c** at different temperatures (Scheme 55)

Temperature (°C)	**243** (% ee)	Conversion (%)	s^a
18	28 (*S*)	18	0.5
−15	0	55	1.0
−40	45(*R*)	33	3.3

[a] Selectivity calculated according to eqn (2).

These investigations nicely show how excess energy of an electronically excited species can be released in a very controlled manner leading to highly selective transformations. As has already been pointed out, this property of photochemical reactions is essential for application to organic synthesis. Similar discussions may be performed for many other organic photochemical reactions.

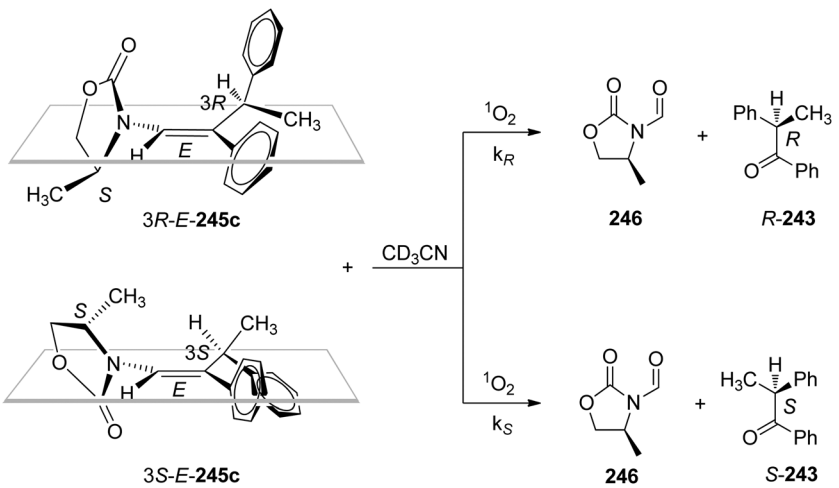

Scheme 55 Stereoselective photooxygenation of two ene carbamate epimers.

7 Photochemical reactions in micro and continuous flow reactors

Photochemical reactions on the laboratory-scale are traditionally performed in batch mode using either immersion well or chamber reactors.[213] Immersion well systems (Fig. 12a) enable individual irradiations of larger volumes (≤1 L) and comprise a central mercury pressure lamp, an immersion well (effectively a cooler for the lamp) and an outer reaction vessel. Chamber reactors utilize an outer array of fluorescent tubes and reaction vessels are inserted into the vacant inner chamber (Fig. 12b). These more flexible systems are typically used for small-scale synthesis (≤250 mL).

Conventional batch photoreactors have a number of disadvantages that have restricted their applications on large, technical scales. As a consequence of the Beer–Lambert law,[214] light is rapidly absorbed by the chromophoric reagent. Consequently, photochemical processes require high dilutions and narrow reaction vessels. The constant irradiation of the reaction mixture additionally favors degradations and polymerizations of light-sensitive products, thus reducing yields and necessitating resource-demanding purifications. Iron and polymer deposits on glass parts around the light source are also common and demand constant cleaning and maintenance. The intense heat generation of most mercury pressure lamps furthermore demands excessive cooling.

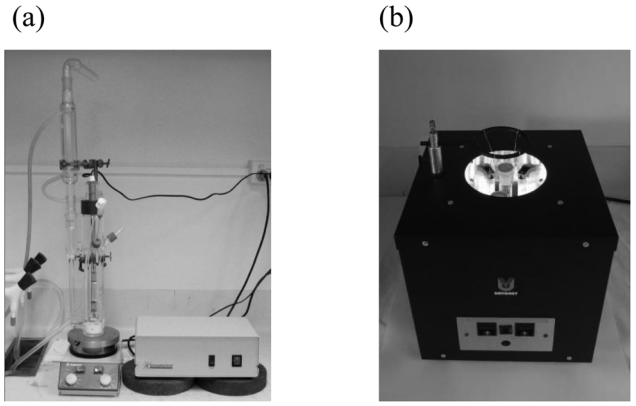

Fig. 12 (a) Immersion well batch reactor (UV-LRS-1; UV-Consulting Peschl, Germany). (b) Rayonet chamber reactor (RMR-600; Southern New England Ultraviolet Company, USA).

Recently, continuous microflow reactors have emerged as new, resource-efficient synthesis tools and have found widespread applications in synthetic organic chemistry.[215] These devices are characterized by very narrow inner dimensions (by definition <1 mm in at least one direction, typically depth or diameter), which makes them suitable for photochemical applications.[216,217] Fixed reactor models such as the dwell device by Mikroglas Chemtech have the reaction channel embedded in the reactor block (Fig. 13a). Complete commercially available microreactor systems have now been developed. The advanced UV-150 flow reactor by Vapourtec (Fig. 13b), for example, utilizes a microcapillary unit in combination with a 150 W mercury-lamp and allows for multi-gram scale synthesis.[134c] A flexible multi-microcapillary flow reactor (MμCFR) (Fig. 13c) for parallel microflow photochemistry operations has been recently described.[218] This reactor has been adopted for process optimization, process validation, scale-up and parallel library synthesis.

Although earlier examples of flow-photochemical reactions exist, the photopinacolization of benzophenone **130** (0.5 M) in isopropanol is regarded as the first comprehensive microreactor comparison study (Scheme 56).[219] The initial microchip reactor was fabricated by bonding a patterned silicon wafer to a Pyrex plate and incorporated a serpentine reaction channel. The device was coupled with a separate detection chip for on-line UV detection. An improved model consisted of a sandwich structure of a silicon wafer between two quartz plates. The chip incorporated a serpentine reaction channel with an integrated detection point for instant on-line UV analysis. The reaction mixtures were pumped through the chips with a syringe pump and irradiated with a small UVA lamp. With an

Fig. 13 (a) Dwell device (Mikroglas Chemtech GmbH, Germany) under a UV-panel (Luzchem Research Inc., Canada). (b) UV-150 E-series flow chemistry system (Vapourtec Ltd, UK). (c) Multi-microcapillary flow reactor (MμCFR).

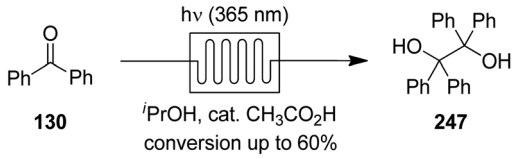

Scheme 56 Photopinacolization of **130** in isopropanol.

optimum flow rate of approximately 4 μl min^{-1}, high conversions of **130** of 60% (by HPLC) were achieved without blockage of the channel. The photodimer **247** readily crystallized in the product vessel, thus allowing easy isolation.

The 4,4′-dimethoxybenzophenone (DMBP) sensitized addition of isopropanol to furanones **164** was chosen to investigate different flow reactor setups (Scheme 57).[220] Reactor Type I consisted of a commercially available dwell device, which was placed under a UVA light panel (5 × 8 W). Reactor Type II combined a microchip with a UVA-LED array (6 × 75 mW), while reactor Type III utilized a dual polytetrafluoroethylene (PTFE) capillary tower equipped with a single UVA tube (8 W) at its center. The small UVA-LED microchip gave high conversions of **164** with a residence time of just 2.5 min, while all other microreactors and the conventional batch reactor required 5 min. Despite high space-time-yields (STY) and energy-efficiency estimations, however, the productivity of the microchip remained low. The flexible and open capillary system was thus further advanced into a 10-microcapillary flow reactor (MμCFR) for parallel microflow photochemistry.[218]

The steroid myriceric acid (**251**), a potent endothelin A receptor antagonist, is available from the intermediary nitrite **249** *via* the Barton reaction. The conversion of **249** to the corresponding oxime **250** was therefore investigated in different microreactor setups (Scheme 58).[221] A glass-covered, stainless steel microreactor (Type I) in combination with a 300 W high-pressure mercury lamp was chosen for process optimization. A soda lime cover gave the best yield of oxime **250** with 59% as its cut-off wavelength at >320 nm prevented further photodegradation. Yields of 71% and 70% (by HPLC) were increased when a 15 W black light (UVA) lamp or a UV-LED array (48 × 35 mW) in combination with a Pyrex glass top were used instead. Utilizing two stainless steel reactors in-series (Type II), a set of 8 × 20 W black light lamps, DMF and a residence time of 32 min, continuous operation for 20 h gave 3.1 g

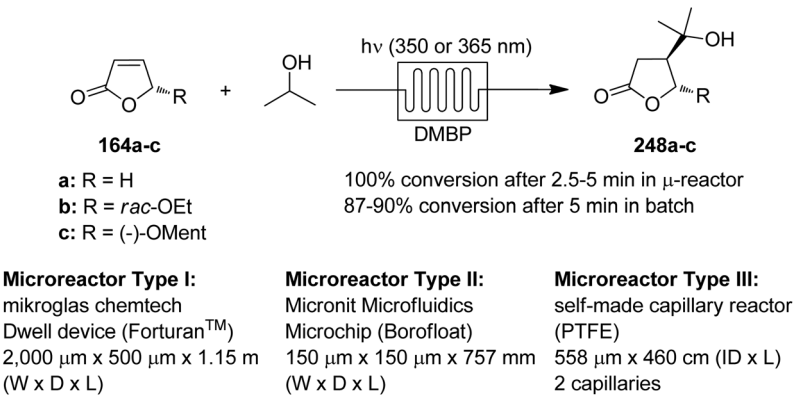

Scheme 57 DMBP-sensitized addition of isopropanol to furanones.

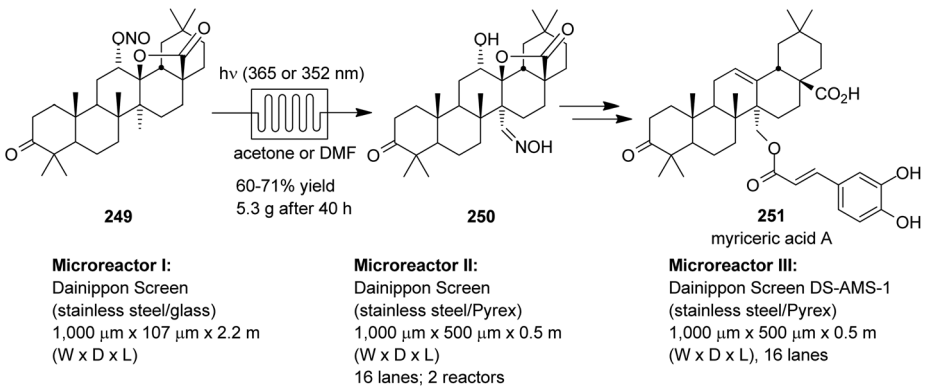

Scheme 58 The Barton reaction as a key step in the synthesis of myriceric acid A (**251**).

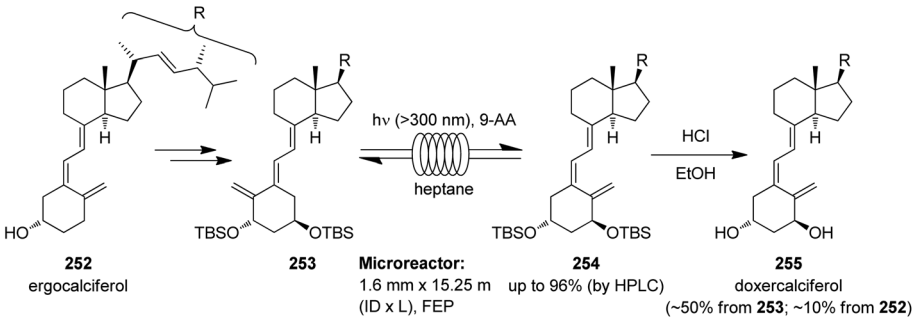

Scheme 59 Synthesis of doxercalciferol (**255**) from ergocalciferol (**252**).

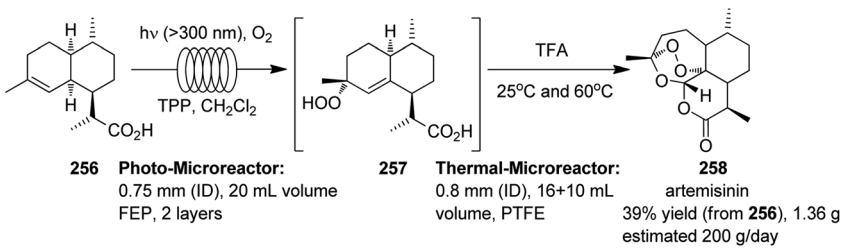

Scheme 60 Continuous synthesis of artemisinin (**258**) *via* a tandem photochemical–thermal process.

of pure **250** (60% yield). In an extension, a fully automated process for the synthesis of **250** was realized in a single multi-lane stainless steel reactor (Type III) equipped with six evenly positioned 15 W black light bulbs. After operation for 40 h and using a residence time of 20 min, the reactor plant produced 5.3 g of **250** (61% yield).

The synthesis of doxercalciferol (1α-hydroxyvitamin D_2; **255**) from ergocalciferol (**252**) has likewise been realized using a continuous flow photochemical key-step.[222] The photoisomerization of the bis-*tert*-butyldimethylsilyl (bis-TBS) ether **253** was accomplished in a fluorinated ethylene propylene (FEP) microcapillary reactor using 9-acetylanthracene (9-AA) as a sensitizer (Scheme 59). The capillary was wrapped around an immersion well fitted with a Pyrex sleeve and a 450 W mercury pressure lamp. Removal of the sensitizer was achieved in-line *via* filtration over a short carbon/Celite (1 : 2 w/w) column. Consequent optimization of the reaction conditions produced **254** in up to 96% yield (by HPLC). Overall, **255** was obtained in about 10% from ergocalciferol (**252**) without purification by chromatography.

The synthesis of the antimalarial compound artemisinin (**258**) *via* a tandem photochemical–thermal continuous flow process has been recently achieved (Scheme 60).[223] Dihydroartemisinic acid (**256**) is converted by photooxygenation with tetraphenylporphyrin (TPP) into the hydroperoxide intermediate **257**. A slow stream of oxygen is injected into the liquid reagent stream creating a slug flow pattern inside a FEP capillary. Irradiation is conducted with a 450 W medium pressure mercury lamp. Subsequently, trifluoroacetic acid (TFA) is injected into the product stream from the photochemistry module. This mixture enters a second, thermal (60 °C) reactor module made of polytetrafluoroethylene (PTFE) tubing, where **257** is converted into artemisinin (**256**). Using this continuous flow plant, **258** is isolated in an overall yield of 39% with the capability of producing 200 g of **258** per day.

8 Conclusion

In conclusion, photochemistry represents an elegant enabling methodology for the synthesis of complex natural products, commodity chemicals or novel chemical entities. Photochemistry has thus expanded the synthesis portfolio of organic chemistry. The traditionally strong links between organic photochemistry and physical chemistry enable a high level of understanding of these reactions.[1,2,4] Profound investigations of reaction mechanisms are frequently carried out in this domain which significantly facilitates the optimization and the application of these organic photochemical reactions. Light can be easily tuned and controlled with a 'flick of a switch', thus allowing safe operations. Despite these advantages, industrial photochemistry is limited to certain commodity chemicals.[224] With the development of novel reactor systems and light sources,[130,217,225,226] it is hoped that photochemical reactions will become more widespread in the future. The recently established industrial synthesis of artemisinin (**A3**) and the innovative Heraeus Noblelight process for the synthesis of anti-cancer precursors represent encouraging examples.[227,228]

References

1 (*a*) P. Klán and J. Wirz, *Photochemistry of Organic Compounds*, Wiley, Chichester, 2009; (*b*) N. J. Turro, V. Ramamurthy and J. C. Scaiano, *Modern Molecular Photochemistry of Organic Molecules*, University Science Books, Sausalito, 2010.

2 (*a*) N. J. Turro, *Angew. Chem., Int. Ed. Engl.*, 1986, **25**, 882–901; (*b*) M. Olivucci and F. Santoro, *Angew. Chem., Int. Ed.*, 2008, **47**, 6322–6325; (*c*) I. Schapiro, F. Melaccio, E. N. Laricheva and M. Olivucci, *Photochem. Photobiol. Sci.*, 2011, **10**, 867–886.

3 H. E. Zimmerman, *Angew. Chem., Int. Ed. Engl.*, 1969, **8**, 1–11.

4 (*a*) N. Hoffmann, *Chem. Rev.*, 2008, **108**, 1052–1103; (*b*) T. Bach and J. P. Hehn, *Angew. Chem., Int. Ed.*, 2011, **50**, 1000–1045; (*c*) C.-L. Ciana and C. G. Bochet, *Chimia*, 2007, **61**, 650–654.

5 (*a*) *CRC Handbook of Organic Photochemistry and Photobiology*, ed. A. Griesbeck, M. Oelgemöller and F. Ghetti, CRC Press, Boca Raton, 3rd edn, 2012; (*b*) *Handbook of Synthetic Photochemistry*, ed. A. Albini and M. Fagnoni, Wiley-VCH, Weinheim, 2010; (*c*) *Synthetic Organic Photochemistry*, ed. A. G. Griesbeck and J. Mattay, Marcel Dekker, New York, 2005.

6 (*a*) Y. Inoue, *Chem. Rev.*, 1992, **92**, 741–770; (*b*) *Chiral Photochemistry*, ed. Y. Inoue and V. Ramamurthy, Marcel Dekker, New York, 2004.

7 H. Hopf, *Classics in Hydrocarbon Chemistry*, Wiley-VCH, Weinheim, 2000.

8 N. Hoffmann, *Photochem. Photobiol. Sci.*, 2012, **11**, 1613–1641.

9 (*a*) A. Albini and M. Fagnoni, *Green Chem.*, 2004, **6**, 1–6; (*b*) M. Oelgemöller, C. Jung and J. Mattay, *Pure Appl. Chem.*, 2007, **79**, 1939–1947; (*c*) S. Protti, D. Dondi, M. Fagnoni and A. Albini, *Green Chem.*, 2009, **11**, 239–249; (*d*) M. Oelgemöller, *J. Chin. Chem. Soc.*, 2014, **61**, 743–748; (*e*) M. Oelgemöller, *Chem. Rev.*, 2016, DOI: 10.1021/acs.chemrev.5b00720.

10 (*a*) P. Wessig and O. Mühling, in *Synthetic Organic Photochemistry*, ed. A. G. Griesbeck and J. Mattay, Marcel Dekker, New York, 2005, pp. 41–87; (*b*) P. J. Wagner, in *Synthetic Organic Photochemistry*, ed. A. G. Griesbeck and J. Mattay, Marcel Dekker, New York, 2005, pp. 11–39.

11 (*a*) J. R. Scheffer, M. Garcia-Garibay and O. Nalamasu, *Org. Photochem.*, 1987, **8**, 249–347; (*b*) H. Ihmels and J. R. Scheffer, *Tetrahedron*, 1999, **55**, 885–907.

12 M. Leibovich, G. Olovsson, J. R. Scheffer and J. Trotter, *J. Am. Chem. Soc.*, 1998, **120**, 12755–12769.

13 (*a*) M. Abe, *Chem. Rev.*, 2013, **113**, 7011–7088; (*b*) M. Abe, J. Ye and M. Mishima, *Chem. Soc. Rev.*, 2012, **41**, 3808–3820.

14 (*a*) L. Salem and D. Rowland, *Angew. Chem., Int. Ed. Engl.*, 1972, **11**, 92–111; (*b*) L. Carlacci, C. Doubleday Jr., T. R. Furlani, H. F. King and J. W. McIver Jr., *J. Am. Chem. Soc.*, 1987, **109**, 5323–5329; (*c*) J. Michl, *J. Am. Chem. Soc.*, 1996, **118**, 3568–3579. See also: (*d*) J. C. Scaiano, *Tetrahedron*, 1982, **38**, 819–824.

15 A. G. Griesbeck, H. Mauder and S. Stadtmüller, *Acc. Chem. Res.*, 1994, **27**, 70–75.

16 A. G. Griesbeck, M. Abe and S. Bondock, *Acc. Chem. Res.*, 2004, **37**, 919–928.

17 (*a*) M. W. Nau, F. L. Cozens and J. C. Scaiano, *J. Am. Chem. Soc.*, 1996, **118**, 2275–2282. See also: (*b*) B. Giese, P. Wettstein, C. Stähli, F. Barbosa, M. Neuburger, M. Zehnder and P. Wessig, *Angew. Chem., Int. Ed.*, 1999, **38**, 2586–2587.

18 A. G. Griesbeck and H. Heckroth, *J. Am. Chem. Soc.*, 2002, **124**, 396–403.

19 (*a*) V. Ramamurthy and K. Venkateban, *Chem. Rev.*, 1987, **87**, 433–481; (*b*) B. L. Feringa and R. A. van Delden, *Angew. Chem., Int. Ed.*, 1999, **38**, 3418–3438; (*c*) M. Sakamoto, *J. Photochem. Photobiol., C*, 2006, **7**, 183–196; (*d*) C. Yang and W. Xia, *Chem. – Asian J.*, 2009, **4**, 1774–1784.

20 M. Leibovich, G. Olovsson, J. R. Scheffer and J. Trotter, *J. Am. Chem. Soc.*, 1997, **119**, 1462–1463.

21 I. Turowska-Tyrk, E. Trzop, J. R. Scheffer and S. Chen, *Acta Crystallogr., Sect. B: Struct. Sci.*, 2006, **62**, 128–134.

22 (*a*) P. Kissel, D. J. Murray, W. J. Wulftange, V. J. Catalano and B. T. King, *Nat. Chem.*, 2014, **6**, 774–778; (*b*) M. J. Kory, M. Wörle, T. Weber, P. Payamyar, S. W. van de Poll, J. Dshemuchadse, N. Trapp and A. D. Schlüter, *Nat. Chem.*, 2014, **6**, 779–784.

23 N. R. Champness, *Nat. Chem.*, 2014, **6**, 757–759.

24 P. J. Wagner, in *CRC Handbook of Organic Photochemistry and Photobiology*, ed. W. Horspool and F. Lenci, CRC Press, Boca Raton, 2nd edn, 2004, pp. 58/1–58/70.

25 G. Descotes, *Top. Curr. Chem.*, 1990, **154**, 39–76.

26 A. Herrera, M. Rondón and E. Suárez, *J. Org. Chem.*, 2008, **73**, 3384–3391.

27 D. Álvarez-Dorta, E. I. León, A. R. Kennedy, C. Riesco-Fagundo and E. Suárez, *Angew. Chem., Int. Ed.*, 2008, **47**, 8917–8919.

28 R. Breslow, *Acc. Chem. Res.*, 1980, **13**, 170–177.

29 (*a*) T. Bach, *Synthesis*, 1998, 683–703; (*b*) M. T. Crimmins and T. L. Reinhold, *Org. React.*, 1993, **44**, 297–588; (*c*) J. Iriondo-Alberti and M. F. Greaney, *Eur. J. Org. Chem.*, 2007, 4801–4815.

30 (*a*) R. Alibés, J. L. Bourdelande, J. Font, A. Gregori and T. Parella, *Tetrahedron*, 1996, **52**, 1267–1278; (*b*) G. Lejeune, J. Font, T. Parella, R. Alibés and M. Figueredo, *J. Org. Chem.*, 2015, **80**, 9437–9445. See also: (*c*) P. de March, F. Figueredo, J. Font, J. Raya, A. Alvarez-Larena and J. F. Piniella, *J. Org. Chem.*, 2003, **68**, 2437–2447.

31 See for example: (*a*) H. Kreigh and F. S. Richardson, *J. Chem. Soc., Perkin Trans. 2*, 1976, 1674–1677; (*b*) J. K. Gawronski, A. van Oeveren, H. van der Deen, C. W. Leung and B. L. Feringa, *J. Org. Chem.*, 1996, **61**, 1513–1515.

32 R. Jahjah, A. Gassama, V. Bulach, C. Suzuki, M. Abe, N. Hoffmann, A. Martinez and J.-M. Nuzillard, *Chem. – Eur. J.*, 2010, **16**, 3341–3354.

33 (*a*) R. Bonneau, *J. Am. Chem. Soc.*, 1980, **102**, 3816–3822; (*b*) A. C. Chan and D. I. Schuster, *J. Am. Chem. Soc.*, 1986, **108**, 4561–4567; (*c*) S. Yamauchi, N. Hirota and J. Higuchi, *J. Phys. Chem.*, 1988, **92**, 2129–2133; (*d*) D. I. Schuster, D. A. Dunn, G. E. Heibel, P. B. Brown, J. M. Rao, J. Woning and R. Bonneau, *J. Am. Chem. Soc.*, 1991, **113**, 6245–6255; (*e*) M. Reguero, M. Olivucci, F. Bernardi and M. A. Robb, *J. Am. Chem. Soc.*, 1994, **116**, 2103–2114; (*f*) S. Wilsey, L. González, M. A. Robb and K. N. Houk, *J. Am. Chem. Soc.*, 2000, **122**, 5866–5876; (*g*) M. Fréneau, P. de Sainte-Claire, M. Abe and N. Hoffmann, *J. Phys. Chem.*, 2016, DOI: 10.1002/poc.3560.

34 (*a*) K. Wiesner, *Tetrahedron*, 1975, **31**, 1655–1658; (*b*) G. Marini-Bettòlo, S. P. Sahoo, G. A. Poulton, T. Y. R. Tsai and K. Wiesner, *Tetrahedron*, 1980, **36**, 719–721; (*c*) N. Braussaud, N. Hoffmann and H.-D. Scharf, *Tetrahedron*, 1997, **53**, 14701–14712; (*d*) D. Becker, M. Nagler, Y. Sahali and N. Haddad, *J. Org. Chem.*, 1991, **56**, 4537–4543.

35 N. Hoffmann, H. Buschmann, G. Raabe and H.-D. Scharf, *Tetrahedron*, 1994, **50**, 11167–11186.

36 K. Hayday and R. D. McKelvey, *J. Org. Chem.*, 1976, **41**, 2222–2223.

37 (*a*) N. Hoffmann, *J. Phys. Org. Chem.*, 2015, **28**, 121–136; (*b*) N. Hoffmann, *Synthesis*, 2016, 1782–1802.

38 (*a*) P. Wessig, in *CRC Handbook of Organic Photochemistry and Photobiology*, ed. A. Griesbeck, M. Oelgemöller and F. Ghetti, CRC Press, Boca Raton, 3rd edn, 2012, pp. 201–211; (*b*) P. Wessig and O. Muehling, *Eur. J. Org. Chem.*, 2007, 2219–2232.

39 (*a*) P. Wessig and O. Muehling, *Angew. Chem., Int. Ed.*, 2005, **44**, 6778–6781; (*b*) P. Wessig and O. Muehling, *Chem. – Eur. J.*, 2008, **14**, 7951–7960.

40 (*a*) G. Cainelli, D. Giacomini and P. Galletti, *Chem. Commun.*, 1999, 567–572; (*b*) Y. Inoue, T. Wada, S. Asaoka, H. Sato and J.-P. Pete, *Chem. Commun.*, 2000, 251–259.

41 (*a*) F. Nerdel and W. Brodowski, *Chem. Ber.*, 1968, **101**, 1398–1406; (*b*) M. Pfau, S. Combrisson, J. E. Rowe Jr. and N. D. Heindel, *Tetrahedron*, 1978, **34**, 3459–3468; (*c*) R. M. Wilson, K. Hannemann, W. R. Heineman and J. R. Kirchhoff, *J. Am. Chem. Soc.*, 1987, **109**, 4743–4745.

42 P. G. Sammes, *Tetrahedron*, 1976, **32**, 405–422.

43 (*a*) P. Klán, J. Wirz and A. D. Gudmundsdottir, in *CRC Handbook of Organic Photochemistry and Photobiology*, ed. A. Griesbeck, M. Oelgemöller and F. Ghetti, CRC Press, Boca Raton, 3rd edn, 2012, pp. 627–652; (*b*) P. Wagner and H.-S. Park, *Org. Photochem.*, 1991, **11**, 227–366.

44 P. Klán, T. Šolomek, C. G. Bochet, A. Blanc, R. Givens, M. Rubina, V. Popik, A. Kostikov and J. Wirz, *Chem. Rev.*, 2013, **113**, 119–191.

45 P. Wan and D. Shukla, *Chem. Rev.*, 1993, **93**, 571–584.

46 J. Wirz, *Adv. Phys. Org. Chem.*, 2010, **44**, 325–356.

47 V. S. Padalkar and S. Seki, *Chem. Soc. Rev.*, 2015, **45**, 169–202.

48 N. Basarić, K. Mlinarić-Majerski and M. Kralj, *Curr. Org. Chem.*, 2014, **18**, 3–18.

49 N. Hoffmann, in *Reference Module in Chemistry, Molecular Sciences and Chemical Engineering*, ed. J. Reedijk, Elsevier, Waltham, 2014, DOI: 10.1016/B978-0-12-409547-2.11017-0.

50 (*a*) O. Piva, R. Mortezaei, F. Henin, J. Muzart and J.-P. Pete, *J. Am. Chem. Soc.*, 1990, **112**, 9263–9272; (*b*) F. Hénin, S. Létinois and J. Muzart, *Tetrahedron: Asymmetry*, 2000, **11**, 2037–2044.

51 H. Buschmann, H.-D. Scharf, N. Hoffmann and P. Esser, *Angew. Chem., Int. Ed. Engl.*, 1991, **30**, 477–515.

52 O. A. Mukhina, N. N. B. Kumar, T. M. Arisco, R. A. Valiulin, G. A. Metzel and A. G. Kutateladze, *Angew. Chem., Int. Ed.*, 2011, **50**, 9423–9428.

53 R. B. Woodward and R. Hoffmann, *Angew. Chem., Int. Ed. Engl.*, 1969, **8**, 781–853.

54 O. A. Mukhina, W. C. Cronk, N. N. B. Kumar, M. C. Sekhar, A. Samanta and A. G. Kutateladze, *J. Phys. Chem. A*, 2014, **118**, 10487–10496.

55 (*a*) W. J. Umstead, O. A. Mukhina and A. G. Kutateladze, *Eur. J. Chem.*, 2015, 2205–2213; (*b*) W. C. Cronk, O. A. Mukhina and A. G. Kutateladze, *J. Org. Chem.*, 2014, **79**, 1235–1246; (*c*) N. S. Nandurkar, N. N. B. Kumar, O. A. Mukhina and A. G. Kutateladze, *ACS Comb. Sci.*, 2013, **15**, 73–76; (*d*) N. N. B. Kumar, O. A. Mukhina and A. G. Kutateladze, *J. Am. Chem. Soc.*, 2013, **135**, 9608–9611.

56 (*a*) B. Li, C. Yang, W. Xia and W. Xia, *Synlett*, 2015, 1997–2000; (*b*) Y. Shao, C. Yang, W. Gui, Y. Liu and W. Xia, *Chem. Commun.*, 2012, **48**, 3560–3562.

57 (*a*) I. V. Alabugin, W.-Y. Yang and R. Pal, in *CRC Handbook of Organic Photochemistry and Photobiology*, ed. A. Griesbeck, M. Oelgemöller and F. Ghetti, CRC Press, Boca Raton, 3rd edn, 2012, pp. 549–592; (*b*) R. K. Mohamed, P. W. Peterson and I. V. Alabugin, *Chem. Rev.*, 2013, **113**, 7089–7129. For a particular case of a thermal reaction see: (*c*) A. Baroudi, J. Mauldin and I. V. Alabugin, *J. Am. Chem. Soc.*, 2010, **132**, 967–979.

58 (*a*) M. Winkler and W. Sander, *Angew. Chem., Int. Ed.*, 2000, **39**, 2014–2016; (*b*) M. Winkler and W. Sander, *J. Org. Chem.*, 2006, **71**, 6357–6367.

59 M. Fagnoni and A. Albini, *Acc. Chem. Res.*, 2005, **38**, 713–721.

60 V. Dichiarante and M. Fagnoni, *Synlett*, 2008, 787–800.

61 H. Qrareya, C. Raviola, S. Protti, M. Fagnoni and A. Albini, *J. Org. Chem.*, 2013, **78**, 6016–6024.

62 S. Lazzaroni, D. Dondi, M. Fagnoni and A. Albini, *J. Org. Chem.*, 2008, **73**, 206–211.

63 (*a*) M. Freccero, M. Fagnoni and A. Albini, *J. Am. Chem. Soc.*, 2003, **125**, 13182–13190; (*b*) K. K. Laali, G. Rasul, G. K. S. Prakash and G. A. Olah, *J. Org. Chem.*, 2002, **67**, 2913–2918; (*c*) M. Aschi and J. N. Harvey, *J. Chem. Soc., Perkin Trans. 2*, 1999, 1059–1062; (*d*) M. Slegt, H. S. Overkleeft and G. Lodder, *Eur. J. Org. Chem.*, 2007, 5364–5375.

64 V. Dichiarante, M. Fagnoni and A. Albini, *J. Org. Chem.*, 2008, **73**, 1282–1289.

65 (*a*) H. Mayr, B. Kempf and A. R. Ofial, *Acc. Chem. Res.*, 2003, **36**, 66–77; (*b*) H. Mayr and A. R. Ofial, *J. Phys. Org.*

Chem., 2008, **21**, 584–595; (*c*) H. Mayr, *Tetrahedron*, 2015, **71**, 5095–5111.
66 B. Guizzardi, M. Mella, M. Fagnoni and A. Albini, *Tetrahedron*, 2000, **56**, 9383–9390.
67 S. Protti, M. Fagnoni and A. Albini, *Org. Biomol. Chem.*, 2005, **3**, 2868–2871.
68 A. Fraboni, M. Fagnoni and A. Albini, *J. Org. Chem.*, 2003, **68**, 4886–4893.
69 S. Protti, M. Fagnoni and A. Albini, *J. Am. Chem. Soc.*, 2006, **128**, 10670–10671.
70 (*a*) E. Paternò and G. Chieffi, *Gazz. Chim. Ital.*, 1909, **39**, 341–361; (*b*) G. Büchi, C. G. Inman and E. S. Lipinski, *J. Am. Chem. Soc.*, 1954, **76**, 4327–4331.
71 (*a*) M. D'Auria, in *CRC Handbook of Organic Photochemistry and Photobiology*, ed. A. Griesbeck, M. Oelgemöller and F. Ghetti, CRC Press, Boca Raton, 3rd edn, 2012, pp. 653–681; (*b*) T. Bach, *Synthesis*, 1998, 683–703; (*c*) V. H. Rawal, A. Eschbach, C. Dufour and S. Iwasa, *Pure Appl. Chem.*, 1996, **68**, 675–678; (*d*) J. A. Porco and S. L. Schreiber, in *Comprehensive Organic Synthesis*, ed. B. M. Trost, I. Fleming and L. A. Paquette, Plenum Press, New York, 1991, vol. 5, pp. 151–192.
72 M. Abe, in *Handbook of Synthetic Photochemistry*, ed. A. Albini and M. Fagnoni, Wiley-VCH, Weinheim, 2010, pp. 217–239.
73 D. R. Arnold, *Adv. Photochem.*, 1968, **6**, 301–423.
74 I. J. Palmer, I. N. Ragazos, R. Bernardi, M. Olivucci and M. A. Robb, *J. Am. Chem. Soc.*, 1994, **116**, 2121–2132.
75 J. Mattay, J. Gersdorf and K. Buchkremer, *Chem. Ber.*, 1987, **120**, 307–318.
76 J. Gersdorf, J. Mattay and H. Görner, *J. Am. Chem. Soc.*, 1987, **109**, 1203–1209.
77 M. Abe, Y. Shirodai and M. Nojima, *J. Chem. Soc., Perkin Trans. 1*, 1998, 3253–3260.
78 A. G. Griesbeck and S. Stadtmüller, *Chem. Ber.*, 1990, **123**, 357–362.
79 A. G. Griesbeck, S. Buhr, M. Fiege, H. Schmickler and J. Lex, *J. Org. Chem.*, 1998, **63**, 3847–3854.
80 M. Abe, M. Ikeda and M. Nojima, *J. Chem. Soc., Perkin Trans. 1*, 1998, 3261–3266.
81 H. Buschmann, H.-D. Scharf, N. Hoffmann, M. W. Plath and J. Runsink, *J. Am. Chem. Soc.*, 1989, **111**, 5367–5373.
82 N. J. Turro, J. C. Dalton, K. Dawes, G. Farrington, R. Hautala, D. Morton, M. Niemczyk and N. Schore, *Acc. Chem. Res.*, 1972, **5**, 92–101.
83 (*a*) A. G. Griesbeck and S. Stadtmüller, *J. Am. Chem. Soc.*, 1991, **113**, 6923–6928; (*b*) A. G. Griesbeck, H. Mauder, K. Peters, E.-M. Peters and H. G. von Schnering, *Chem. Ber.*, 1991, **124**, 407–410; (*c*) A. G. Griesbeck and S. Stadtmüller, *J. Am. Chem. Soc.*, 1990, **112**, 1281–1282.
84 S. Bondock and A. G. Griesbeck, *Int. J. Photoenergy*, 2005, **7**, 23–25.
85 A. G. Kutateladze, *J. Am. Chem. Soc.*, 2001, **123**, 9279–9282.
86 A. G. Griesbeck, M. Fiege, S. Bondock and M. S. Gudipati, *Org. Lett.*, 2000, **2**, 3623–3625.
87 A. G. Griesbeck, S. Bondock and M. S. Gudipati, *Angew. Chem., Int. Ed.*, 2001, **40**, 4684–4687.
88 G. Cainelly, D. Giacomini and P. Galletti, *Chem. Commun.*, 1999, 567–572.
89 L. Liu and Q.-X. Guo, *Chem. Rev.*, 2001, **101**, 673–695.
90 (*a*) W. Linert and R. F. Jameson, *Chem. Soc. Rev.*, 1989, **18**, 477–505; (*b*) W. Linert, *Chem. Soc. Rev.*, 1994, **23**, 429–438.
91 M. Abe, T. Kawakami, S. Ohata, K. Nozaki and M. Nojima, *J. Am. Chem. Soc.*, 2004, **126**, 2838–2846.
92 E. Juaristi and G. Cuevas, *The Anomeric Effect*, CRC Press, Boca Raton, 1995.
93 (*a*) W. Adam, K. Peters, E. M. Peters and V. R. Stegmann, *J. Am. Chem. Soc.*, 2000, **122**, 2958–2959; (*b*) W. Adam and V. R. Stegmann, *Synthesis*, 2001, 1203–1214; (*c*) M. D'Auria, L. Emanuele, G. Poggi, R. Racioppi and G. Romaniello, *Tetrahedron*, 2002, **58**, 5045–5051; (*d*) M. D'Auria, L. Emanuele and R. Racioppi, *Photochem. Photobiol. Sci.*, 2004, **3**, 927–932; (*e*) M. D'Auria, L. Emanuele, R. Racioppi and A. Valente, *Photochem. Photobiol. Sci.*, 2008, **7**, 98–103.
94 T. Bach, H. Bergmann and K. Harms, *J. Am. Chem. Soc.*, 1999, **121**, 10650–10651.
95 (*a*) L. K. Sydnes, K. I. Hansen, D. L. Oldroyd, A. C. Weedon and E. Jørgensen, *Acta Chem. Scand.*, 1993, **47**, 916–924; (*b*) S. McN. Sieburth and K. F. McGee Jr., *Org. Lett.*, 1999, **1**, 1775–1777; (*c*) A. Yokoyama and K. Mizuno, *Org. Lett.*, 2000, **2**, 3457–2459.
96 S. Iwata and K. Morokuma, *J. Am. Chem. Soc.*, 1973, **95**, 7563–7575.
97 (*a*) U. Pischel and W. M. Nau, *Photochem. Photobiol. Sci.*, 2002, **1**, 141–147; (*b*) J. E. Del Bene and J. D. Watts, *Int. J. Quantum Chem.*, 2000, **77**, 187–191; (*c*) C. N. R. Rao and A. S. N. Murthy, *Theor. Chim. Acta*, 1971, **22**, 392–395; (*d*) J. C. Scaiano, *J. Photochem.*, 1973, **2**, 81–118.
98 A. G. Griesbeck and S. Bondock, *J. Am. Chem. Soc.*, 2001, **123**, 6191–6192.
99 Y. Yabuno, Y. Hiraga, R. Takagi and M. Abe, *J. Am. Chem. Soc.*, 2011, **133**, 2592–2604.
100 (*a*) J. Mattay, R. Conrads and R. Hoffmann, in *Houben-Weyl, Methods of Organic Chemistry, Vol. E21: Stereoselective Synthesis*, ed. G. Helmchen, R. W. Hoffmann, J. Mulzer and E. Schaumann, Thieme Verlag, Stuttgart, 1993, pp. 3085–3132; (*b*) J. P. Hehn, C. Müller and T. Bach, in *Handbook of Synthetic Photochemistry*, ed. A. Albini and M. Fagnoni, Wiley-VCH, Weinheim, 2010, pp. 171–215; (*c*) D. I. Schuster, G. N. Lem and A. Kaprinidis, *Chem. Rev.*, 1993, **93**, 3–22.
101 (*a*) R. Brimioulle, D. Lenhart, M. M. Maturi and T. Bach, *Angew. Chem., Int. Ed.*, 2015, **54**, 3872–3890; (*b*) C. Müller and T. Bach, *Aust. J. Chem.*, 2008, **61**, 557–564.
102 (*a*) R. Brimioulle and T. Bach, *Science*, 2013, **342**, 840–843; (*b*) R. Brimioulle, A. Bauer and T. Bach, *J. Am. Chem. Soc.*, 2015, **137**, 5170–5176.
103 (*a*) F. D. Lewis and S. V. Barancyk, *J. Am. Chem. Soc.*, 1989, **111**, 8653–8661; (*b*) H. Görner and T. Wolff, *Photochem. Photobiol.*, 2008, **84**, 1224–1230.

104 H. Wang, X. Cao, X. Chen, W. Fang and M. Dolg, *Angew. Chem., Int. Ed.*, 2015, **127**, 14295–14298.
105 J. Du, K. L. Skubi, D. M. Schultz and T. P. Yoon, *Science*, 2014, **344**, 392–396.
106 R. Telmesani, S. H. Park, T. Lynch-Colameta and A. B. Beeler, *Angew. Chem., Int. Ed.*, 2015, **54**, 11521–11525.
107 H. D. Roth, *Top. Curr. Chem.*, 1990, **156**, 1–19.
108 (*a*) S. L. Mattes and S. Farid, in *Organic Photochemistry*, ed. A. Padwa, Marcel Dekker, New York, 1982, vol. 6, pp. 233–326; (*b*) J. Mattay, *Angew. Chem., Int. Ed. Engl.*, 1987, **26**, 825–845; (*c*) J. Mattay, *Synthesis*, 1989, 233–252; (*d*) A. G. Griesbeck and S. Schieffer, in *Electron Transfer in Chemistry*, ed. A. Balzani, 2000, vol. 2, pp. 457–493.
109 L. Eberson, *Electron Transfer Reactions in Organic Chemistry*, Springer, Berlin, 1987.
110 (*a*) G. J. Kovarnos and N. J. Turro, *Chem. Rev.*, 1986, **86**, 401–449; (*b*) J. Mattay and M. Vondenhof, *Top. Curr. Chem.*, 1991, **159**, 219–255; (*c*) G. J. Kovarnos, *Fundamentals of Photoinduced Electron Transfer*, VCH Publishers, New York, 1993; (*d*) *Electron Transfer in Chemistry*, ed. V. Balzani, Wiley-VCH, Weinheim, 2001, vol. 1 and 2; (*e*) M. Oelgemöller, J.-O. Bunte and J. Mattay, in *Synthetic Organic Photochemistry*, ed. A. G. Griesbeck and J. Mattay, Marcel Dekker, New York, 2004, pp. 267–295.
111 (*a*) D. Rehm and A. Weller, *Isr. J. Chem.*, 1970, **8**, 259–271; (*b*) D. Rehm and A. Weller, *Ber. Bunsenges. Phys. Chem.*, 1969, **73**, 834–839.
112 P. J. Wagner, *Acc. Chem. Res.*, 1983, **16**, 461–467.
113 M. A. Fox, *Adv. Photochem.*, 1986, **13**, 237–272.
114 T. Majima, C. Pac, A. Nakasone and H. Sakurai, *J. Am. Chem. Soc.*, 1981, **103**, 4499–4508. Pac *et al.* were probably the first who introduced "redox photosensitization" which is synonymous to "co-sensitization".
115 J. Mattay, G. Trampe and J. Runsink, *Chem. Ber.*, 1988, **121**, 1991–2005.
116 (*a*) H. Görner, M. Oelgemöller and A. G. Griesbeck, *J. Phys. Chem. A*, 2002, **106**, 1458–1464; (*b*) H. Görner, A. G. Griesbeck, T. Heinrich, W. Kramer and M. Oelgemöller, *Chem. – Eur. J.*, 2001, **7**, 1530–1538; (*c*) V. Wintgens, P. Valat, J. Kossanyi, L. Biczok, A. Demeter and T. Bérces, *J. Chem. Soc., Faraday Trans.*, 1994, **90**, 411–421; (*d*) A. G. Griesbeck and H. Görner, *J. Photochem. Photobiol., A*, 1999, **129**, 111–119; (*e*) H. Hayashi, S. Nagakura, Y. Kubo and K. Maruyama, *Chem. Phys. Lett.*, 1980, **72**, 291–294; (*f*) J. D. Coyle, A. Harriman and G. L. Newport, *J. Chem. Soc., Perkin Trans. 2*, 1979, 799–802; (*g*) P. B. Filho, V. G. Toscano and M. J. Politi, *J. Photochem. Photobiol., A*, 1988, **43**, 51–58.
117 (*a*) M. Oelgemöller, A. G. Griesbeck, J. Lex, A. Haeuseler, M. Schmittel, M. Niki, D. Hesek and Y. Inoue, *Org. Lett.*, 2001, **3**, 1593–1596; (*b*) M. Oelgemöller, A. Haeuseler, M. Schmittel, A. G. Griesbeck, J. Lex and Y. Inoue, *J. Chem. Soc., Perkin Trans. 2*, 2002, 676–686; (*c*) D. W. Leedy and D. L. Muck, *J. Am. Chem. Soc.*, 1971, **93**, 4264–4270; (*d*) G. Farnia, A. Romanin, G. Capobianco and F. Torzo, *J. Electroanal. Chem.*, 1971, **33**, 31–44; (*e*) G. Capobianco, G. Farnia and F. Torzo, *Ric. Sci.*, 1968, **38**, 842–844.
118 (*a*) M. Hovart, K. Mlinarić-Majerski and N. Basarić, *Croat. Chem. Acta*, 2010, **83**, 179–188; (*b*) G. McDermott, D. J. Yoo and M. Oelgemöller, *Heterocycles*, 2005, **65**, 2221–2257; (*c*) M. Oelgemöller and A. G. Griesbeck, *J. Photochem. Photobiol., C*, 2002, **3**, 109–127; (*d*) M. Oelgemöller and A. G. Griesbeck, in *CRC Handbook of Organic Photochemistry and Photobiology*, ed. W. M. Horspool and F. Lenci, CRC Press, Boca Raton, 2nd edn, 2004, pp. 84/1–84/19; (*e*) M. Oelgemöller, A. G. Griesbeck, W. Kramer and F. Nerowski, *J. Inf. Rec.*, 1998, **24**, 87–94; (*f*) J. D. Coyle, in *Synthetic Organic Photochemistry*, ed. W. M. Horspool, Plenum Press, New York, 1984, pp. 259–284; (*g*) P. H. Mazzocchi, *Org. Photochem.*, 1981, **5**, 421–471; (*h*) Y. Kanaoka, *Acc. Chem. Res.*, 1978, **11**, 407–413.
119 N. J. Pienta, in *Photoinduced Electron Transfer*, ed. M. A. Fox and M. Chanon, Elsevier, Amsterdam, 1988, pp. 421–486.
120 (*a*) Y. Hatanaka, Y. Sato, H. Nakai, M. Wada, T. Mizoguchi and Y. Kanaoka, *Liebigs Ann. Chem.*, 1992, 1113–1123; (*b*) Y. Sato, H. Nakai, M. Wada, T. Mizoguchi, Y. Hatanaka, Y. Migata and Y. Kanaoka, *Liebigs Ann. Chem.*, 1985, 1099–1118.
121 (*a*) Y. Sato, H. Nakai, M. Wada, T. Mizoguchi, Y. Hatanaka and Y. Kanaoka, *Chem. Pharm. Bull.*, 1992, **40**, 3174–3180; (*b*) M. Wada, H. Nakai, K. Aoe, K. Kotera, Y. Sato, Y. Hatanaka and Y. Kanaoka, *Tetrahedron*, 1983, **39**, 1273–1279; (*c*) M. Wada, H. Nakai, Y. Sato, Y. Hatanaka and Y. Kanaoka, *Chem. Pharm. Bull.*, 1983, **31**, 429–435.
122 (*a*) M. Machida, H. Takechi and Y. Kanaoka, *Chem. Pharm. Bull.*, 1982, **30**, 1579–1587; (*b*) J. D. Coyle, L. E. Smart, J. F. Challiner and E. J. Haws, *J. Chem. Soc., Perkin Trans. 1*, 1985, 121–129; (*c*) J. D. Coyle and G. L. Newport, *Synthesis*, 1979, 381–382.
123 (*a*) U. C. Yoon and P. S. Mariano, *Acc. Chem. Res.*, 2001, **34**, 523–533; (*b*) U. C. Yoon, Y. X. Jin, S. W. Oh, D. W. Cho, K. H. Park and P. S. Mariano, *J. Photochem. Photobiol., A*, 2002, **150**, 77–84; (*c*) A. G. Griesbeck, M. Oelgemöller, J. Lex, A. Haeuseler and M. Schmittel, *Eur. J. Org. Chem.*, 2001, 1831–1843.
124 (*a*) K. Maruyama, T. Ogawa, Y. Kubo and T. Araki, *J. Chem. Soc., Perkin Trans. 1*, 1985, 2025–2031; (*b*) M. Machida, K. Oda and Y. Kanaoka, *Tetrahedron*, 1985, **41**, 4995–5001; (*c*) P. H. Mazzocchi and G. Fritz, *J. Org. Chem.*, 1986, **51**, 5362–5364; (*d*) K. Maruyama and Y. Kubo, *J. Org. Chem.*, 1981, **46**, 3612–3622.
125 (*a*) P. H. Mazzocchi, D. Shook and L. Liu, *Heterocycles*, 1987, **26**, 1165–1167; (*b*) K. Maruyama and Y. Kubo, *Chem. Lett.*, 1978, **7**, 851–854.
126 J. Xue, L. Zhu, H.-K. Fun and J.-H. Xu, *Tetrahedron Lett.*, 2000, **41**, 8553–8557.
127 L. Eberson, in *Electron Transfer Reactions in Organic Chemistry (Reactivity and Structure-Concepts in Organic Chem-*

istry), ed. K. Hafner, Springer-Verlag, Berlin, 1987, vol. 25, pp. 39–66.

128 (*a*) A. G. Griesbeck, W. Kramer and M. Oelgemöller, *Synlett*, 1999, 1169–1178; (*b*) A. G. Griesbeck, A. Henz, W. Kramer, J. Lex, F. Nerowski, M. Oelgemöller, K. Peters and E.-M. Peters, *Helv. Chim. Acta*, 1997, **80**, 912–933; (*c*) W. Kramer, A. G. Griesbeck, F. Nerowski and M. Oelgemöller, *J. Inf. Rec.*, 1998, **24**, 81–85.

129 (*a*) A. G. Griesbeck, T. Heinrich, M. Oelgemöller, A. Molis and A. Heidtmann, *Helv. Chim. Acta*, 2002, **85**, 4561–4578; (*b*) A. G. Griesbeck, F. Nerowski and J. Lex, *J. Org. Chem.*, 1999, **64**, 5213–5217; (*c*) D. J. Yoo, E. Y. Kim, M. Oelgemöller and S. C. Shim, *Heterocycles*, 2001, **54**, 1049–1055; (*d*) Y.-J. Lee, D.-H. Ahn, K.-S. Lee, A. R. Kim, D. J. Yoo and M. Oelgemöller, *Tetrahedron Lett.*, 2011, **52**, 5029–5031; (*e*) A. R. Kim, K.-S. Lee, C.-W. Lee, D. J. Yoo, F. Hatoum and M. Oelgemöller, *Tetrahedron Lett.*, 2005, **46**, 3395–3398.

130 (*a*) A. G. Griesbeck, N. Maptue, S. Bondock and M. Oelgemöller, *Photochem. Photobiol. Sci.*, 2003, **2**, 450–451; (*b*) A. G. Griesbeck, W. Kramer and M. Oelgemöller, *Green Chem.*, 1999, **1**, 205–207.

131 (*a*) O. Shvydkiv, K. Nolan and M. Oelgemöller, *Beilstein J. Org. Chem.*, 2011, **7**, 1055–1063; (*b*) O. Shvydkiv, S. Gallagher, K. Nolan and M. Oelgemöller, *Org. Lett.*, 2010, **12**, 5170–5173; (*c*) M. Oelgemöller, S. Gallagher and K. McCarthy, *Processes*, 2014, **2**, 158–166; (*d*) H. M. Pordanjani, C. Faderl, J. Wang, C. A. Motti, P. Junk and M. Oelgemöller, *Aust. J. Chem.*, 2015, **68**, 1662–1667.

132 (*a*) A. G. Griesbeck, W. Kramer and J. Lex, *Angew. Chem., Int. Ed.*, 2001, **40**, 577–579; (*b*) A. G. Griesbeck, W. Kramer and J. Lex, *Synthesis*, 2001, 1159–1166; (*c*) A. G. Griesbeck, W. Kramer, T. Heinrich and J. Lex, *Photochem. Photobiol. Sci.*, 2002, **1**, 237–239; (*d*) A. G. Griesbeck, W. Kramer, A. Bartoschek and H. Schmickler, *Org. Lett.*, 2001, **3**, 537–539.

133 T. Šumanovac Ramljak, M. Sohora, I. Antol, D. Kontrec, N. Basarić and K. Mlinarić-Majerski, *Tetrahedron Lett.*, 2014, **55**, 4078–4081.

134 (*a*) V. Belluau, P. Noeureuil, E. Ratzke, A. Skvortsov, S. Gallagher, C. A. Motti and M. Oelgemöller, *Tetrahedron Lett.*, 2010, **51**, 4738–4741; (*b*) F. Hatoum, J. Engler, C. Zelmer, J. Wißen, C. A. Motti, J. Lex and M. Oelgemöller, *Tetrahedron Lett.*, 2012, **53**, 5573–5577; (*c*) S. Josland, S. Mumtaz and M. Oelgemöller, *Chem. Eng. Technol.*, 2016, **39**, 81–87; (*d*) F. Hatoum, S. Gallagher, L. Baragwanath, J. Lex and M. Oelgemöller, *Tetrahedron Lett.*, 2009, **50**, 6335–6338; (*e*) M. Oelgemöller, P. Cygon, J. Lex and A. G. Griesbeck, *Heterocycles*, 2003, **59**, 669–684.

135 R. Jahjah, A. Gassama, F. Dumur, S. Marinković, S. Richert, S. Landgraf, A. Lebrun, C. Cadiou, P. Sellès and N. Hoffmann, *J. Org. Chem.*, 2011, **76**, 7104–7118.

136 L. Strekowski, M. Hojjat, S. E. Patterson and A. S. Kiselyov, *J. Heterocycl. Chem.*, 1994, **31**, 1413–1416.

137 (*a*) M. Periasamy, N. Kishorebabu and K. N. Jayakumar, *Tetrahedron Lett.*, 2003, **44**, 8939–8941; see also: (*b*) W. A. Moradi and S. L. Buchwald, *J. Am. Chem. Soc.*, 2001, **123**, 7996–8002.

138 S. Barata-Vallejo, M. M. Flesia, B. Lantaño, J. E. Argüello, A. Peñéñory and A. Postigo, *Eur. J. Org. Chem.*, 2013, 981–1008.

139 (*a*) *Homogeneous Photocatalysis*, ed. M. Chanon, Wiley, Chichester, 1997; (*b*) M. Fagnoni, D. Dondi, D. Ravelli and A. Albini, *Chem. Rev.*, 2007, **107**, 2725–2756; (*c*) D. Ravelli, D. Dondi, M. Fagnoni and A. Albini, *Chem. Soc. Rev.*, 2009, **38**, 1999–2011; (*d*) D. Ravelli, M. Fagnoni and A. Albini, *Chem. Soc. Rev.*, 2013, **42**, 97–113; (*e*) R. E. Galian and J. Pérez-Prieto, *Energy Environ. Sci.*, 2010, **3**, 1488–1498.

140 M. Julliard and M. Chanon, *Chem. Rev.*, 1983, **83**, 425–506.

141 (*a*) A. Heumann and M. Chanon, in *Applied Homogeneous Catalysis with Organometallic Compounds*, ed. B. Cornils and W. A. Herrmann, Wiley-VCH, Weinheim, 2nd edn, 2002, pp. 1030–1978; (*b*) H. Henning, R. Billing and H. Knoll, in *Photosensitization and Photocatalysis Using Inorganic and Organometallic Compounds*, ed. K. Kayanasundaram and M. Gräzel, Kluwer Academic Publishers, Dordrecht, 1993, pp. 51–69; (*c*) H. Kisch, in *Photocatalysis, Fundamentals and Applications*, ed. N. Serpone and E. Pelizzetti, Wiley, New York, 1989, pp. 1–8; (*d*) A. Albini, *J. Chem. Educ.*, 1986, **63**, 383–386; (*e*) F. Chanon and M. Chanon, in *Photocatalysis, Fundamentals and Applications*, ed. N. Serpone and E. Pelizzetti, Wiley, New York, 1989, pp. 489–540.

142 N. Hoffmann, *J. Photochem. Photobiol., C*, 2008, **9**, 43–60.

143 (*a*) N. Hoffmann, S. Bertrand, S. Marinković and J. Pesch, *Pure Appl. Chem.*, 2006, **78**, 2227–2246; (*b*) A. G. Griesbeck, N. Hoffmann and K. D. Warzecha, *Acc. Chem. Res.*, 2007, **40**, 128–140.

144 (*a*) S. Bertrand, C. Glapski, N. Hoffmann and J.-P. Pete, *Tetrahedron Lett.*, 1999, **40**, 3169–3172; (*b*) S. Bertrand, N. Hoffmann and J.-P. Pete, *Eur. J. Org. Chem.*, 2000, 2227–2238.

145 See also: E. Santiago de Alvarenga and J. Mann, *J. Chem. Soc., Perkin Trans. 1*, 1993, 2141–2142.

146 S. G. Cohen, A. H. Parola and G. H. Parsons Jr., *Chem. Rev.*, 1973, **73**, 141–161.

147 N. Hoffmann and H. Görner, *Chem. Phys. Lett.*, 2004, **383**, 451–455.

148 H. Fischer and L. Radom, *Angew. Chem., Int. Ed.*, 2001, **40**, 1340–1371.

149 (*a*) S. Marinković and N. Hoffmann, *Chem. Commun.*, 2001, 1576–1578; S. Marinković and N. Hoffmann, *Int. J. Photoenergy*, 2003, **5**, 175–182.

150 A. Bauer, F. Westkämper, S. Grimme and T. Bach, *Nature*, 2005, **436**, 1139–1140.

151 S. Z. Zard, *Angew. Chem., Int. Ed. Engl.*, 1997, **36**, 672–685.

152 (*a*) S. Yamago and Y. Nakamura, *Polymer*, 2013, **54**, 981–894; (*b*) G. Moad, E. Rizzardo and S. H. Thang, *Aust. J. Chem.*, 2012, **65**, 985–1076; (*c*) C. Boyer, V. Bulmus, T. P. Davis, V. Ladmiral, J. Liu and S. Perrier, *Chem. Rev.*, 2009, **109**, 5402–5436.

153 D. Harakat, D. Pesch, S. Marinković and N. Hoffmann, *Org. Biomol. Chem.*, 2006, **4**, 1202–1205.

154 A. Gassama, C. Ernenwein and N. Hoffmann, *ChemSusChem*, 2009, **2**, 1130–1137.

155 (*a*) E. Riguet and N. Hoffmann, in *Encyclopedia of Radicals in Chemistry, Biology and Materials*, ed. C. Chatgilialoglu and A. Studer, Wiley-VCH, Chichester, 2012, vol. 2, pp. 1217–1241; (*b*) U. Wille, in *CRC Handbook of Organic Photochemistry and Photobiology*, ed. A. Griesbeck, M. Oelgemöller and F. Ghetti, CRC Press, Boca Raton, 3rd edn, 2012, pp. 329–345; (*c*) *Radicals in Organic Synthesis*, ed. P. Renaud and M. Sibi, Wiley-VCH, Weinheim, 2001, vol. 1 and 2; (*d*) L. F. Tietze, G. Brasche and K. M. Gericke, *Domino Reactions in Organic Synthesis*, Wiley-VCH, Weinheim, 2006.

156 S. Bertrand, N. Hoffmann, S. Humbel and J.-P. Pete, *J. Org. Chem.*, 2000, **65**, 8690–8703.

157 S. Marinković, C. Brulé, N. Hoffmann, E. Prost, J.-M. Nuzillard and V. Bulach, *J. Org. Chem.*, 2004, **69**, 1646–1651.

158 (*a*) S. Marinković and N. Hoffmann, *Eur. J. Org. Chem.*, 2004, 3102–3107; (*b*) N. Hoffmann, *Aust. J. Chem.*, 2015, **68**, 1621–1639.

159 J. Tang, G. Grampp, Y. Liu, B.-X. Wang, F.-F. Tao, L.-J. Wang, X.-Z. Liang, H.-Q. Xiao and Y.-M. Shen, *J. Org. Chem.*, 2015, **80**, 2724–2732.

160 (*a*) G. Pandey and S. R. Gadre, *ARKIVOC*, 2003, 45–54; (*b*) G. Pandey, *Top. Curr. Chem.*, 1993, **168**, 175–221; (*c*) G. Pandey, *Synlett*, 1992, 546–552.

161 (*a*) C. K. Prier, D. A. Rankic and D. W. C. MacMillan, *Chem. Rev.*, 2013, **113**, 5322–5363; (*b*) M. Reckenthähler and A. G. Griesbeck, *Adv. Synth. Catal.*, 2013, **355**, 2727–2744; (*c*) L. Shi and W. Xia, *Chem. Soc. Rev.*, 2012, **41**, 7687–7697; (*d*) J. M. R. Narayanam and C. R. J. Stephenson, *Chem. Soc. Rev.*, 2011, **40**, 102–113; (*e*) T. P. Yoon, M. A. Ischay and J. Du, *Nat. Chem.*, 2010, **2**, 527–532; (*f*) K. Zeitler, *Angew. Chem., Int. Ed.*, 2009, **48**, 9785–9789; (*g*) *Chemical Photocatalysis*, ed. B. König, Walter de Gruyter, Berlin, 2013.

162 (*a*) N. Hoffmann, *ChemSusChem*, 2012, **5**, 352–371; (*b*) F. Teplý, *Collect. Czech. Chem. Commun.*, 2011, **76**, 859–917.

163 (*a*) A. Juris, V. Balzani, F. Barigelletti, S. Campagna, P. Belzer and A. von Zelewski, *Coord. Chem. Rev.*, 1988, **84**, 85–277; (*b*) S. Champagna, F. Puntoriero, F. Nastasi, G. Bergamini and V. Balzani, *Top. Curr. Chem.*, 2007, **280**, 117–214; (*c*) J. W. Tucker and C. R. J. Stephenson, *J. Org. Chem.*, 2013, **77**, 1617–1622.

164 For some older examples see: (*a*) T. J. van Bergen, D. M. Hedstrand, W. H. Kruizinga and R. M. Kellogg, *J. Org. Chem.*, 1979, **44**, 4953–4962; (*b*) H. Cano-Yelo and A. Deronzier, *J. Chem. Soc., Perkin Trans. 2*, 1984, 1093–1098; (*c*) C. Pac, Y. Miyauchi, O. Ishitani, M. Ihama, M. Yasuda and H. Sakurai, *J. Org. Chem.*, 1984, **49**, 26–34; (*d*) R. Maidan, Z. Goren, J. Y. Becker and I. Willner, *J. Am. Chem. Soc.*, 1984, **106**, 6217–6222; (*e*) K. Hironaka, S. Fukuzumi and T. Tanaka, *J. Chem. Soc., Perkin Trans. 2*, 1984, 1705–1709.

165 D. A. Nicewicz and D. W. C. MacMillan, *Science*, 2008, **322**, 77–80.

166 D. D. M. Wayner, J. J. Dannenberg and D. Griller, *Chem. Phys. Lett.*, 1986, **131**, 189–191.

167 C. R. Bock, J. A. Connor, A. R. Gutierrez, T. J. Meyer, D. G. Whitten, B. P. Sullivan and J. K. Nagle, *J. Am. Chem. Soc.*, 1979, **101**, 4815–4824.

168 S. Fukuzumi, S. Mochizuki and T. Tanaka, *J. Phys. Chem.*, 1990, **94**, 722–726.

169 D. A. Nagib, M. E. Scott and D. W. C. MacMillan, *J. Am. Chem. Soc.*, 2009, **131**, 10875–10877.

170 (*a*) J. D. Slinker, A. A. Gorodetsky, M. S. Lowry, J. Wang, S. Parker, R. Rohl, S. Bernhard and G. G. Malliaras, *J. Am. Chem. Soc.*, 2004, **126**, 2763–2767; (*b*) L. Flamigni, A. Barbieri, C. Sabatini, B. Ventura and F. Barigelletti, *Top. Curr. Chem.*, 2007, **281**, 143–203.

171 (*a*) M. Neumann, S. Füldner, B. König and K. Zeitler, *Angew. Chem., Int. Ed.*, 2011, **50**, 951–954; (*b*) K. Fidaly, C. Ceballos, A. Falguières, M. S.-I. Veitia, A. Guy and C. Ferroud, *Green Chem.*, 2012, **14**, 1293–1297.

172 M. Cherevatskaya, M. Neumann, S. Füldner, C. Harlander, S. Kümmel, S. Dankesreiter, A. Pfitzner, K. Zeitler and B. König, *Angew. Chem., Int. Ed.*, 2012, **51**, 4062–4066.

173 (*a*) H. Zollinger, *Color Chemistry*, Verlag Helvetica Chimica Acta, Zürich, 2003; (*b*) H. Langhals, *Helv. Chim. Acta*, 2005, **88**, 1309; (*c*) L. Chen, C. Li and K. Müllen, *J. Mater. Chem. C*, 2014, **2**, 1938; (*d*) C. Li and H. Wonneberger, *Adv. Mater.*, 2012, **24**, 613–636; (*e*) X. Zhan, A. Facchetti, S. Barlow, T. J. Marks, M. A. Ratner, M. R. Wasielewski and S. R. Marder, *Adv. Mater.*, 2011, **23**, 268; (*f*) F. Würthner, *Chem. Commun.*, 2004, 1564; (*g*) D. Wöll, E. Braeken, A. Deres, F. C. De Schryver, H. Uji-i and J. Hofkens, *J. Chem. Soc. Rev.*, 2009, **38**, 313–328.

174 For recent systematic studies on a large compound family see: (*a*) M. Queste, C. Cadiou, B. Pagoaga, L. Giraudet and N. Hoffmann, *New J. Chem.*, 2010, **34**, 2537–2545; (*b*) B. Pagoaga, L. Giraudet and N. Hoffmann, *Eur. J. Org. Chem.*, 2014, 5178–5195; (*c*) B. Pagoaga, O. Mongin, M. Caselli, D. Vanossi, F. Momicchioli, M. Blanchard-Desce, G. Lemercier, N. Hoffmann and G. Ponterini, *Phys. Chem. Chem. Phys.*, 2016, **18**, 4924–4941.

175 I. Ghosh, T. Ghosh, J. I. Bardagi and B. König, *Science*, 2014, **346**, 725–728.

176 (*a*) D. Gosztola, M. P. Niemczyk, W. Svec, A. S. Lukas and M. R. Wasielewski, *J. Phys. Chem. A*, 2000, **104**, 6545–6551; (*b*) M. J. Tauber, R. F. Kelley, J. M. Giaimo, B. Rybtchinski and M. R. Wasielewski, *J. Am. Chem. Soc.*, 2006, **128**, 1782–1783.

177 (*a*) G. Chen, H. Qiu, P. N. Prasad and X. Chen, *Chem. Rev.*, 2014, **114**, 5161–5214; (*b*) F. Auzel, *Chem. Rev.*, 2004, **104**, 139–174; (*c*) T. F. Schulze and T. W. Schmidt, *Energy Environ. Sci.*, 2015, **8**, 103–125; (*d*) T. W. Schmidt and F. N. Castellano, *J. Phys. Chem. Lett.*, 2014, **5**, 4062–4072.

178 M. Majek, U. Faltermeier, B. Dick, R. Pérez-Ruiz and A. Jacobi von Wangelin, *Chem. – Eur. J.*, 2015, **21**, 15496–15501.

179 (*a*) K. P. C. Vollhardt, *Angew. Chem., Int. Ed. Engl.*, 1984, **23**, 539–556; (*b*) V. Gandon, C. Aubert and M. Malacria, *Chem. Commun.*, 2006, 2209–2217; (*c*) P. R. Chopade and J. Louie, *Adv. Synth. Catal.*, 2006, **348**, 2307–2327; (*d*) G. Dominguez and J. Pérez-Castells, *Chem. Soc. Rev.*, 2011, **40**, 3430–3444; (*e*) N. Weding and M. Hapke, *Chem. Soc. Rev.*, 2011, **40**, 4525–4538.

180 (*a*) H. Bönnemann, *Angew. Chem., Int. Ed. Engl.*, 1985, **24**, 248–262; (*b*) G. Chelucci, *Tetrahedron: Asymmetry*, 1995, **6**, 811–826; (*c*) B. Heller and M. Hapke, *Chem. Soc. Rev.*, 2007, **36**, 1085–1094; (*d*) J. A. Varela and C. Saa, *Synlett*, 2008, 2571–2578.

181 W. Schulz, H. Pracejus and G. Oehme, *Tetrahedron Lett.*, 1989, **30**, 1229–1232.

182 B. Heller, *Nachr. Chem., Tech. Lab.*, 1999, **47**, 9–14.

183 G. Chelucci, M. Falorni and G. Giacomelli, *Synthesis*, 1990, 1121–1122.

184 A. Gutnov, B. Heller, C. Fischer, H.-J. Drexler, A. Spannenberg, B. Sundermann and C. Sundermann, *Angew. Chem., Int. Ed.*, 2004, **43**, 3795–3797.

185 (*a*) G. Oehme, B. Heller and P. Wagler, *Energy*, 1997, **22**, 327–336; (*b*) P. Wagler, B. Heller, J. Ortner, K.-H. Funken and G. Oehme, *Chem. Ing. Tech.*, 1996, **68**, 823–826.

186 (*a*) B. Heller, D. Heller and G. Oehme, *J. Mol. Catal. A: Chem.*, 1996, **110**, 211–219; (*b*) B. Heller, D. Heller, P. Wagler and G. Oehme, *J. Mol. Catal. A: Chem.*, 1998, **136**, 219–233.

187 J. A. K. Du Plessis and J. S. Viljoen, *J. Mol. Catal. A: Chem.*, 1995, **99**, 71–76.

188 H. Bönnemann, *Angew. Chem., Int. Ed. Engl.*, 1985, **24**, 248–262.

189 B. Heller and G. Oehme, *J. Chem. Soc., Chem. Commun.*, 1995, 179–180.

190 D. I. Perez, M. M. Grau, I. W. C. E. Arends and F. Hollmann, *Chem. Commun.*, 2009, 6848–6850.

191 E. Churakova, M. Kluge, R. Ullrich, I. Arends, M. Hofrichter and F. Hollmann, *Angew. Chem., Int. Ed.*, 2011, **50**, 10716–10719.

192 F. Hollmann, A. Taglieber, F. Schulz and M. T. Reetz, *Angew. Chem., Int. Ed.*, 2007, **46**, 2903–2906.

193 N. J. Turro, V. Ramamurthy and J. C. Scaiano, *Modern Molecular Photochemistry of Organic Molecules*, University Science Books, Sausalito, 2010, pp. 1003–1008.

194 B. F. Minaev, *Russ. Chem. Rev.*, 2007, **76**, 988–1010.

195 (*a*) B. F. Minaev and H. Ågren, *THEOCHEM*, 1998, **434**, 193–206; (*b*) A. Riahi, J. Muzart, M. Abe and N. Hoffmann, *New J. Chem.*, 2013, **37**, 2245–2249.

196 (*a*) G. O. Schenck, *Naturwissenschaften*, 1948, **35**, 28–29; (*b*) H. H. Wasserman and J. L. Ives, *Tetrahedron*, 1981, **37**, 1825–1852; (*c*) E. L. Clennan, *Tetrahedron*, 2000, **56**, 9151–9179; (*d*) M. Stratakis and M. Orfanopoulos, *Tetrahedron*, 2000, **56**, 1595–1615; (*e*) T. Montagnon, D. Noutsias, I. Alexopoulou, M. Tofi and G. Vassilikogiannakis, *Org. Biomol. Chem.*, 2011, **9**, 2031–2039; (*f*) W. J. Kinart, C. M. Kinart and M. Sendecki, *Curr. Org. Synth.*, 2013, **10**, 337–346; (*g*) M. Zamadar and A. Greer, in *Handbook of Synthetic Photochemistry*, ed. A. Albini and M. Fagnoni, Wiley-VCH, Weinheim, 2010, pp. 353–386.

197 C. S. Foot, *Acc. Chem. Res.*, 1968, **1**, 104–110.

198 W. Fudickar and T. Linker, *Aust. J. Chem.*, 2014, **67**, 320–327.

199 K. Yamaguchi, Y. Ikeda and T. Fueno, *Tetrahedron*, 1985, **41**, 2099–2107.

200 (*a*) H. Rau, *Chem. Rev.*, 1983, **83**, 535–347; (*b*) A. G. Griesbeck and U. J. Meierhenrich, *Angew. Chem., Int. Ed.*, 2002, **41**, 3147–3154.

201 J. Sivaguru, M. R. Solomon, T. Poon, S. Jockusch, S. G. Bosio, W. Adam and N. J. Turro, *Acc. Chem. Res.*, 2008, **41**, 387–400.

202 W. Adam, S. G. Bosio, N. J. Turro and B. T. Wolff, *J. Org. Chem.*, 2004, **69**, 1704–1715.

203 S. Inagaki, H. Fujimoto and K. Fukui, *Chem. Lett.*, 1976, 749–752.

204 S. Masamune, W. Choy, J. S. Petersen and L. R. Sita, *Angew. Chem., Int. Ed. Engl.*, 1985, **24**, 1–30.

205 J. Sivaguru, M. R. Solomon, H. Saito, T. Poon, S. Jockusch, W. Adam, Y. Inoue and N. J. Turro, *Tetrahedron*, 2006, **62**, 6707–6717.

206 M. Prein and W. Adam, *Angew. Chem., Int. Ed. Engl.*, 1996, **35**, 477–494.

207 T. Poon, J. Sivaguru, R. Franz, S. Jockusch, C. Martinez, I. Washington, W. Adam, Y. Inoue and N. J. Turro, *J. Am. Chem. Soc.*, 2004, **126**, 10498–10499.

208 J. Sivaguru, T. Poon, C. Hooper, H. Saito, M. R. Solomon, S. Jockusch, W. Adam, Y. Inoue and N. J. Turro, *Tetrahedron*, 2006, **46**, 10647–10659.

209 H. B. Kagan and J. C. Fiaud, *Top. Stereochem.*, 1988, **18**, 249–330.

210 (*a*) J. E. Leffler, *J. Org. Chem.*, 1955, **20**, 1202; (*b*) J. E. Leffler and E. Grunwald, *Rates and Equilibria of Organic Reactions*, J. Wiley & Sons, New York, 1963, ch. 9, pp. 318–402; (*c*) O. Exner, *Collect. Czech. Chem. Commun.*, 1975, **40**, 2762–2780; (*d*) O. Exner, *Collect. Czech. Chem. Commun.*, 1975, **40**, 2781–2791; (*e*) W. Linert, *Inorg. Chim. Acta*, 1988, **141**, 233–242; (*f*) B. Giese, *Acc. Chem. Res.*, 1984, **17**, 438–442; (*g*) N. Hoffmann, H. Buschmann, G. Raabe and H.-D. Scharf, *Tetrahedron*, 1994, **50**, 11167–11186; (*h*) Y. Inoue and T. Wada, *Adv. Supramol. Chem.*, 1997, **4**, 55–96.

211 N. J. Turro, *Tetrahedron*, 1985, **41**, 2089–2098.

212 (*a*) G. Peters and M. A. J. Rodgers, *J. Am. Chem. Soc.*, 1981, **103**, 6759–6761; (*b*) M. A. J. Rodgers, *J. Am. Chem. Soc.*, 1983, **105**, 6201–6205.

213 (*a*) A. E. Cassano, C. A. Martin, R. J. Brandi and O. M. Alfano, *Ind. Eng. Res.*, 1995, **34**, 2155–2201; (*b*) A. M. Braun, M. Maurette and E. Oliveros, *Photochemical Technology*, Wiley, Chichester, 1991.

214 J. M. Parnis and K. B. Oldham, *J. Photochem. Photobiol., A*, 2013, **267**, 6–10.

215 (*a*) J. Wegner, S. Ceylan and A. Kirschning, *Adv. Synth. Catal.*, 2012, **354**, 17–57; (*b*) C. Wiles and P. Watts, *Green Chem.*, 2012, **14**, 38–54; (*c*) J.-i. Yoshida, H. Kim and A. Nagaki, *ChemSusChem*, 2011, **4**, 331–340; (*d*) P. T. Baraldi and V. Hessel, *Green Process. Synth.*, 2012, **1**, 149–167; (*e*) L. Malet-Sanz and F. Susanne, *J. Med. Chem.*, 2012, **55**, 4062–4098; (*f*) N. G. Anderson, *Org. Process Res. Dev.*, 2012, **16**, 852–869; (*g*) K. S. Elvira, X. Casadevall i Solvas, R. C. R. Wootton and A. J. deMello, *Nat. Chem.*, 2013, **5**, 905–915; (*h*) K. Jähnisch, V. Hessel, H. Löwe and M. Baerns, *Angew. Chem., Int. Ed.*, 2004, **43**, 406–446.

216 (*a*) T. Aillet, K. Loubière, O. Dechy-Cabaret and L. Prat, *Int. J. Chem. React. Eng.*, 2014, **12**, 257–269; (*b*) T. Aillet, K. Loubière, O. Dechy-Cabaret and L. Prat, *Chem. Eng. Process.*, 2013, **64**, 38–47; (*c*) K. Loubière, M. Oelgemöller, T. Aillet, O. Dechy-Cabaret and L. Prat, *Chem. Eng. Process.*, 2016, **104**, 120–132.

217 (*a*) K. Gilmore and P. H. Seeberger, *Chem. Rec.*, 2014, **14**, 410–418; (*b*) M. Oelgemöller, N. Hoffmann and O. Shvydkiv, *Aust. J. Chem.*, 2014, **67**, 337–342; (*c*) M. Oelgemöller, *Chem. Eng. Technol.*, 2012, **35**, 1144–1152; (*d*) M. Oelgemöller and O. Shvydkiv, *Molecules*, 2011, **16**, 7522–7550; (*e*) E. E. Coyle and M. Oelgemöller, *Photochem. Photobiol. Sci.*, 2008, **7**, 1313–1322.

218 A. Yavorskyy, O. Shvydkiv, N. Hoffmann, K. Nolan and M. Oelgemöller, *Org. Lett.*, 2012, **14**, 4342–4345.

219 H. Lu, M. A. Schmidt and K. F. Jensen, *Lab Chip*, 2001, **1**, 22–28.

220 (*a*) O. Shvydkiv, A. Yavorskyy, K. Nolan, A. Youssef, E. Riguet, N. Hoffmann and M. Oelgemöller, *Photochem. Photobiol. Sci.*, 2010, **9**, 1601–1603; (*b*) A. Yavorskyy, O. Shvydkiv, K. Nolan, N. Hoffmann and M. Oelgemöller, *Tetrahedron Lett.*, 2011, **52**, 278–280; (*c*) O. Shvydkiv, A. Yavorskyy, S. B. Tan, K. Nolan, N. Hoffmann, A. Youssef and M. Oelgemöller, *Photochem. Photobiol. Sci.*, 2011, **10**, 1399–1404.

221 (*a*) A. Sugimoto, Y. Sumino, M. Takagi, T. Fukuyama and H. Ryu, *Tetrahedron Lett.*, 2006, **47**, 6197–6200; (*b*) A. Sugimoto, T. Fukuyama, Y. Sumino, M. Takagi and I. Ryu, *Tetrahedron*, 2009, **65**, 1593–1598.

222 B. G. Anderson, W. E. Bauta and W. R. Cantrell, *Org. Process Res. Dev.*, 2012, **16**, 967–975.

223 (*a*) F. Lévesque and P. H. Seeberger, *Angew. Chem., Int. Ed.*, 2012, **51**, 1706–1709; (*b*) D. Kopetzki, F. Lévesque and P. H. Seeberger, *Chem. – Eur. J.*, 2013, **19**, 5450–5456.

224 (*a*) M. Fischer, *Angew. Chem., Int. Ed. Engl.*, 1978, **17**, 16–26; (*b*) K. Gollnick, *Chim. Ind.*, 1982, **63**, 156–166.

225 (*a*) G. Shama, C. Peppiatt and M. Biguzzi, *J. Chem. Technol. Biotechnol.*, 1996, **65**, 56–64; (*b*) S. D. Pask, O. Nuyken and Z. Cai, *Polym. Chem.*, 2012, **3**, 2698–2707; (*c*) V. Pareek, *Chem. Eng.*, 2005, **764**, 28.

226 (*a*) E. A. Sosnin, T. Oppenländer and V. F. Tarasenko, *J. Photochem. Photobiol., C*, 2006, **7**, 145–163; (*b*) N. T. Kalyania and S. J. Dhoble, *Renewable Sustainable Energy Rev.*, 2012, **16**, 2696–2723; (*c*) G. Kreisel, S. Meyer, D. Tietze, T. Fidler, R. Gorges, A. Kirsch, B. Schäfer and S. Rau, *Chem. Ing. Tech.*, 2007, **79**, 153–159.

227 J. Turconi, F. Griolet, R. Guevel, G. Oddon, R. Villa, A. Geatti, M. Hvala, K. Rossen, R. Göller and A. Burgard, *Org. Process Res. Dev.*, 2014, **18**, 417–422.

228 S. Werner, R. Seliger, H. Rauter and F. Wissmann, *EP* 2065387A2, 2009; *Chem. Abstr.*, 2009, **150**, 376721.

229 M. Oelgemöller and M. Bolte, *Green Process. Synth.*, 2014, **3**, 163–165.

